# EVIDENCE FOR POST-HISPANIC ENVIRONMENTAL CHANGE IN GUERRERO, MEXICO FROM HIGH-RESOLUTION LACUSTRINE SEDIMENT CORES

A Thesis
Presented to the Faculty of the Graduate School
of Cornell University
In Partial Fulfillment of the Requirements for the Degree of
Master of Science

by
William James Guerra
May 2012

# EVIDENCE FOR POST-HISPANIC ENVIRONMENTAL CHANGE IN GUERRERO, MEXICO FROM HIGH-RESOLUTION LACUSTRINE SEDIMENT CORES

William James Guerra
Cornell University, 2012

The cumulative impact of the Spanish Contact (c. 1520CE) and the Little Ice Age (c. 1300-1850CE) for environmental change in Mexico is still much debated. We present a sub-decadal resolution paleoecological record of environmental change for Laguna Ojo de Mar (LOM), a ~4 ha lake in eastern Guerrero, Mexico. Two sediment cores (2m and 2.9m) were collected from LOM, and AMS radiocarbon dating indicates the basal sediments were deposited approximately c. 1490CE ± 117 (1 SD). Reconstruction of environmental history is based on geochemical data including high-resolution magnetic susceptibility, carbon isotopes, carbon/nitrogen ratio, and loss-on-ignition analysis. Macroscopic charcoal and seed data are used to reconstruct paleoecology and anthropogenic impacts. The combined multi-proxy data suggest low agriculture intensity post-contact through the early 18th century and drought conditions resulting in declining lake levels from the mid-18th century to early 19th century.

# BIOGRAPHICAL SKETCH

William Guerra was born in Massachusetts in 1986. Developing an interest in the natural sciences at an early age, he was soon on a path to study Environmental Science at the University of Vermont and later graduate summa cum laude from the University of Massachusetts in May 2008 with a double degree in Earth Systems Sciences and Geology. He decided to pursue graduate school immediately afterward and began working with Dr. Michelle Goman first in Mexico and later in the Cornell Paleoecology Laboratory. While working on his degree, William met his wife Mary, a fellow Cornell Graduate student, and they married in August 2010. In total, William worked on his master's project for two years at Cornell and continued the project in absentia, while employed by the U.S. Army Corps of Engineers in Baltimore, MD.

# ACKNOWLEDGEMENTS

I would like to thank the Cornell Department of Earth and Atmospheric Sciences, Cornell College of Engineering, and the NASA Space Grant program for generously providing financial support during the two years I was in Ithaca. I'd especially like to thank my advisor, Dr. Michelle Goman who provided countless hours of support, edited innumerable drafts of proposals, abstracts, and manuscripts, and coordinated nearly all of my research activities. Thanks as well to Dr. Sturt Manning for providing much expertise, particularly toward disentangling the complicated core chronology. Additionally, much of the analysis would not have been possible without the support of grants from the Geological Society of America, The Cornell Biodiversity and Biocomplexity IGERT Program, and the National Lacustrine Core Laboratory.

Finally, thanks to my family (and especially my wife Mary) for providing me with the emotional support to keep pushing toward the completion of this manuscript. It would not have been possible without them.

## Table of Contents

## LIST OF FIGURES

# LIST OF TABLES

## Section 1. Introduction

### 1.1 Research Question

This paper presents temporally high-resolution multi-proxy paleolimnological evidence for human impact and climatic change in the Southern Mexican highlands from the time of European contact (c. 1520 CE) to the present. We utilize geochemical and biologic archives of environmental change from the sediments of a mid-elevation lake in eastern Guerrero, Mexico. Our research seeks to fill a significant gap in the understanding of regional environmental change and investigate climatic conditions during the LIA.

### 1.2 Prior Research

The assumption that Spanish settlers encountered a sustainably managed, if not 'pristine' landscape (Melville, 1990) has been much discredited by extensive research showing a history of environmental degradation in Mesoamerica (Deevey et al. 1979; Metcalfe, 1989; Denevan, 1992, O'Hara et al. 1993; Redman, 1999). However, the cumulative environmental impact of Spanish settlement on this already altered landscape is still much debated. It is known from historical records that the Spanish settlement brought considerable changes to Central and Southern Mexico. The dramatic decrease in indigenous population (Acuna-Soto, 2005), and the introduction of plough and animal-based agriculture (Simpson, 1952) resulted in new patterns of land use and settlement. Some research has provided evidence for increased erosion during the early colonial era due to abandonment of indigenous fields and settlements (Fisher et al. 2003), Spanish deforestation (Elliot et al. 2010), or Spanish settlement and mineral exploitation (Davies et al. 2005), followed by decreased erosion during the 18th century as local population rebounded. Other studies have detected no significant difference in erosion (Metcalfe et al.

2007) or even catchment stability (Davies et al. 2004) during the colonial period.

A major complication to studying environmental change is that the greatest impacts are local in scale, but detailed regional and sub-regional prior research is available from only a few areas throughout Mexico and with clear biases or preferences for only a few contexts. The volcanic highlands of Central Mexico have been much studied, particularly for the agricultural history (Ranere et al. 2009; Piperno et al. 2007; Smith, 1997), and the Yucatan Peninsula for the prospect of understanding Mayan cultural evolution (Curtis, 1996; Hodell 2001; Whitmore, 1996, Hodell et al. 2007). Studies from other regions, including Veracruz (eg. Goman and Byrne, 1998; Lozano-Garcia et al. 2007) and Oaxaca (eg. Joyce and Mueller, 1997; Goman et al. 2005; Goman et al. 2010) have sought to provide perspective on human impacts, though they have typically lacked the resolution to discern environmental changes on decadal, much less sub-decadal temporal scales. These focal points of research and the lack of temporal resolution has led to substantial gaps in the overall understanding of Mexican landscape evolution.

Quantifying the extent of human impact is further complicated by climate variability during the same period. Spanish colonization occurred during the Little Ice Age (LIA) (Diaz et al. 2011), an important but inadequately understood climatic period in Central America. While there is much agreement on the existence of a large-scale Late Classic drought across Mesoamerica (Haug et al. 2003; Hodell et al. 2005a; Metcalfe et al. 2010), understanding LIA impacts has proved more complicated. Frequent droughts are documented in historical records from Central and Southern Mexico throughout the LIA (O'Hara and Metcalfe, 1997), but some paleolimnological research has suggested increased winter precipitation (Lozano-Garcia et al. 2007).

## 2. Study Site

### 2.1 Physical Setting

Laguna Ojo de Mar, hereafter referred to LOM (17° 48' N, 98° 34' W, WGS1984) is located in the Tlapaneco river valley of the Sierra Madre del Sur physiological province at 880m above sea level in the Mexican state of Guerrero (Figures 1 and 2) (Tamayo, 1962). The lake basin lies in a steep sided valley and has an area extent of 3.5 ha. The maximum depth is approximately 20m, but coring was conducted on the shallower shelf (~5m deep) that extends around the lake due to equipment limitations. The lake is bounded on the eastern side by a steep, approximately 400m mountain face largely devoid of vegetation, and to the west by a heavily agricultural floodplain along the Tlapaneco River, a tributary of the Balsas. LOM is 1 km east of the Tlapaneco, and lies at approximately the same elevation as the river. The predominant geology in the valley is quaternary sedimentary soils, but the upland terrain is underlain by Early Tertiary gypsum to the west and Lower Cretaceous limestone to the east (Servicio Geológico Mexicano. 1981).

The climate of Southern Mexico is complex due to topography, proximity to both the Gulf of Mexico and the Pacific Ocean, and latitudinal location in the subtropics. LOM is situated on the leeward slope of the Sierra Madres del Sur and experiences a Seasonally Humid Tropical (Köppen: Aw) climate. Minimum temperatures range from 15-21˚C, and maximum temperatures from 30-36˚C. The average annual precipitation is approximately 800mm but most occurs from May-October. Precipitation predominantly results from convection driven by the northerly migration of the Intertropical Convergence Zone (ITCZ) (O'Hara and Metcalfe, 1997). Central and Southern Mexico experiences a mid-summer drought or canícula (Small, 2007). During this period, typically July and August, the splitting of the subtropical high-pressure

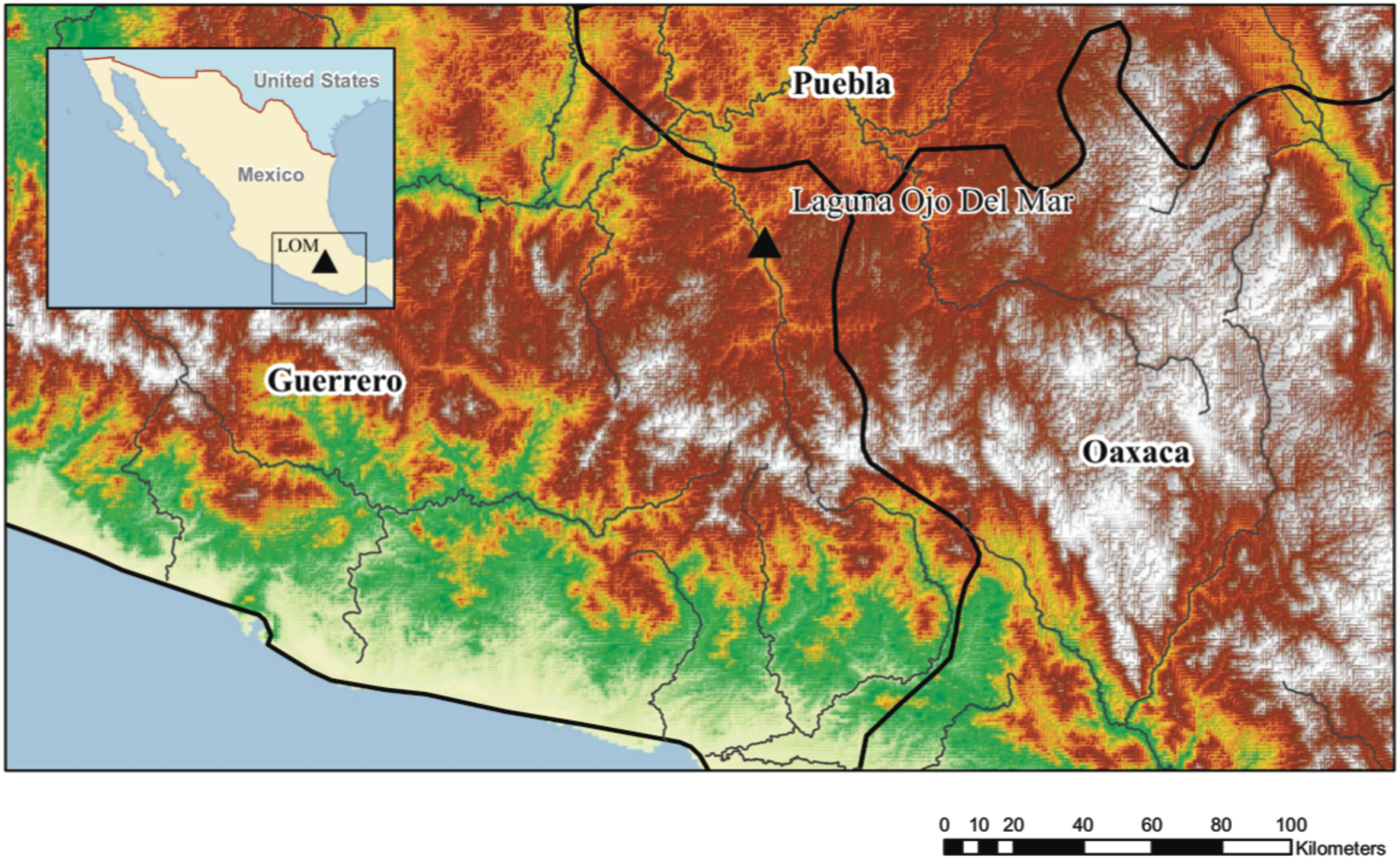


Figure 1. Laguna Ojo de Mar overview map. Shading shows topography of the Sierra Madre del Sur mountain range.

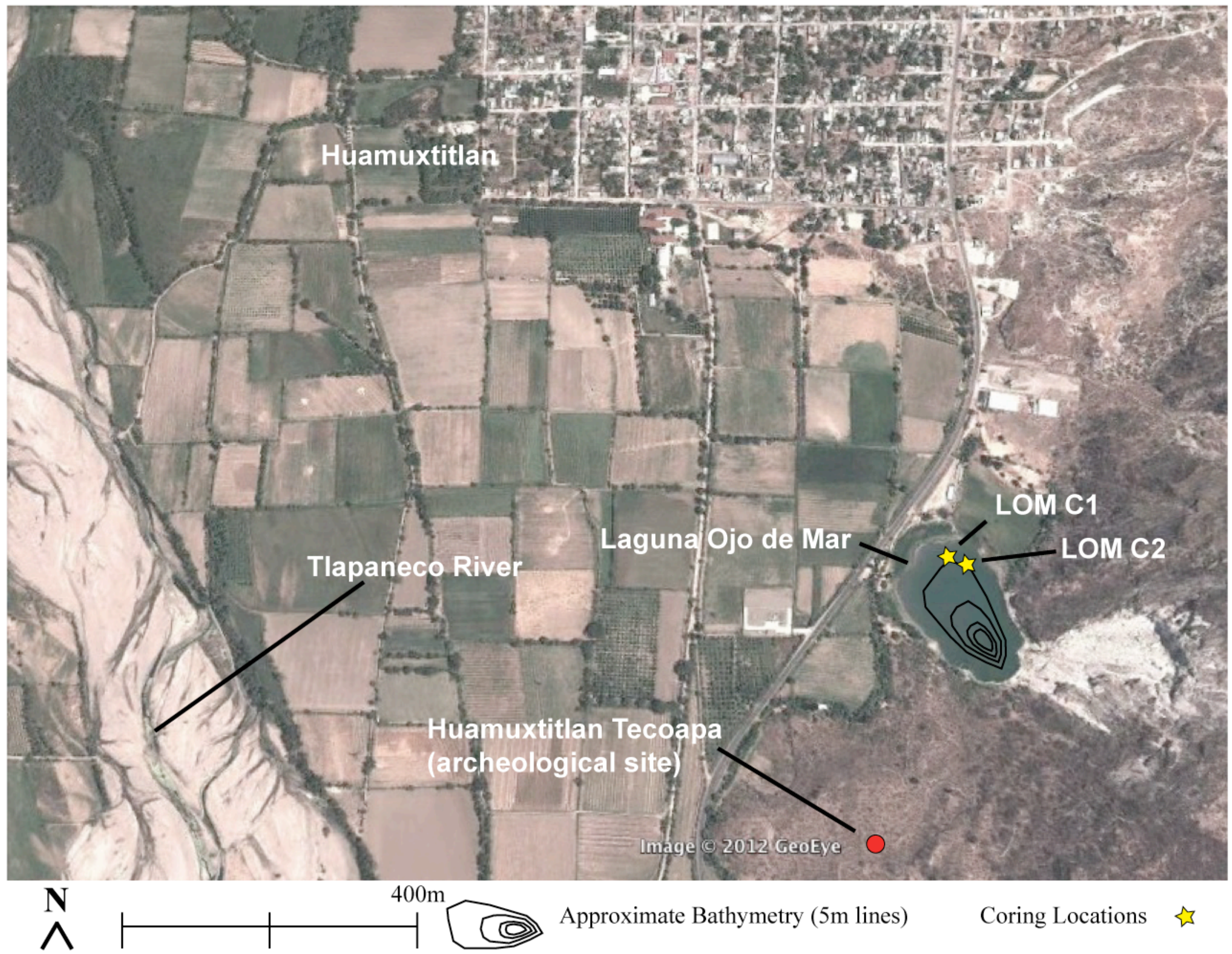


Figure 2. Laguna Ojo de Mar Local area map. Location of lake to Tlapaneco River, city of Huamuxtitlan, and Huamuxtitlan Tecoapa archeological site and approximate bathymetry of LOM is included. Note the lack of vegetation on cliffs to the southeast of the lake.

system results in northerly atmospheric flow, which provides dry air from northern Mexico but also allows increased moist air from the Pacific. The region receives supplementary rainfall from tropical cyclones from the Atlantic and Pacific oceans. El Niño-Southern Oscillation (ENSO) is a major driver of interannual variability. Drier conditions occur during El Niño events because the ITCZ is displaced to the south, and La Niña events appear to produce increased summer rainfall (Magaña et al. 2003; Pavia et al. 2006).

## 2.2 Cultural Setting

LOM is situated near the modern municipality of Huamuxtitlan in the Tlapaneco river valley. The region has an extensive history of human occupation. Strong political and economic alliances were formed by the pre-classic period (1500BCE - 300CE) (Gutiérrez, 2002). From the mid 15th century to early 16th century, the region surrounding Huamuxtitlan (Tlapa-Tlachinollan) expanded greatly, reaching a population of more than 150,000 people (Gutiérrez, 2002). Huamuxtitlan was later incorporated into the New Spanish encomienda system in the 16th century (Gerhard, 1993). Under colonial authority, 'encomenderos', or appointed leaders of local encomiendas imposed tributes and exacted indigenous labor. Huamaxtitlan was part of the encomienda of Chiautla in the 1520's and later added to the encomienda of Tlapa in the 1550's (Gerhard, 1993). As with many parts of Central America, a collapse of the local population occurred in the 16th and early 17th century, likely as high as 80-90% (Acuna-Soto, 2005), primarily due to the introduction of diseases from Europe (Cook and Borah, 1987). According to colonial census data, the number of tribute-paying households in the Tlapa district was 10,718 in 1548 CE and fell to 5,500 in 1600 CE, and possibly as low as 1,600 households in 1626 CE (Gerhard, 1993). Population eventually increased to 7,649 households by 1696 CE, and locals reoccupied many of the settlements abandoned during the population crash. The region remained in Spanish control until the war for independence in the early 1800's (Meyer et al. 1999). Modern Huamuxtitlan is densely farmed with most cropland following the Tlapaneco River. Domesticated animals including chickens, pigs, and donkeys are common in the region.

## 2.3 Vegetation and Land Use

LOM is located in the tropical deciduous forest zone. Trees in this region typically reach 8-12m and drop their leaves for 5-8 months each year. The dominant vegetation includes tree species from the genera *Bursera* and *Ceiba,* and cacti (*Neobuxbaumia*). The genera *Amphipterygium, Bomba, Cercium, Crataeva, Ipomea, Guazuma, Plumeria, Tabeuia* are also frequently found in this region (Rzedowski, 1978). Crop agriculture includes production of maize, rice, and mamey. Historically, agricultural production has utilized the "Trompezón" system. This type of wetland agriculture involves building barriers (trompezónes) of rocks and woody material to restrain and reroute river waters and trap sediments for farming. Trompezón agriculture is still practiced in the Tlapaneco River Valley.

Much additional land is dedicated to animal husbandry including cattle, pigs, sheep, goats, and horses. Widespread use of domesticated animals began in 1540 when Francisco Vásquez introduced many pigs and horses across present-day Mexico. Soon afterward, sheep, goats, chickens, ducks, and donkeys were introduced into Spanish settlements across then New Spain. The introduction of grazing animals represented a significant change of land-use, though there is much debate as to the extent of environmental degradation brought about by this change (Butzer and Butzer, 1997; Melville, 1994). It has been suggested that these animals increased erosion and flood frequency by decreasing brush cover (Melville, 2000).

## 3. Methods

### 3.1 Core Collection

In July 2008, two cores were collected from Laguna Ojo de Mar using a 1m Livingstone Corer. Collected sediment was extruded into polyethylene tubes and wrapped with tape for transport. Both cores were sampled from the northern side of the lake, approximately 20m from shore. LOM C1 was sampled at a water depth of 4.50m and LOM C2 at 5.07m depth. LOM C1 was cored to a depth of 1.99m and LOMC2 to a depth of 2.90m. A sandy sediment layer prevented further coring at both sites. Sediment compaction during coring was calculated from the difference of total depth cored and core recovery. Stretching and compaction was assumed uniform within individual core segments. Cores were transported back to Cornell for analysis, and placed in cold storage. Unfortunately, LOM C2, push 1 was lost in transport.

### 3.2 Core Chronology

Accelerator Mass Spectrometry (AMS) Radiocarbon (RC) dates were determined for 6 samples from LOM C2 and 3 samples from LOM C1 (Table 1). Samples were collected using sterilized scalpels and tweezers, dried in a 100°C oven, and weighed using a digital scale. Of the 9 total samples, 3 were of woody material and 6 were of bulk lake sediment. Radiocarbon calibration and age-modelling was carried out using OxCal v 4.1.7 (Figure 3)(Bronk Ramsey 2010; Bronk Ramsey 2009). Atmospheric data was from Reimer et al. (2009). The chronological model utilizes the three AMS RC dates from plant macrofossils (all from LOM C2) in a Poisson Sequence Deposition model (Bronk Ramsey, 2008). One boundary was incorporated in the age model to account for a lithological change at 200cm depth.

Table 1: Radiocarbon Data. Samples included in the age model are highlighted in bold. Calibrated age and modelled age are reported as mean of the modelled distribution ± the standard deviation. Note: Data are from: Keck Laboratory: UC Irvine, (Keck); Beta Analytic: Miami, FL (Beta); University of Waikato: Waikato, New Zealand (WNZ). All samples pretreated with acid/alkali/acid washes.

| Lab ID | Sample Name | Core # | Core Depth | Type of Sample: | Measured Age (BP) | ± 1 SD | Calibrated Age (BP) | ± 1 SD | Modelled Age (CE) | ± 1 SD |
|---|---|---|---|---|---|---|---|---|---|---|
| WNZ - 28723 | LOMC1P1 68-70cm | 1 | 69 | Lake sediment | 1921 | 29 | 1867 | 35 | N/A | N/A |
| WNZ - 28724 | LOMC1P1 84-86cm | 1 | 85 | Lake sediment | 1090 | 30 | 1001 | 36 | N/A | N/A |
| WNZ - 28725 | LOMC1P2 32-34cm | 1 | 137.3 | Lake sediment | No data | N/A | N/A | N/A | N/A | N/A |
| Beta - 280034 | LOMC1P3 16-17cm | 1 | 207 | Lake sediment | 3120 | 40 | 3339 | 49 | N/A | N/A |
| **Keck - 58011** | **LOMC2P2 108-109 cm** | **2** | **108.5** | **Unidentified plant material** | **130** | **15** | **135** | **80** | **1877** | **37** |
| WNZ - 28726 | LOMC2P3 6-8cm | 2 | 164.6 | Lake sediment | 632 | 38 | 606 | 35 | N/A | N/A |
| WNZ - 28727 | LOMC2P4 8-10cm | 2 | 203.9 | Lake sediment | 560 | 30 | 582 | 37 | N/A | N/A |
| **Beta - 280035** | **LOMC2P4 35-36cm** | **2** | **230.1** | **Unidentified plant material** | **210** | **40** | **183** | **100** | **1677** | **43** |
| **Keck - 58010** | **LOMC2P5 33-34cm** | **2** | **264.8** | **Unidentified plant material** | **420** | **100** | **435** | **102** | **1569** | **75** |
| WNZ - 28728 | LOMC2P6 12-14cm | 2 | 282.4 | Lake sediment | 503 | 30 | 530 | 22 | N/A | N/A |

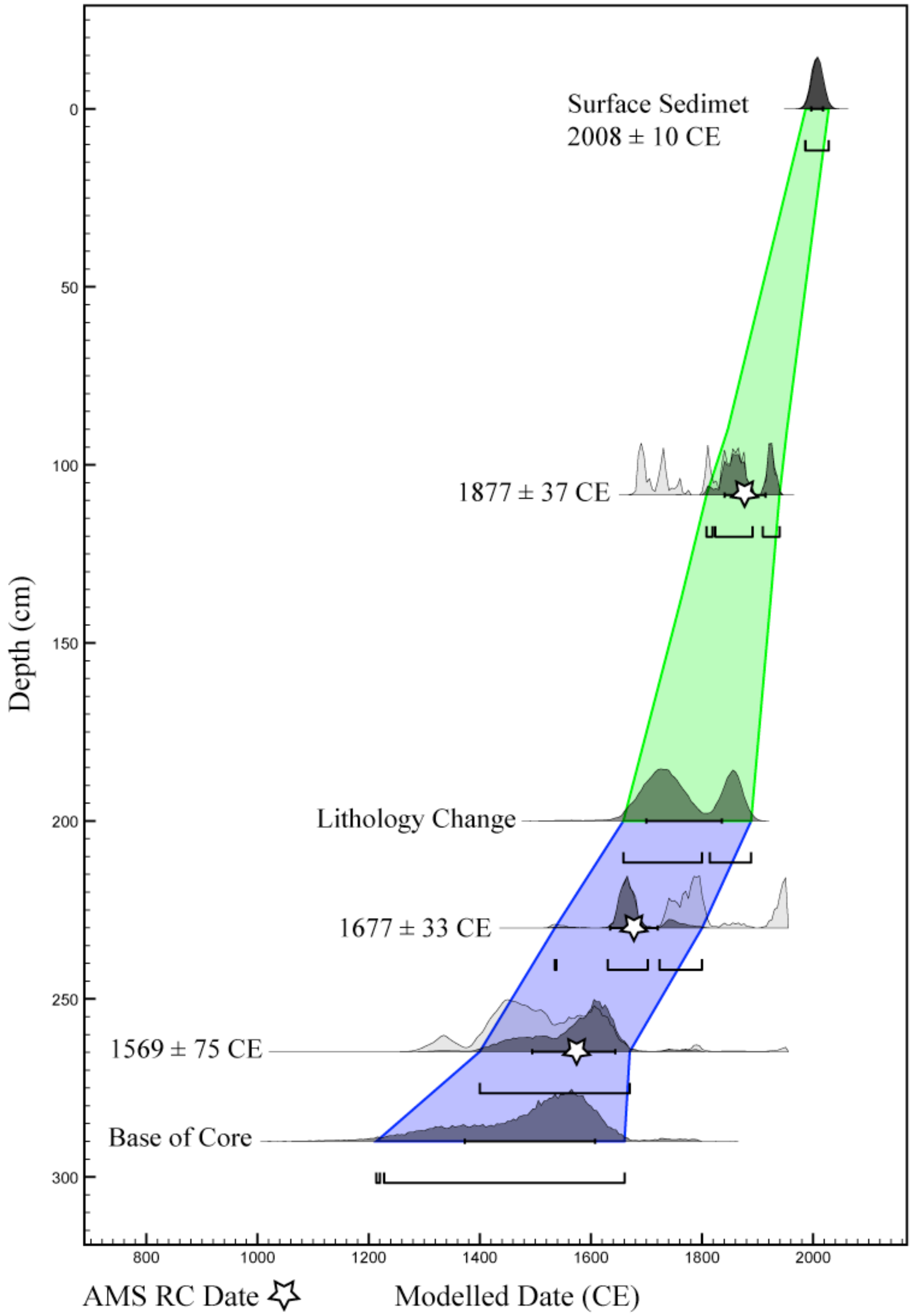


Figure 3. Poisson Deposition Age Model from OxCal version 4.1.7. Light gray shading represents likelihood based on calibrated ages. Blue, green, and black shading represents the 95.4% probability of the deposition model. Listed dates are mean probability of model data ± 1 standard deviation. $A_{model}$ Index = 100.5. $A_{overall}$ Index = 99.7.

The OxCal run file is as follows:

*P_Sequence(1) { Boundary("Base of Core") { z=290; }; R_Date("264.8cm, 420, 100){ z=264.8; }; R_Date("230.1", 210, 40) { z=230.1; }; Boundary("lithology change") { z=200; }; R_Date("108.5", 130, 15) { z=108.5; C_Date("Surface Sediment", 2008, 10) { z=0; }; Boundary("Top of Core") { z=0; }; };*

7 samples from the surface sediment from LOM C1 and 2 soil samples collected near the lake were analyzed for a 210Pb chronology. Samples of approximately 5cc were dried for 24 hours at 100°C, ground using a mortar and pestle, and analyzed by the Rochester Institute of Technology, Bopp Lab.

### 3.3 Stratigraphic and Geochemical Analysis

Digital computed radiographs of LOM C1 and LOM C2 were collected at the Cornell University Hospital for Animals using a Kodak CR 500. The unopened cores were analyzed with a Geotek Multi-Sensor Core Logger (MSCL) at the National Lacustrine Core Facility (LacCore) to determine density, magnetic susceptibility, and electrical resistivity data at continuous 1cm resolution. Cores were cut using parallel circular saws and split using aluminum blades. The surface sediment was cleaned using polished microscope slides. Cores were digitally imaged immediately after splitting using a Geotek Geoscan-III line-scan CCD camera at 254dpi resolution, and then analyzed with a Geotek XYZ core scanner for contiguous 0.5cm resolution point-sensor high-resolution magnetic susceptibility (HRMS) measurements. Magnetic susceptibility data has been commonly used in Mexico to infer periods of catchment instability (eg. Lozano-Garcia and Ortega-Guerrero, 1994; Caballero et a. 2002; Davies et al. 2005; Goman et al. 2010) because high MS reflects an increased flux of ferromagnetic particles of terrestrial origin (Thompson and Oldfield, 1986).

Cores were described using standard Munsell colors, grain size by hand feel, major and minor components of the sediment, and bedding type (i.e. laminated or massive) at the Cornell Quaternary Paleoecology Lab. Samples were analyzed at 1-cm intervals for charcoal, macrofossil, and Loss on Ignition analysis (LOI). 1.5 cc of sediment was sampled for LOI, and analysis followed from Heiri et al (2001). LOI data are used to determine the organic and carbonate content of sediment (Dean, 1974) and have been used detect evaporative precipitation (Metcalfe et al. 2007) or erosion (Caballero et al. 2006). Approximately 5cc of sediment was used for macroscopic charcoal and aquatic macrofossils counts with exact sample volume determined by displacement. Preparation procedures followed Whitlock and Larson (2001). Charcoal (125μm and 250μm fractions) and seeds were identified and quantified using an Olympus dissecting microscope. Charcoal accumulation rate (CHAR) is used to infer local fire history including burning for agriculture (eg. Clement and Horn 2001; Conserva and Byrne, 2002; Goman and Byrne, 1998; Lane et al. 2004), and was determined using the sedimentary accumulation rate calculated from the radiocarbon chronology and the formula *(Whitlock and Anderson, 2001)*:

*CHAR = {total charcoal counted} / {volume sediment sampled (cm$^3$)} x {sediment deposited(cm))/year}*

Because no AMS RC dates from LOMC1 were used in the constructed age model, CHAR for LOMC1 utilizes the sedimentation rate derived from the LOMC2 chronology. Background charcoal accumulation rate and peak identification (fire events) were calculated through statistical analyses from Kelly et al. 2011, Higuera et al. 2010, and Higuera et al. 2009 using the program CharAnalysis (available freely at http://sites.google.com/site/charanalysis/).

Identification of statistically significant fire events helps to interpret charcoal variability in cases where total charcoal counted reflects delivery rather as well as production (Higuera et al. 2010).

Carbon and nitrogen isotope analysis was conducted at approximately 8-cm resolution. Samples were analyzed for percent carbon and nitrogen of total sediment, and for abundance of $^{13}C$ and $^{15}N$ verses PDB ($^{13}C$) and air ($^{15}N$) to determine the source of carbon and nitrogen in the lake sediments. Grasslands plants (C4 metabolic pathway) typically have a ∂13C isotopic ratio of approximately -13‰ vs PDB whereas woody taxa have a ratio of approximately -28‰ (Peterson and Fry, 1987). ∂13C data has also been used to detect changes in plant productivity (Leng et al. 2005), or in maize agriculture activity (eg. Lane et al. 2004; Lane et al. 2009; Goman et al., 2010) because of the shift in sedimentary isotopic ratio when forests (C3) are cleared for cultivation of C4 plants. Stable isotope and carbon/nitrogen analysis was conducted on 2cc samples and procedures followed from Lane et al. (2004). Samples were analyzed at the Cornell Stable Isotope Lab (COIL) using a Finnigan MAT Delta Plus isotope ratio mass spectrometer (IRMS).

## 4. Results

### 4.1 Chronology and Stratigraphic Correlation

Nine AMS 14C dates were obtained for LOMC1 and LOMC2 (Table 1). The measured RC ages ranged from 130BP to 3120BP. Unfortunately bulk lake sediment samples from LOM returned radiocarbon ages much older and not in chronological sequence than those from the plant macrofossils, but this is attributed to the hardwater effect, whereby lakes in carbonate-rich environments produce inconsistent dates due to carbonate present in the sediment, groundwater or lake water (Deevy et al. in 1954, Broecker and Walton, 1959; Ogden, 1967; Andree et al., 1986; Saarnisto, 1988). Hardwater is a major concern at LOM, as the bedrock surrounding the lake is primarily limestone and limestone-lutite-gysum, and much of the lake sediment in comprised of greater than 20% carbonate content. Under these conditions, the magnitude of error for bulk radiocarbon dating of North American lakes is commonly 500-2000 years, and as much as 8000 years (Grimm et al. 2009). The greatest errors tend to occur in small, deep lakes due to the slower mixing of $CO_2$ within the water body, and in sediments with low organic content (Turner et al. 1983), both characteristic of LOM. Considering the regional geology, low organic content of the lake sediment, high carbonate percentage of the lake sediment, and slow $CO_2$mixing regime at LOM, we reject the bulk sedimentary dates. The carbon reservoir at LOM varies greatly with depth and ranges from approximately 250 - 3000 years.

For this reason, the age-model was based on a linear interpolation of the three AMS 14C dates from plant macrofossils, all from LOMC2. The resulting age-model for LOMC2 suggests a rapid rate of sedimentation of approximately 0.84cm/yr between 0-200cm and 0.31cm/yr from 200-290cm and a basal age of 1490 ±117 CE (Figure 4). The proposed rapid sedimentation rate is further supported by the low 210Pb activity in the surface lake sediment of LOMC1. The rapid rate of sedimentation at LOM suggested by the AMS RC dates of plant macrofossils allows for sub-decadal scale resolution.

Correlation of LOMC1 and LOMC2 (Figure 5) utilizes stratigraphic markers including a sharp contact at 1767 ± 68 CE (C1: 138cm; C2: 200cm), and high-resolution magnetic susceptibility data. Charcoal and Loss-on-ignition data show a high degree of correlation and strongly support the proposed chronology. Additionally, a deposit of coarse sand underlies the basal sediments of both cores, suggesting the lateral continuity of basal sediments.

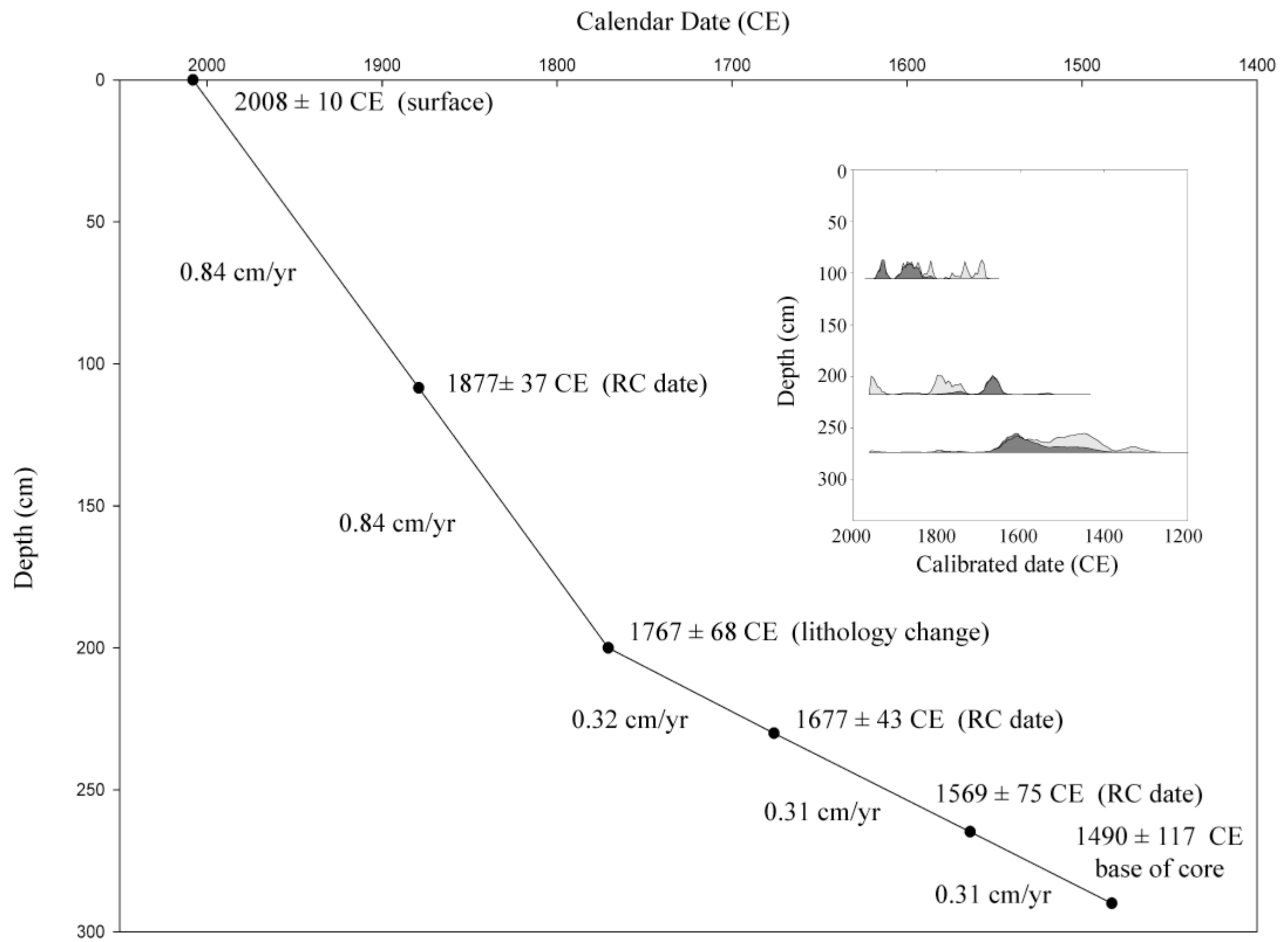


Figure 4. LOM Core 2 Age-Depth plot sediment accumulation rate based on the proposed Poisson deposition model. Dates are mean probabilities of model data ± 1 standard deviation. The inset (top right) shows the probability distributions of calibrated ages used in generation of the model. The lithology change at 200cm was determined from sediment classification and geochemical data.

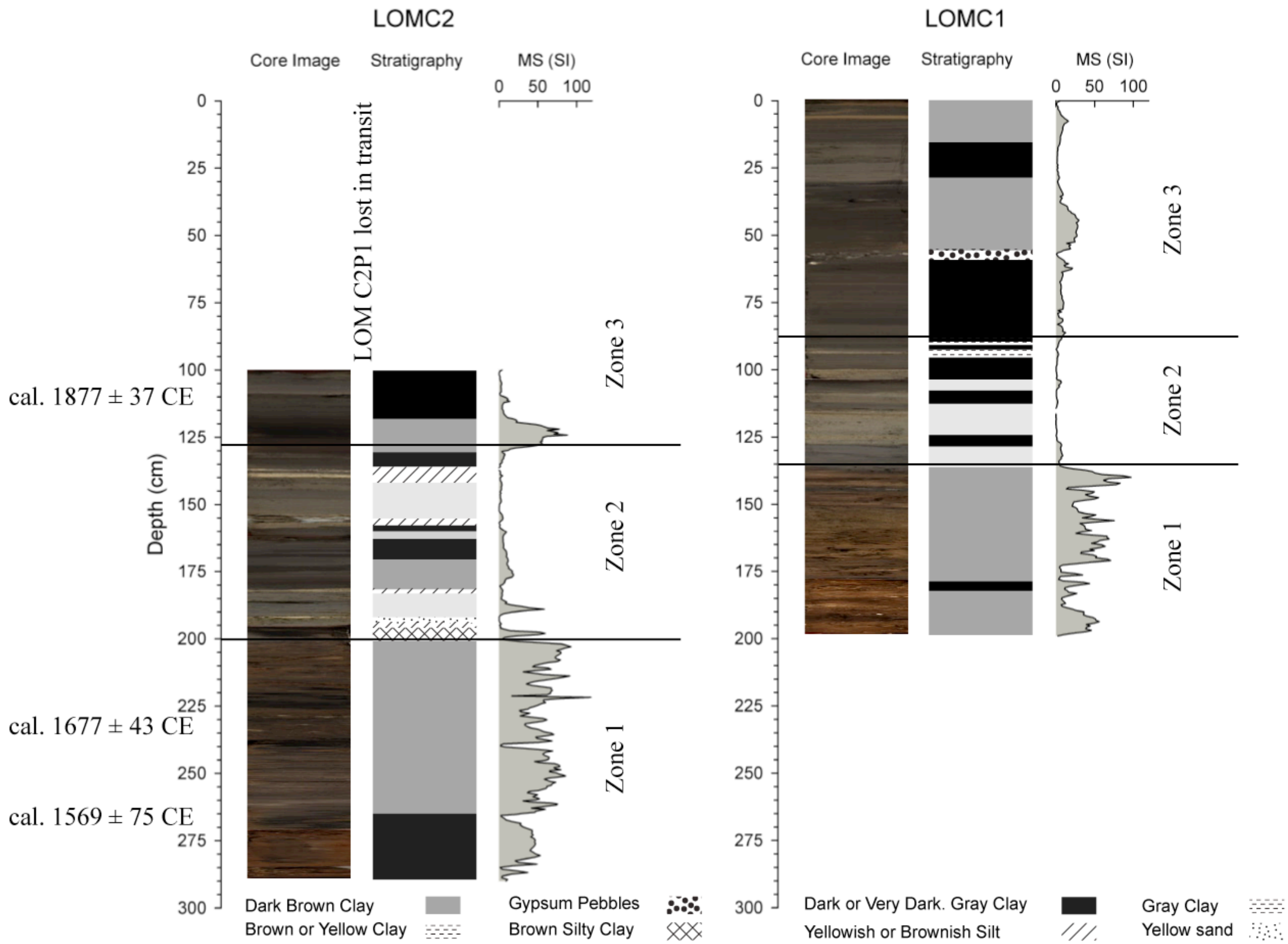


Figure 5. Stratigraphy and correlation of LOMC1 and LOMC2. Calendar dates for LOMC2 are based on Poisson deposition model.

4.2 Sediment Lithostratigraphy (Figure 5)

Sediments from both cores are predominantly medium to thinly bedded clay and silty-clay clastics with bedding planes punctuated by several thin beds of mm-scale precipitated carbonates and one bed comprised of gypsum pebbles (as determined by reaction with HCL). The basal sediment lies above a deposit of coarse sand, which was observed but could not be recovered. The sediments exhibit sharp contacts in both lithology and color, providing a clear basis for both stratigraphic correlation of the cores, and for dividing the sediment into three lithostratigraphic zones; Zone 1: 1490 ±117 CE - 1767 ± 68 CE, Zone 2: 1767 ± 68 CE - 1877 ± 37 CE, and Zone 3: 1877 ± 37 CE to present. These zones correspond to depths of 199cm - 138cm; 138cm - 87cm; 87cm - surface for LOM C1 and 290cm - 200cm; 200cm - 127cm; 127 - 100 cm for LOM C2 (due to missing segment LOMC2P1).

The sediment of zone 1 is predominantly Dark Grayish Brown or Dark Yellowish Brown Clay for both cores. There is approximately 20cm of dark grey and very dark gray clay at the base of LOMC2, and LOMC1 has a <5cm section of dark grey and very dark gray clay at approximately 180cm. In zone 2, there are several small to medium beds of yellowish or brownish silt, as well gray clay. In LOMC1, the base of zone 2 is comprised of grayish brown silty clay and a thin bed of grayish yellow sand. Zone 3 is mostly dark gray or very dark gray clay at the bottom of the zone, and mostly dark grayish brown or dark yellowish brown clay near the top of the core. A thin bed of gypsum pebbles occurs in LOMC1 at 57cm depth.

4.3 Geochemical Data (Figures 6 and 7)

*Magnetic Susceptibility*

The variation in magnetic susceptibility strongly correlates with the core lithology. MS

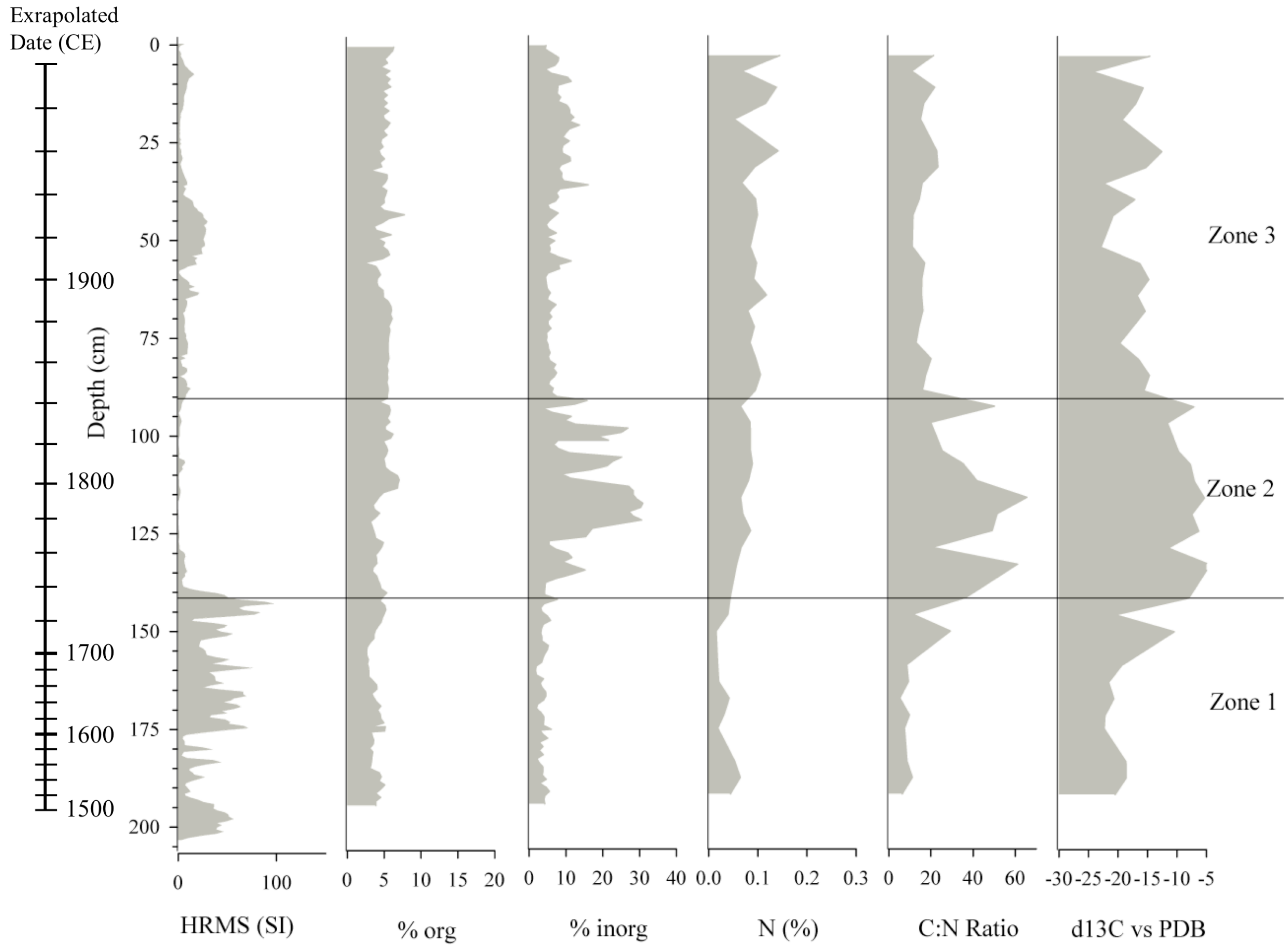


Figure 6. LOMC1 Geochemical Indices by depth and extrapolated age. Chronology for LOMC1 extrapolated from LOMC2 Poisson deposition model.

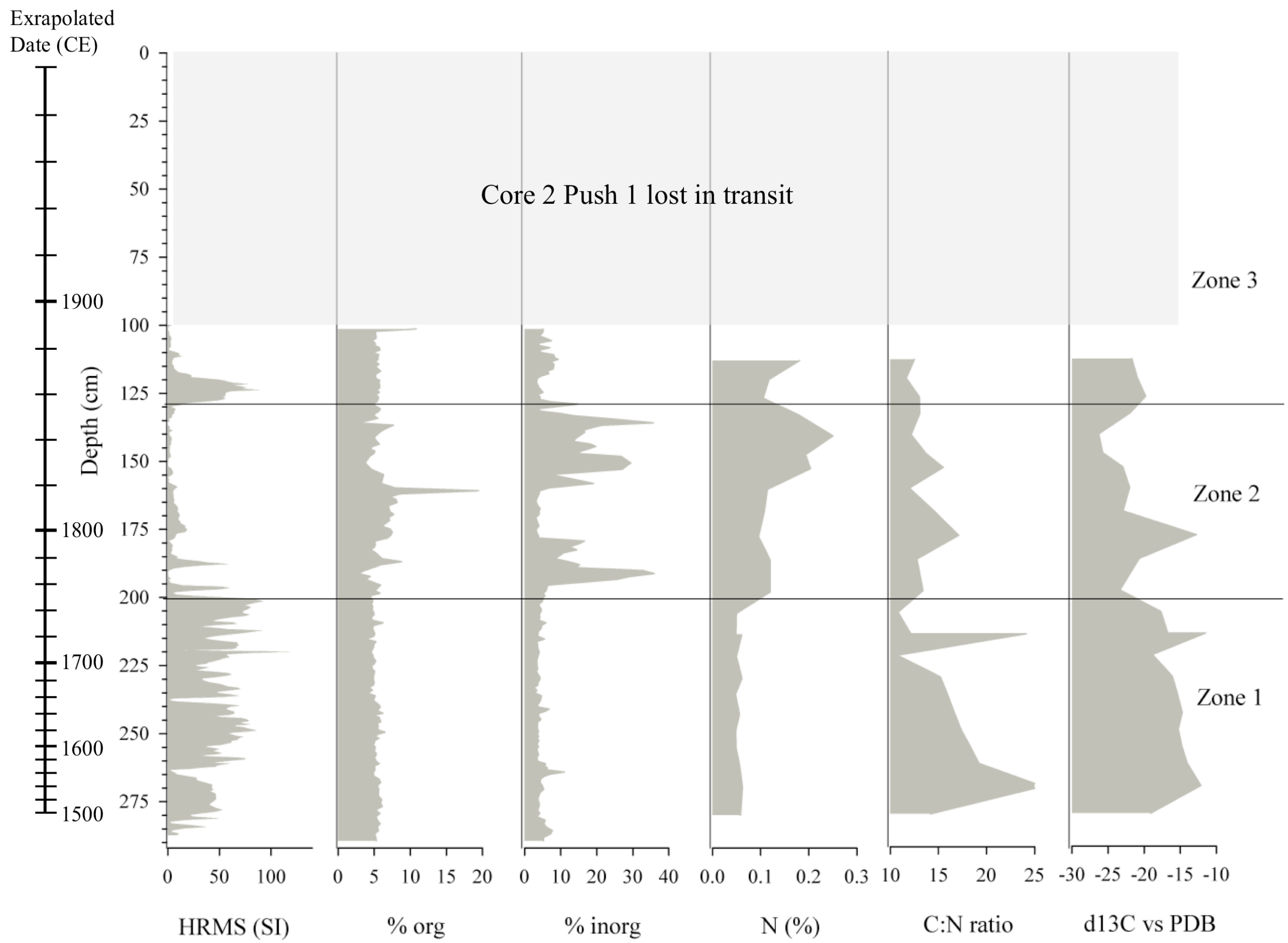


Figure 7. LOMC2 Geochemical Indices by depth and extrapolated age. Chronology extrapolated from Poisson deposition model.

values are low (5-10 SI) for the basal sediment, but rapidly increase to approximately 50 SI, then remain high but variable throughout zone 1. MS sharply decreases at the beginning of zone 2. MS remains low throughout zone 2 and zone 3 with the exception of two temporally short excursions present in LOMC2 at approximately 185cm and 125cm) and in LOMC1 at 50cm and 7cm.

*Loss on Ignition Data*

Percent organic carbon (%org) remains constant between 4-6% for most of zone 1, except for an outlier sample from topmost sediment of LOMC2. Percent inorganic carbon (%inorg) remains approximately 5% throughout Zone 1. In zone 2 %inorg levels are at a maximum. Several %inorg peaks of >25% occur in 5-10cm beds dominated by precipitated carbonate. These beds are visible in the core images as cm-scale silty layers, and under the dissecting microscope, mm-scale fibrous carbonate precipitates are observed to dominate sediment from these layers. In zone 3, %org is approximately 5% throughout, and %inorg fluctuates between 4.5% and 16% with the highest values occurring in the top ~40cm of C1.

*Carbon isotopes*

The ∂13C ratio differs greatly between C1 and C2. For LOMC1 the ∂13C ratio is generally depleted (-18 and -22 ‰ vs pdb) for the bottom half of zone 1 but becomes enriched near the transition to zone 2. C1 remains highly enriched throughout zone 2 with the ∂13C ratio ranging between -5 and -10‰ for most of zone. In zone 3, the variability of ∂13C values increased and ratios alternate between an enriched state (-12 to -16‰) and a depleted state (-19 to -24‰). LOMC2 is enriched near the base of the core (-20 to -25‰) and transitions to a depleted state by the middle of zone 2 (approximately -15‰).

*Percent Nitrogen of Sediment (%N)*

In zone 1, the %N was low for both cores, ranging between 0.015-0.065% in C1 and 0.045-0.06% in C2. %N greatly increased at the beginning of zone 2 in both cores to more than double the level in zone 1. The %N continued to increase in zone 3, especially in the top 30cm of core 1.

*Carbon: Nitrogen Ratio (C:N)*

Similar to the ∂13C ratio, the C:N ratio differed greatly between LOMC1 and LOMC2. C:N ratio was low (< 20) for C1 for the majority of zone 3, but increased to C:N > 40 in the lower part of zone 2, while for C2, C:N remained low throughout ( C:N < 20). During zone 2, C:N fluctuated greatly for C1, alternating between high C:N (> 50) and C:N of approximately 20. For C2, C:N continued to decrease from approximately 25 at the top of zone 2 to between 10-15 at the top of the zone. In zone 3, C:N was between 10-20 for C1 and 10-15 for C2.

4.4 Biological Data (Figures 8, 9, and 10)

*Charcoal*

The charcoal accumulation rate (CHAR) was lower in C1 (0-40 $cm^2$/yr) than C2 (0-120 $cm^2$/yr), but exhibited similar overall trends. CHAR was generally low from the base of the core until the middle of zone 1, and then increased through the middle of zone 2 in both cores. CHAR was lower overall for the second half of zone 2 through the top of the core, but low CHAR periods were punctuated by several periods of rapid charcoal deposition in C1. Charanalysis identified 12 fire events in LOMC1, 2 in zone 2 and 10 in zone 3. Most fires events occurred in two periods: approximately 1958-2008 CE (6 fires) and approximately 1864-1902 CE (4 fires)

*Seeds*

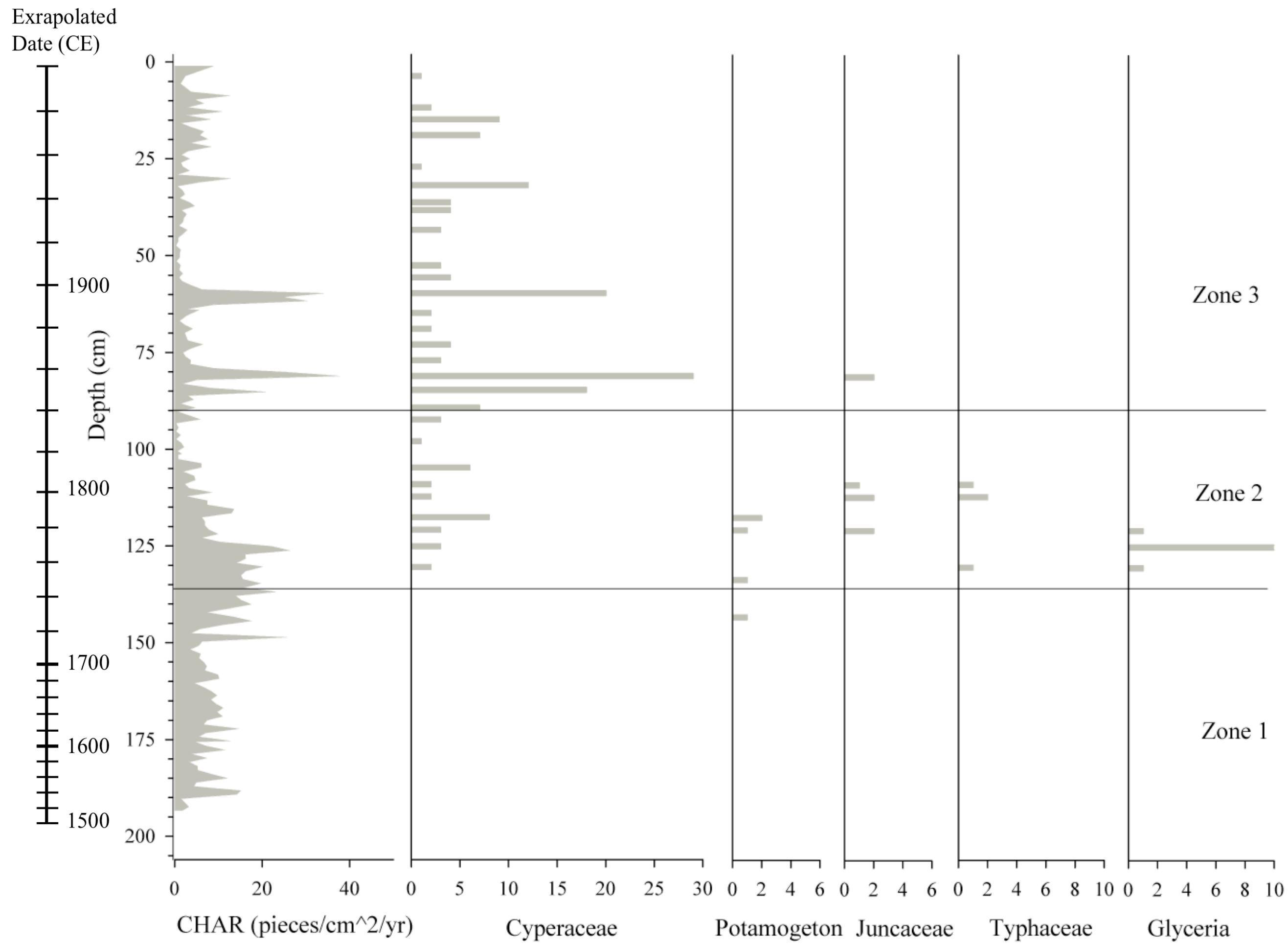


Figure 8. LOMC1 Biological Indices by depth and extrapolated age. Chronology for LOMC1 extrapolated from LOMC2 Poisson deposition model.

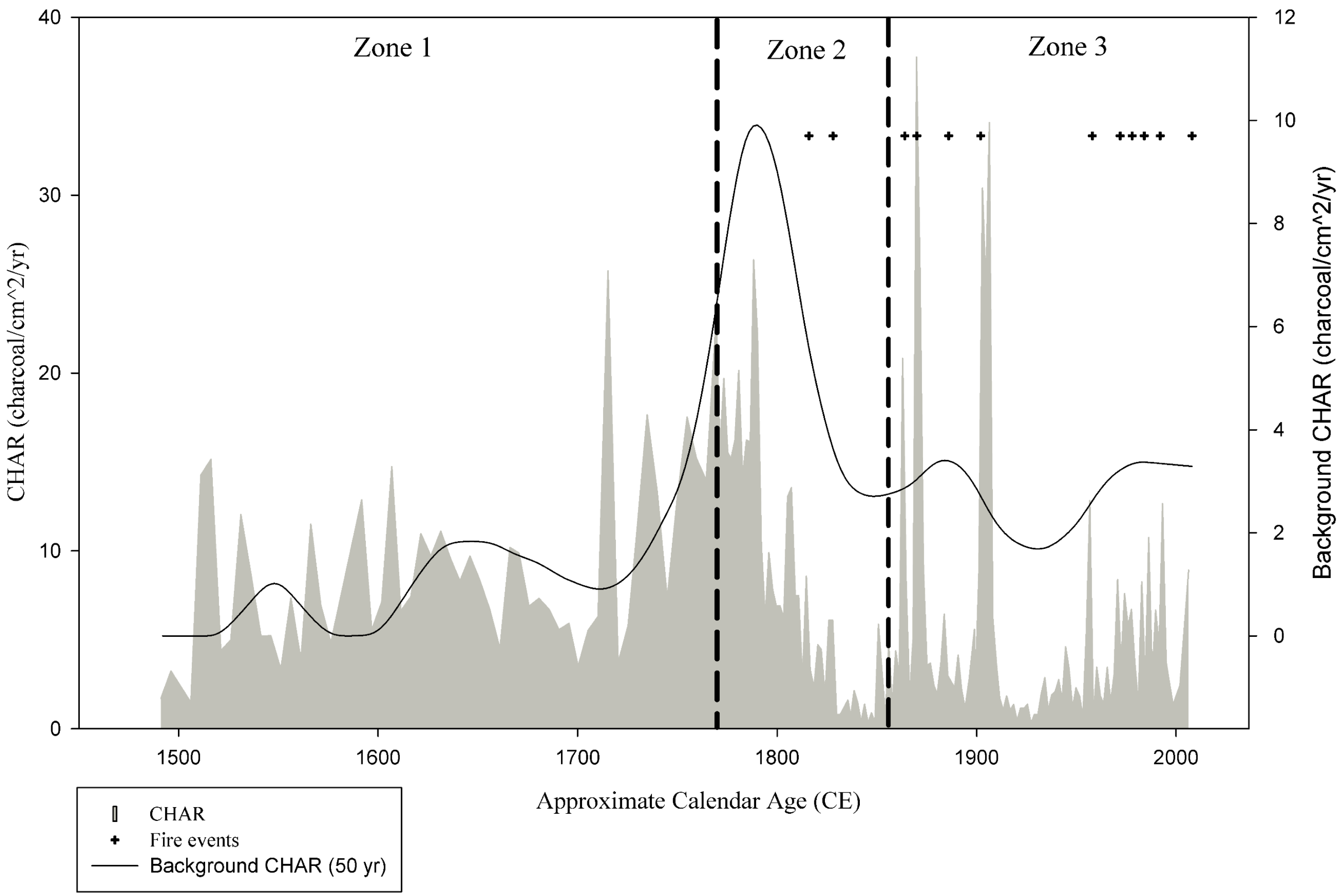


Figure 10. LOMC1 Charcoal Accumulation Rates and Fire Events. Chronology for LOMC1 extrapolated from LOMC2 Poisson deposition model.

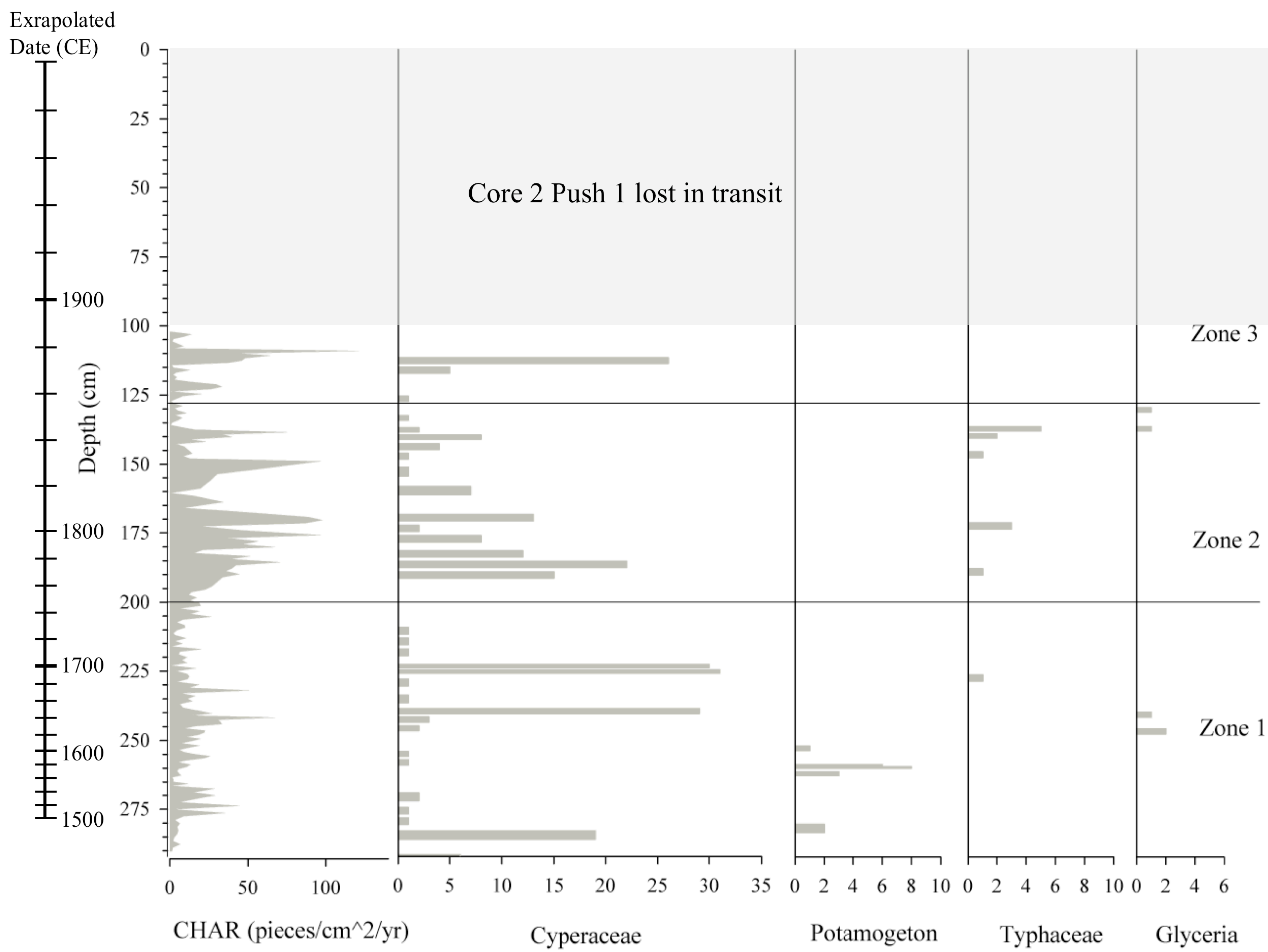


Figure 9. LOMC2 Biological Indices by depth and extrapolated age. Chronology extrapolated from Poisson deposition model

Seeds from five aquatic or wetland plant taxa of were identified with Cyperaceae the most common in both cores. Cyperaceae seeds were identified throughout C2, and in the lower half of C1. *Potamogeton*, Typhaceae, and Poaceae were present in the lower half of C1, and Juncaceae in the middle of C1. Typhaceae was identified in the middle and lower section of Zone 2 in C2, and Poaceae in near the top of the zone. Seed diversity was greatest in zone 2 and decreased in zone 3 with Cyperaceae and Juncaceae seeds present only in the bottom of the zone.

## 5. Interpretation

### 5.1 Zone 1, 1490 ± 117CE - 1767 ± 68 CE

The exceptionally high magnetic susceptibility throughout the zone, a proxy for erosion (Thompson and Oldfield, 1986), suggests that this period was marked by catchment disturbance. The carbon isotopic data is conflicting between the cores but the slight trend toward greater depletion of ∂13C values suggests forest expansion overall. With catchment instability, erosion typically increases, but the radiocarbon chorology suggests a lower sedimentation rate during this period. Median grain size of sediment in both cores varies very little throughout the sedimentary record (~4.5-6.5μm), so it is unlikely that the Tlapaneco River migrated as far as LOM at any period.

The low charcoal accumulation rate throughout zone 1 likely indicates a limited level of agricultural intensity as charcoal accumulation rate is typically linked with burning for agriculture (Patterson et al. 1987; Clement and Horn, 2001). However, periodic increases in the charcoal accumulation rate during this period suggest persistent agricultural activities despite population losses. The basal sediments of LOM, c. 1490CE, lie in the pre-colonial era. The region began to experience population loss near the time the basal sediments were deposited, and regional population continued to decline until a nadir at approximately 1625CE. After 1625, many settlements abandoned during the population decrease were reoccupied (Gerhard, 1993).

5.2 Zone 2, 1767 ± 68 CE - 1877 ± 37 CE

Exceptionally low magnetic susceptibility during this period provides evidence for a stable catchment, however, the sedimentation rate increased. The change in sediment color at the beginning of zone 2 may be the result of progressive erosion of upland terrain to an unweathered soil horizon, or may reflect a transition to plough agriculture (Ohara et al. 1993). CHAR is exceptionally high during zone 2, particularly in the lower to middle part of the zone. Increased CHAR during this period likely indicates resurgence in agricultural activity near the lake. As with zone 1, the carbon isotopic data is conflicting between the cores, with core 1 suggesting an increase in C4 taxa (grassland or maize agriculture) and core 2 suggesting an increase in C3 taxa (forest expansion). The seed data exhibits more diversity than other zones, especially for wetland taxa, which may have resulted from a fall in lake level that moved the shoreline closer to the core site. Additionally, the increase in total nitrogen during Zone 2 may have had environmental impacts for LOM. Percent nitrogen in lacustrine sediment may be increased by the addition of nitrogen from the watershed to the lake basin from fertilizers or animal waste (Carpenter et al. 1998), thus the nitrogen increase could have been driven by an increase in domesticated animals near the lake.

Percent inorganic carbon rapidly increased to >15%, and sometimes >30% at several times during the zone during precipitation of mm-scale fibrous carbonates. A possible source of episodic increases in carbonate precipitates is evaporative precipitation of carbonate resulting from fall in lake level (Bradbury, 2000; Eugster and Hardie, 1978). This occurs in closed basins when the hydrologic precipitation/evaporation balance is negative and carbonates are concentrated within the lake basin. Algal growth is also known cause carbonate precipitation (Leng et al. 2006; Valero-Garces et al. 1995) so it is possible that increased algal productivity was a contributor to or even the source of increased %inorg. However, C/N of LOM was very high during carbonate deposition in core 1 and C/N ratios >20 typically indicate high input of terrestrial organic matter whereas values <10 often result from high algal productivity (Meyers, 1994; Meyers and Lallier-Verges, 1999).

### 5.3 Zone 3, 1856CE - Present

The most recent period is marked by relatively high catchment stability, as indicated by low magnetic susceptibility. The one exception to this trend, occurring at the beginning of the zone, may be related to forest clearance, evidenced by enrichment of ∂13C at the end of Zone 2. The ∂13C ratio appears to show alternation between landscapes dominated by C4 (grassland/agriculture) and C3 (woody) taxa respectively. CHAR is somewhat lower overall in Zone 3 but fire event frequency increased during this period. The increase in larger fires may be related to the multiple transitions between forest and grassland/agriculture indicated by the ∂13C record. Nitrogen enrichment continued in zone 3, but exhibited more variability. %N closely follows the C3/C4 alternation with ∂13C enrichment corresponding to higher %N. The cessation of carbonate precipitation events probably signals a return to more stable lake levels.

## 6. Discussion

### 6.1 Landscape History

The rapid rate of sedimentation at LOM suggested by the AMS RC dates of plant macrofossils (approximately 0.31-0.84cm/year) allows for sub-decadal scale resolution, which is much greater temporal than most records from Central and Southern Mexico. Even the most high-resolution studies from the region (e.g. Caballero et al. 2006; Davies et al. 2004) have achieved only multi-decadal to centennial resolution, and only one study, a varve chronology from Central Mexico, has achieved sub-decadal resolution (Kienel et al. 2009).

Data from LOM provide insights into the impacts of a changing landscape at the study site. The record from LOM includes the period before the Spanish arrival, so it is a valuable source to assess whether erosion increased during the occupation. The findings of this record are consistent with the work of Fisher (2003) and Elliot (2010), whereby the MS-derived erosion intensity at LOM is inversely proportional to the indigenous population during the early colonial period, and suggests landscape stabilization in the mid 18th century when the local population recovered. Abandonment appears the most likely cause of catchment instability at LOM, as there is documentation of major population losses in the Tlapa region concurrent with high MS. Furthermore, the nearby (<1km) terraced archeological sites including "Huamuxtitlan-Tecoapa" and "Huamuxtitlan Plaza Vieja" (Gutierrez, 2002) would be susceptible to decay without maintenance. The relatively low CHAR concentration during the population loss and recovery may indicate diminished agricultural intensity, further supporting the abandonment hypothesis.

The overall trend in charcoal at LOM, whereby the CHAR flux generally increases after approximately 1700CE is consistent with the work from Dull et al. (2010) that showed a low rate of charcoal accumulation during and immediately after population losses in Mesoamerica, but a increase beginning in the mid-18th century. In particular, their record from Lago Herradura suggests a major increase in CHAR during this period. Similarly, Marlon et al. (2009) observed a slight increase in charcoal influx for Central and South American sites from 1600CE to present. However, the LOM CHAR record contrasts with the trend of lower CHAR from the early 18th century-present found by Conserva and Byrne (2002) and the consistent charcoal influx before and after Spanish contact found by Figeuroa-Rangel et al. (2010). This regional variability confirms the great need for local charcoal records to accurately interpret environmental history.

The likely source of charcoal in LOM is agricultural burning (eg. Clement and Horn 2001; Conserva and Byrne, 2002; Goman and Byrne, 1998; Lane et al. 2004), and other geochemical indicators can often be used to confirm this assumption. Studies have shown a strong connection between ∂13C enrichment and maize agriculture using pollen data (eg. Lane et al. 2004; Lane et al. 2009; Goman et al., 2010), and the ∂13C at LOM does provide evidence of isotopic enrichment during periods with increased charcoal flux. However, the carbon isotope data is inconsistent between core 1 and core 2 for much of the record, possibly due to the local depositional environment. Specifically, the proximity of the core site to wetland or floating vegetation such as *Potamogeton* could influence the source of organic deposition. The differing seed diversity between core 1 and core 2 confirms that the sites receive different organic inputs, despite their proximity to each other. Future research on the pollen record at LOM, could help to determine the source of fluctuating ∂13C values, and solidify the relationship between charcoal and agriculture.

## 6.2 Lake History

A secondary environmental impact evident in the sedimentary record is the nutrient enrichment of LOM. Eutrophication is a well-documented problem in Mexican lakes (Alcocer and Bernal-Brooks, 2010), and the rapid increase in %N in this record provides evidence that

LOM may have experienced nutrient enrichment as early as the mid-18th century. The tripling of the % N of sediment from in the early 17th century to the 19th century may have stimulated algal growth within LOM, as nitrogen is sometimes the limiting nutrient in Mexican Lakes (Ramırez-Olvera et al. 2009) and very often a co-limiting nutrient (Hernandez-Aviles et al. 2001).

This trend corresponds well with the work of Davies et al. (2005) which detected nutrient enrichment in two lakes from the Central Mexican highlands beginning in the mid-18th century, and Taylor (2011) who saw nitrogen concentrations increase after about 600BP (though the record only extends to approximately 400BP). The observed nitrogen enrichment may reflect an increased concentration of animals near the lake. The impact of animals on the landscape has been a topic of much debate (Butzer and Butzer, 1997; Melville, 1994), and the record from LOM is well situated to produce comparisons to pre-Hispanic conditions. The nitrogen data from LOM suggest a similar to result to Berrio et al. (2006), a nearby lake (<100km west of LOM). In this study, the authors observed eutrophication in the lake basin to following the Spanish introduction of domesticated animals using fungal spores to detect the presence of domesticated animals. The addition of phosphorous from animals created a nitrogen-limited environment, thereby encouraging nitrogen-fixing cynaobacteria blooms. However, without diatom assemblage data (eg. Bradbury, 2000; Davies, 2004), there is still considerable uncertainty in the trophic state of LOM. Furthermore, it seems improbable that animals were related to the previously discussed increase of erosion because the nutrient enrichment occurred mostly during a period of low MS.

## 6.3 Climate Changes

From the early 18th century to late 19th century, changes in sedimentary input to the lake appears to be most impacted by drought conditions, rather than land use changes. It is possible that this timeframe represents the peak of the LIA impacts in Central America (Jauregui, 1997), and that the LIA should produce a drier climate overall by displacing the ITCZ to the south (Dilley, 1996). Historical records tend to confirm this assumption, as drought, low crop yields and water scarcities dominate the historical period from the mid 1600's to early 1900's (O'Hara and Metcalfe, 1995; Endfield, 2007). According to O'Hara and Metcalfe (1997), conditions were most severe during the mid-late 1700's and late 1800's. These severe drought periods appear to correspond with the deposition of mm-scale carbonates precipitates at LOM at various depths between approximately 1770 and 1850CE, possibly indicating decreases in lake level. This result is similar to nearby paleolimnological studies that also detected drought conditions in the study region from the mid-18th century into the mid-early 19th century. Caballero et al. (2006) and O'Hara (1993) both attributed declines in lake level during this period to drought conditions, and Berrio et al. (2006) observed an expansion of the dry deciduous forest from ca. 725-225 cal. yr BP, suggesting a drying climate during this period. Other paleolimnological studies that suggest 18th century drought conditions in Mexico include the Hodell et al (2005b) Yucatan lake core record, Figueroa-Rangel (2010) from west central Mexico, and the Haug et al. (2003) record from the Cariaco Basin. It should be noted that not all records from this region support uniformly dry conditions in southern Mexico during the LIA. Lozano-García et al. (2007) presented data from three lakes (two from Central Mexico, one from Yucatan) that appear to show increases in water availability during the LIA attributed to less evapotranspiration due to cooler temperatures and increased winter precipitation from a greater incursion of polar air masses.

## 7. Conclusions and future work

Data from LOM shows significant impacts from drought and landscape changes during the post-Hispanic period, and provides insights at a more precise temporal scale than most studies from the region. The magnetic susceptibility record strongly suggests that the catchment around LOM has been significantly more stable over the last two centuries than from the late 16th through the mid 18th century. The significant decrease in erosion during a period of population growth is striking, and provides another example of the complexity in determining the overall impact of humans on the landscape. At LOM it appears that erosion may have resulted from the detrimental landscape impact of local abandonment in Central America following cultural upheaval. The eutrophication of the lake basin may be related to their presence of animals in the watershed overall though this should be investigated further using fungal spores, phosphorous concentration, or local records to better determine the impact of grazing animals on the landscape.

The $\delta$13C record suggests distinct periods of maize agriculture throughout the record, but the disagreement between core 1 and core 2 complicates this interpretation. The utilization of pollen archives could resolve this disagreement, and answer additional questions regarding the expansion or diminishment of upland forest from Spanish contact to the mid 18th century.

Finally, this record is an important paleoclimatic archive for the understudied period from 1500CE-present, providing further support of the assertion that the LIA was dry in Central America. Climatic changes at LOM are evidenced by lithostratigraphic and geochemical changes in the sediment indicative of fall in lake level. By demonstrating the sensitivity of lakes in Southwestern Mexico to decadal-scale changes climate, this study provides many possibilities for the future study of LIA climate in Mexico.

REFERENCES

ACUNA-SOTO, R., STAHLE, D. W., THERRELL, M. D., CHAVEZ, S. G. & CLEAVELAND, M. K. 2005. Drought, epidemic disease, and the fall of classic period cultures in Mesoamerica (AD 750-950). Hemorrhagic fevers as a cause of massive population loss. *Medical Hypotheses,* 65**,** 405-409.

ALCOCER, J. & BERNAL-BROOKS, F. W. 2010. Limnology in Mexico. *Hydrobiologia,* 644**,** 15-68.

ANDREE, M., OESCHGER, H., SIEGENTHALER, U., RIESEN, T., MOELL, M., AMMANN, B. & TOBOLSKI, K. 1986. C-14 Dating of plant macrofossils in lake sediment. *Radiocarbon,* 28**,** 411-416.

BERRIO, J. C., HOOGHIEMSTRA, H., VAN GEEL, B. & LUDLOW-WIECHERS, B. 2006. Environmental history of the dry forest biome of Guerrero, Mexico, and human impact during the last c. 2700 years. *Holocene,* 16**,** 63-80.

BRADBURY, J. P. 2000. Limnologic history of Lago de Patzcuaro, Michoacan, Mexico for the past 48,000 years: impacts of climate and man. *Palaeogeography Palaeoclimatology Palaeoecology,* 163**,** 69-95.

BROECKER, W. S. & WALTON, A. 1959. The geochemistry of C14 in fresh-water systems. *Geochimica et Cosmochimica Acta,* 16**,** 15-38.

BRONK RAMSEY, C. 2008. Deposition models for chronological records. *Quaternary Science Reviews,* 27**,** 42-60.

BRONK RAMSEY, C. 2009. Bayesian analysis of radiocarbon dates. *Radiocarbon,* 51**,** 337-360.

BRONK RAMSEY, C. 2010. *OxCal v. 4.1.5 [software]* [Online]. Available: http://c14.arch.ox.ac.uk/embed.php?File=oxcal.html.

BUTZER, K. W. & BUTZER, E. K. 1997. The 'natural' vegetation of the Mexican Bajio: Archival documentation of a 16th-century savanna environment. *Quaternary International,* 43-4**,** 161-172.

CABALLERO, M. & GUERRERO, B. O. 1998. Lake levels since about 40,000 years ago at Lake

Chalco, near Mexico City. *Quaternary Research,* 50**,** 69-79.

CABALLERO, M., ORTEGA, B., VALADEZ, F., METCALFE, S., MACIAS, J. L. & SUGIURA, Y. 2002. Sta. Cruz Atizapan: a 22-ka lake level record and climatic implications for the late Holocene human occupation in the Upper Lerma Basin, Central Mexico. *Palaeogeography Palaeoclimatology Palaeoecology,* 186**,** 217-235.

CABALLERO, M., VAZQUEZ, G., LOZANO-GARCIA, S., RODRIGUEZ, A., SOSA-NAJERA, S., RUIZ-FERNANDEZ, A. C. & ORTEGA, B. 2006. Present limnological conditions and recent (ca. 340 yr) palaeolimnology of a tropical lake in the Sierra de Los Tuxtlas, eastern Mexico. *Journal of Paleolimnology,* 35**,** 83-97.

CARPENTER, S. R., CARACO, N. F., CORRELL, D. L., HOWARTH, R. W., SHARPLEY, A. N. & SMITH, V. H. 1998. Nonpoint pollution of surface waters with phosphorus and nitrogen. *Ecological Applications,* 8**,** 559-568.

CLEMENT, R. M. & HORN, S. P. 2001. Pre-Columbian land-use history in Costa Rica: a 3000-year record of forest clearance, agriculture and fires from Laguna Zoncho. *Holocene,* 11**,** 419-426.

CONSERVA, M. E. & BYRNE, R. 2002. Late Holocene vegetation change in the Sierra Madre Oriental of central Mexico. *Quaternary Research,* 58**,** 122-129.

COOK, S. F., BORAH, W. W. & UNIVERSITY OF CALIFORNIA PRESS. 1987. *Essays in population history. Vol. III, Mexico and California,* Berkeley, University of California Press,.

CURTIS, J. H., HODELL, D. A. & BRENNER, M. 1996. Climate variability on the Yucatan Peninsula (Mexico) during the past 3500 years, and implications for Maya Cultural Evolution. *Quaternary Research,* 46**,** 37-47.

DAVIES, S. J., METCALFE, S. E., BERNAL-BROOKS, F., CHACON-TORRES, A., FARMER, J. G., MACKENZIE, A. B. & NEWTON, A. J. 2005. Lake sediments record sensitivity of two hydrologically closed upland lakes in Mexico to human impact. *Ambio,* 34**,** 470-475.

DAVIES, S. J., METCALFE, S. E., MACKENZIE, A. B., NEWTON, A. J., ENDFIELD, G. H. & FARMER, J. G. 2004. Environmental changes in the Zirahuen Basin, Michoacan, Mexico, during the last 1000 years. *Journal of Paleolimnology,* 31**,** 77-98.

DEAN, W. E. 1974. Determination of carbonate and organic-matter in calcareous sediments and sedimentary-rocks by loss on ignition - comparison with other methods. *Journal of Sedimentary Petrology,* 44**,** 242-248.

DEEVEY, E. S., GROSS, M. S., HUTCHINSON, G. E. & KRAYBILL, H. L. 1954. The natural C14 contents of materials from hard-water lakes. *Proceedings of the National Academy of Sciences of the United States of America,* 40**,** 285-288.

DEEVEY, E. S., RICE, D. S., RICE, P. M., VAUGHAN, H. H., BRENNER, M. & FLANNERY, M. S. 1979. MAYAN URBANISM - IMPACT ON A TROPICAL KARST ENVIRONMENT. *Science,* 206**,** 298-306.

DENEVAN, W. M. 1992. THE PRISTINE MYTH - THE LANDSCAPE OF THE AMERICA IN 1492. *Annals of the Association of American Geographers,* 82**,** 369-385.

DIAZ, H. F., TRIGO, R., HUGHES, M. K., MANN, M. E., XOPLAKI, E. & BARRIOPEDRO, D. 2011. SPATIAL AND TEMPORAL CHARACTERISTICS OF CLIMATE IN MEDIEVAL TIMES REVISITED. *Bulletin of the American Meteorological Society,* 92**,** 1487-+.

DILLEY, M. 1996. Synoptic controls on precipitation in the Valley of Oaxaca, Mexico. *International Journal of Climatology,* 16**,** 1019-1031.

DULL, R. A., NEVLE, R. J., WOODS, W. I., BIRD, D. K., AVNERY, S. & DENEVAN, W. M. 2010. The Columbian Encounter and the Little Ice Age: Abrupt Land Use Change, Fire, and Greenhouse Forcing. *Annals of the Association of American Geographers,* 100**,** 755-771.

ELLIOTT, M., FISHER, C. T., NELSON, B. A., GARZA, R. S. M., COLLINS, S. K. & PEARSALL, D. M. 2010. Climate, agriculture, and cycles of human occupation over the last 4000 yr in southern Zacatecas, Mexico. *Quaternary Research,* 74**,** 26-35.

ENDFIELD, G. H. 2007. Archival explorations of climate variability and social vulnerability in colonial Mexico. *Climatic Change,* 83**,** 9-38.

EUGSTER, H. P. & KELTS, K. R. 1978. Saline Lakes. *In:* LERMAN, A. (ed.) *Lakes: Chemistry, Geology, Physics.* New York: Springer.

FIGUEROA-RANGEL, B. L., WILLIS, K. J. & OLVERA-VARGAS, M. 2010. Cloud forest dynamics in the Mexican neotropics during the last 1300 years. *Global Change Biology,* 16**,** 1689-1704.

FISHER, C. T., POLLARD, H. P., ISRADE-ALCANTARA, I., GARDUNO-MONROY, V. H. & BANERJEE, S. K. 2003. A reexamination of human-induced environmental change within the Lake Patzcuaro Basin, Michoacan, Mexico. *Proceedings of the National Academy of Sciences of the United States of America,* 100**,** 4957-4962.

GERHARD, P. 1993. *A guide to the historical geography of New Spain*, University of Oklahoma Press.

GOMAN, M. & BYRNE, R. 1998. A 5000-year record of agriculture and tropical forest clearance in the Tuxtlas, Veracruz, Mexico. *Holocene,* 8**,** 83-89.

GOMAN, M., JOYCE, A. & MUELLER, R. 2005. Stratigraphic evidence for anthropogenically induced coastal environmental change from Oaxaca, Mexico. *Quaternary Research,* 63**,** 250-260.

GOMAN, M., JOYCE, A., MUELLER, R. & PASCHYN, L. 2010. Multiproxy paleoecological reconstruction of prehistoric land-use history in the western region of the lower Rio Verde Valley, Oaxaca, Mexico. *Holocene,* 20**,** 761-772.

GRIMM, E. C., MAHER, L. J. & NELSON, D. M. 2009. The magnitude of error in conventional bulk-sediment radiocarbon dates from central North America. *Quaternary Research,* 72**,** 301-308.

GUTIERREZ, G. 2002. The expanding polity: Patterns of the territorial expansion of the post-Classic senorio of Tlapa-Tlachinollan in the Mixteca-Nahuatl-Tlapaneca region of Guerrero.

HAUG, G. H., GUNTHER, D., PETERSON, L. C., SIGMAN, D. M., HUGHEN, K. A. & AESCHLIMANN, B. 2003. Climate and the collapse of Maya civilization. *Science,* 299**,** 1731-1735.

HEIRI, O., LOTTER, A. F. & LEMCKE, G. 2001. Loss on ignition as a method for estimating organic and carbonate content in sediments: reproducibility and comparability of results. *Journal of Paleolimnology,* 25**,** 101-110.

HERNANDEZ-AVILES, J. & BERNAL-BROOKS, F. 2001. The algal growth potential and algae growth-limiting nutrients from 30 of Mexico's lakes and reservoirs. *Verhandlungen Internationale Vereinigung fur Limnologie*, 3583-3588.

HIGUERA, P. E., BRUBAKER, L. B., ANDERSON, P. M., HU, F. S. & BROWN, T. A. 2009. Vegetation mediated the impacts of postglacial climate change on fire regimes in the south-central Brooks Range, Alaska. *Ecological Monographs,* 79**,** 201-219.

HIGUERA, P. E., GAVIN, D. G., BARTLEIN, P. J. & HALLETT, D. J. 2010. Peak detection in sediment-charcoal records: impacts of alternative data analysis methods on fire-history interpretations. *International Journal of Wildland Fire,* 19**,** 996-1014.

HODELL, D. A., BRENNER, M. & CURTIS, J. H. 2005a. Terminal Classic drought in the northern Maya lowlands inferred from multiple sediment cores in Lake Chichancanab (Mexico). *Quaternary Science Reviews,* 24**,** 1413-1427.

HODELL, D. A., BRENNER, M. & CURTIS, J. H. 2007. Climate and cultural history of the northeastern Yucatan Peninsula, Quintana Roo, Mexico. *Climatic Change,* 83**,** 215-240.

HODELL, D. A., BRENNER, M., CURTIS, J. H. & GUILDERSON, T. 2001. Solar forcing of drought frequency in the Maya lowlands. *Science,* 292**,** 1367-1370.

HODELL, D. A., BRENNER, M., CURTIS, J. H., MEDINA-GONZALEZ, R., CAN, E. I. C., ALBORNAZ-PAT, A. & GUILDERSON, T. P. 2005b. Climate change on the Yucatan Peninsula during the Little Ice Age. *Quaternary Research,* 63**,** 109-121.

HODELL, D. A., CURTIS, J. H., JONES, G. A., HIGUERAGUNDY, A., BRENNER, M., BINFORD, M. W. & DORSEY, K. T. 1991. Reconstruction of Caribbean climate change over the past 10,500 years. *Nature,* 352**,** 790-793.

JAUREGUI, E. 1997. Climate changes in Mexico during the historical and instrumented periods. *Quaternary International,* 43-4**,** 7-17.

JOYCE, A. A. & MUELLER, R. G. 1997. Prehispanic human ecology of the Rio Verde drainage basin, Mexico. *World Archaeology,* 29**,** 75-94.

KELLY, R. F., HIGUERA, P. E., BARRETT, C. M. & HU, F. S. 2011. A signal-to-noise index to quantify the potential for peak detection in sediment-charcoal records. *Quaternary Research,* 75**,** 11-17.

KIENEL, U., BOWEN, S. W., BYRNE, R., PARK, J., BOHNEL, H., DULSKI, P., LUHR, J. F., SIEBERT, L., HAUG, G. H. & NEGENDANK, J. F. W. 2009. First lacustrine varve chronologies from Mexico: impact of droughts, ENSO and human activity since AD 1840 as recorded in maar sediments from Valle de Santiago. *Journal of Paleolimnology,* 42**,** 587-609.

LANE, C. S., HORN, S. P. & MORA, C. I. 2004. Stable carbon isotope ratios in lake and swamp sediments as a proxy for prehistoric forest clearance and crop cultivation in the Neotropics. *Journal of Paleolimnology,* 32**,** 375-381.

LANE, C. S., HORN, S. P., MORA, C. I. & ORVIS, K. H. 2009. Late-Holocene paleoenvironmental change at mid-elevation on the Caribbean slope of the Cordillera Central, Dominican Republic: a multi-site, multi-proxy analysis. *Quaternary Science Reviews,* 28**,** 2239-2260.

LENG, M. J. & BARKER, P. A. A review of the oxygen isotope composition of lacustrine diatom silica for palaeoclimate reconstruction. 2006. Elsevier Science Bv, 5-27.

LENG, M. J., METCALFE, S. E. & DAVIES, S. J. 2005. Investigating Late Holocene climate variability in central Mexico using carbon isotope ratios in organic materials and oxygen isotope ratios from diatom silica within lacustrine sediments. *Journal of Paleolimnology,* 34**,** 413-431.

LERMAN, A. & BACCINI, P. 1978. *Lakes--chemistry, geology, physics,* New York, Springer-Verlag.

LOZANO-GARCIA, M. D. & ORTEGA-GUERRERO, B. 1994. Palynological and magnetic-susceptibility records of Lake Chalco, Central Mexico. *Palaeogeography Palaeoclimatology Palaeoecology,* 109**,** 177-191.

LOZANO-GARCÍA, M. 2007. Tracing the effects of the Little Ice Age in the tropical lowlands of eastern Mesoamerica. *Proceedings of the National Academy of Sciences,* 104**,** 16200.

MAGAÑA, V., VÁZQUEZ, J., PÉREZ, J. & PÉREZ, J. 2003. Impact of El Niño on precipitation in Mexico. *Geofisica Internacional - Mexico,* 42**,** 313-330.

MARLON, J. R., BARTLEIN, P. J., CARCAILLET, C., GAVIN, D. G., HARRISON, S. P., HIGUERA, P. E., JOOS, F., POWER, M. J. & PRENTICE, I. C. 2008. Climate and human influences on global biomass burning over the past two millennia. *Nature Geoscience,* 1**,** 697-702.

MARLON, J. R., BARTLEIN, P. J., CARCAILLET, C., GAVIN, D. G., HARRISON, S. P., HIGUERA, P. E., JOOS, F., POWER, M. J. & PRENTICE, I. C. 2009. Climate and human influences on global biomass burning over the past two millennia (vol 1, pg 697, 2008). *Nature Geoscience,* 2**,** 307-307.

MELVILLE, E. G. K. 1990. ENVIRONMENTAL AND SOCIAL-CHANGE IN THE VALLE-DEL-MEZQUITAL, MEXICO, 1521-1600. *Comparative Studies in Society and History,* 32**,** 24-53.

MELVILLE, E. G. K. 1994. *A plague of sheep: environmental consequences of the conquest of Mexico,* New York, Cambridge University Press.

MELVILLE, E. G. K. & SKOPYK, B. 2000. Disease, ecology, and the environment. *In:* MEYER, M. C. & BEEZLEY, W. H. (eds.) *The Oxford history of Mexico.* New York: Oxford University Press.

METCALFE, S. & DAVIES, S. 2007. Deciphering recent climate change in central Mexican lake records. *Climatic Change,* 83**,** 169-186.

METCALFE, S., O'HARA, S., CABALLERO, M. & DAVIES, S. 2000a. Records of late Pleistocene – - Holocene climatic change in Mexico— - A review. *Quaternary Science Reviews,* 19**,** 699-721.

METCALFE, S. E. 1995. Holocene Environmental Change in the Zacapu Basin - A Diatom-Based Record. *Holocene,* 5**,** 196-208.

METCALFE, S. E., DAVIES, S. J., BRAISBY, J. D., LENG, M. J., NEWTON, A. J., TERRETT, N. L. & O'HARA, S. L. 2007. Long and short-term change in the Patzcuaro Basin, central Mexico. *Palaeogeography Palaeoclimatology Palaeoecology,* 247**,** 272-295.

METCALFE, S. E., JONES, M. D., DAVIES, S. J., NOREN, A. & MACKENZIE, A. 2010. Climate variability over the last two millennia in the North American Monsoon region, recorded in laminated lake sediments from Laguna de Juanacatlan, Mexico. *Holocene,* 20**,** 1195-1206.

METCALFE, S. E., O'HARA, S. L., CABALLERO, M. & DAVIES, S. J. 2000b. Records of Late Pleistocene-Holocene climatic change in Mexico - a review. *Quaternary Science Reviews,* 19**,** 699-721.

METCALFE, S. E., STREET-PERROTT, F. A., BROWN, R. B., HALES, P. E., PERROTT, R. A. & STEININGER, F. M. 1989. Late holocene human impact on lake basins in central mexico. *Geoarchaeology,* 4**,** 119-141.

MEXICANO, S. G. 1981. *Carta Geológico-Minera Chilpancingo E14-8, Guerrero, Oaxaca, Puebla, Esc. 1:250,000*. Aguascalientes, Ags. México: Instituto Nacional de Estadística, Geografía e Informática (INEGI).

MEYER, M. C., SHERMAN, W. L. & DEEDS, S. M. 1999. *The course of Mexican history,* New York, Oxford University Press.

MEYERS, P. A. 1994. PRESERVATION OF ELEMENTAL AND ISOTOPIC SOURCE IDENTIFICATION OF SEDIMENTARY ORGANIC-MATTER. *Chemical Geology,* 114**,** 289-302.

MEYERS, P. A. & LALLIER-VERGES, E. 1999. Lacustrine sedimentary organic matter records of Late Quaternary paleoclimates. *Journal of Paleolimnology,* 21**,** 345-372.

O'HARA, S. L. & METCALFE, S. E. 1995. Reconstructing the climate of Mexico from historical records. *The Holocene,* 5**,** 485-490.

O'HARA, S. L., STREETPERROTT, F. A. & BURT, T. P. 1993. Accelerated soil-erosion around a Mexican highland lake caused by Pre-Hispanic agriculture. *Nature,* 362**,** 48-51.

O'HARA, S. L. A. M., S. E. 1997. The climate of Mexico since the Aztec period. *Quaternary International,* 43-4**,** 25-31.

OGDEN, J. G. 1967. Radiocarbon determinations of sedimentation rates from hard and soft-water lakes in Northeastern North America. *Quaternary paleoecology. Vol. 7. Proceedings of the VII Congress of the International Association for Quaternary Research. August - September, 1965. Boulder, Colo***,** 175-183.

PATTERSON, W. A., EDWARDS, K. J. & MAGUIRE, D. J. 1987. MICROSCOPIC CHARCOAL AS A FOSSIL INDICATOR OF FIRE. *Quaternary Science Reviews,* 6**,** 3-23.

PAVIA, E. G., GRAEF, F. & REYES, J. 2006. PDO-ENSO effects in the climate of Mexico. *Journal of Climate,* 19**,** 6433-6438.

PETERSON, B. J. & FRY, B. 1987. STABLE ISOTOPES IN ECOSYSTEM STUDIES. *Annual Review of Ecology and Systematics,* 18**,** 293-320.

PIPERNO, D. R., MORENO, J. E., IRIARTE, J., HOIST, I., LACHNIET, M., JONES, J. G., RANERE, A. J. & CASTANZO, R. 2007. Late pleistocene and holocene environmental history of the iguala valley, central balsas watershed of Mexico. *Proceedings of the National Academy of Sciences of the United States of America,* 104**,** 11874-11881.

RAMIREZ-OLVERA, M. A., ALCOCER, J., MERINO-IBARRA, M. & LUGO, A. 2009. Nutrient limitation in a tropical saline lake: a microcosm experiment. *Hydrobiologia,* 626**,** 5-13.

RANERE, A. J., PIPERNO, D. R., HOLST, I., DICKAU, R. & IRIARTE, J. 2009. The cultural and chronological context of early Holocene maize and squash domestication in the Central Balsas River Valley, Mexico. *Proceedings of the National Academy of Sciences of the United States of America,* 106**,** 5014-5018.

REDMAN, C. L. 1999. *Human impact on ancient environments,* Tucson, University of Arizona Press.

REIMER, P. J., BAILLIE, M. G. L., BARD, E., BAYLISS, A., BECK, J. W., BLACKWELL, P. G., RAMSEY, C. B., BUCK, C. E., BURR, G. S., EDWARDS, R. L., FRIEDRICH, M., GROOTES, P. M., GUILDERSON, T. P., HAJDAS, I., HEATON, T. J., HOGG, A. G., HUGHEN, K. A., KAISER, K. F., KROMER, B., MCCORMAC, F. G., MANNING, S. W., REIMER, R. W., RICHARDS, D. A., SOUTHON, J. R., TALAMO, S., TURNEY, C. S. M., VAN DER PLICHT, J. & WEYHENMEYE, C. E. 2009. INTCAL09 AND MARINE09 RADIOCARBON AGE CALIBRATION CURVES, 0-50,000 YEARS CAL BP. *Radiocarbon,* 51**,** 1111-1150.

RZEDOWSKI, J. & LAURA HUERTA, M. 1978. *Vegetación de México*, Limusa Mexico City.

SAARNISTO, M. 1986. Annually laminated lake sediments. *Handbook of Holocene Palaeoecology and*

*Palaeohydrology,* 17**,** 343.

SIMPSON, L. B. 1952. *Exploitation of land in central Mexico in the sixteenth century,* Berkeley,, University of California Press.

SMALL, R. J. O. & DE SZOEKE, S. P. 2007. The Central American midsummer drought: Regional aspects and large-scale forcing. *Journal of Climate,* 20**,** 4853-4873.

SMITH, B. D. 1997. The initial domestication of Cucurbita pepo in the Americas 10,000 years ago. *Science,* 276**,** 932-934.

TAMAYO, J., HERNANDEZ, P. & HERNANDEZ, M. 1962. Atlas geografico general de Mexico: con cartas fisicas, biológicas, demográficas, sociales, económicas y cartogra mas.

TAYLOR, Z. 2011. *Spatial Variation in Organic Carbon and Stable Isotope Composition of Lake Sediments at Laguna Zoncho, Costa Rica.* PhD, University of Tennessee.

THOMPSON, R. & OLDFIELD, F. 1986. *Environmental magnetism,* London ; Boston, Allen & Unwin.

TURNER, J. V., FRITZ, P., KARROW, P. F. & WARNER, B. G. 1983. Isotopic and geochemical composition of marl lake waters and implications for radiocarbon dating of marl lake-sediments. *Canadian Journal of Earth Sciences,* 20**,** 599-615.

VALERO GARCES, B. L., KELTS, K. & ITO, E. 1995. Oxygen and carbon isotope trends and sedimentological evolution of a meromictic and saline lacustrine system: The Holocene Medicine Lake basin, North American Great Plains, USA. *Palaeogeography Palaeoclimatology Palaeoecology,* 117**,** 253-278.

WHITLOCK, C. & LARSEN, C. 2001. Charcoal as a fire proxy. *Tracking Environmental Change Using Lake Sediments,* 3**,** 75Ð97.

WHITMORE, T. J., BRENNER, M., CURTIS, J. H., DAHLIN, B. H. & LEYDEN, B. W. 1996. Holocene climatic and human influences on lakes of the Yucatan Peninsula, Mexico: An interdisciplinary, palaeolimnological approach. *Holocene,* 6**,** 273-287.

Appendix 1.  LOMC1 Raw Charcoal, Charaphyte, Statoblast data

| Core Label | Segment depth start (cm) | Segment depth end (cm) | Core Depth (cm) | Sed rate (cm/yr) | Sample Volume ($cm^3$) | Charcoal pieces >250um | Charcoal pieces >125um | Total Charcoal | CHAR | Chara-phytes | Stato-blasts |
|---|---|---|---|---|---|---|---|---|---|---|---|
| C1P1 | 0 | 2 | 1 | 0.58 | 2 | 0 | 31 | 31 | 8.9 | 0 | 1 |
| C1P1 | 3 | 4 | 3.5 | 0.58 | 4 | 0 | 17 | 17 | 2.4 | 2 | 2 |
| C1P1 | 5 | 6 | 5.5 | 0.58 | 3 | 0 | 7 | 7 | 1.3 | 0 | 0 |
| C1P1 | 7 | 8 | 7.5 | 0.58 | 4 | 0 | 26 | 26 | 3.7 | 0 | 0 |
| C1P1 | 8 | 9 | 8.5 | 0.58 | 2.5 | 0 | 55 | 55 | 12.7 | 0 | 0 |
| C1P1 | 9 | 10 | 9.5 | 0.58 | 4 | 0 | 32 | 32 | 4.6 | 0 | 2 |
| C1P1 | 10 | 11 | 10.5 | 0.58 | 2.5 | 2 | 27 | 29 | 6.7 | 0 | 3 |
| C1P1 | 11 | 12 | 11.5 | 0.58 | 3.5 | 0 | 18 | 18 | 3 | 0 | 2 |
| C1P1 | 12 | 13 | 12.5 | 0.58 | 3 | 24 | 32 | 56 | 10.7 | 0 | 0 |
| C1P1 | 13 | 14 | 13.5 | 0.58 | 3 | 0 | 14 | 14 | 2.7 | 0 | 6 |
| C1P1 | 14 | 15 | 14.5 | 0.58 | 3 | 4 | 39 | 43 | 8.3 | 0 | 3 |
| C1P1 | 15 | 16 | 15.5 | 0.58 | 4 | 0 | 10 | 10 | 1.4 | 0 | 4 |
| C1P1 | 16 | 17 | 16.5 | 0.58 | 2.5 | 0 | 16 | 16 | 3.7 | 0 | 3 |
| C1P1 | 17 | 18 | 17.5 | 0.58 | 3 | 2 | 33 | 35 | 6.7 | 0 | 6 |
| C1P1 | 18 | 19 | 18.5 | 0.58 | 3 | 0 | 30 | 30 | 5.8 | 0 | 5 |
| C1P1 | 19 | 20 | 19.5 | 0.58 | 2.5 | 2 | 31 | 33 | 7.6 | 0 | 3 |
| C1P1 | 20 | 21 | 20.5 | 0.58 | 4 | 4 | 21 | 25 | 3.6 | 0 | 3 |
| C1P1 | 21 | 22 | 21.5 | 0.58 | 3.5 | 4 | 47 | 51 | 8.4 | 0 | 4 |
| C1P1 | 22 | 23 | 22.5 | 0.58 | 3 | 0 | 16 | 16 | 3.1 | 0 | 2 |
| C1P1 | 23 | 24 | 23.5 | 0.58 | 3 | 0 | 8 | 8 | 1.5 | 0 | 7 |
| C1P1 | 24 | 25 | 24.5 | 0.58 | 4 | 0 | 24 | 24 | 3.5 | 0 | 11 |
| C1P1 | 25 | 26 | 25.5 | 0.58 | 4 | 0 | 10 | 10 | 1.4 | 0 | 0 |
| C1P1 | 26 | 27 | 26.5 | 0.58 | 2.5 | 0 | 8 | 8 | 1.8 | 0 | 0 |
| C1P1 | 27 | 28 | 27.5 | 0.58 | 3.5 | 0 | 21 | 21 | 3.5 | 0 | 3 |
| C1P1 | 28 | 29 | 28.5 | 0.58 | 2 | 0 | 2 | 2 | 0.6 | 0 | 1 |
| C1P1 | 29 | 30 | 29.5 | 0.58 | 3.5 | 3 | 75 | 78 | 12.8 | 0 | 2 |
| C1P1 | 30 | 31 | 30.5 | 0.58 | 3.5 | 1 | 33 | 34 | 5.6 | 0 | 2 |
| C1P1 | 31 | 32 | 31.5 | 0.58 | 3.5 | 0 | 4 | 4 | 0.7 | 0 | 0 |
| C1P1 | 32 | 33 | 32.5 | 0.58 | 5 | 0 | 16 | 16 | 1.8 | 0 | 4 |
| C1P1 | 33 | 34 | 33.5 | 0.58 | 5 | 1 | 19 | 20 | 2.3 | 0 | 5 |
| C1P1 | 34 | 35 | 34.5 | 0.58 | 5 | 0 | 10 | 10 | 1.2 | 0 | 3 |
| C1P1 | 35 | 36 | 35.5 | 0.58 | 6 | 0 | 35 | 35 | 3.4 | 0 | 8 |
| C1P1 | 37 | 38 | 37.5 | 0.58 | 5 | 0 | 14 | 14 | 1.6 | 0 | 2 |

| Core Label | Segment depth start (cm) | Segment depth end (cm) | Core Depth (cm) | Sed rate (cm/yr) | Sample Volume ($cm^3$) | Charcoal pieces >250um | Charcoal pieces >125um | Total Charcoal | CHAR | Chara-phytes | Stato-blasts |
|---|---|---|---|---|---|---|---|---|---|---|---|
| C1P1 | 38 | 39 | 38.5 | 0.58 | 5 | 0 | 24 | 24 | 2.8 | 0 | 6 |
| C1P1 | 39 | 40 | 39.5 | 0.58 | 5.5 | 0 | 20 | 20 | 2.1 | 0 | 2 |
| C1P1 | 40 | 41 | 40.5 | 0.58 | 6 | 1 | 19 | 20 | 1.9 | 0 | 1 |
| C1P1 | 41 | 42 | 41.5 | 0.58 | 6 | 2 | 9 | 11 | 1.1 | 0 | 1 |
| C1P1 | 42 | 43 | 42.5 | 0.58 | 5 | 0 | 25 | 25 | 2.9 | 0 | 3 |
| C1P1 | 43 | 44 | 43.5 | 0.58 | 5 | 0 | 17 | 17 | 2 | 1 | 1 |
| C1P1 | 44 | 45 | 44.5 | 0.58 | 5 | 0 | 7 | 7 | 0.8 | 0 | 3 |
| C1P1 | 45 | 46 | 45.5 | 0.58 | 5 | 0 | 7 | 7 | 0.8 | 0 | 6 |
| C1P1 | 46 | 47 | 46.5 | 0.58 | 5.5 | 0 | 3 | 3 | 0.3 | 0 | 3 |
| C1P1 | 47 | 48 | 47.5 | 0.58 | 5 | 1 | 11 | 12 | 1.4 | 0 | 2 |
| C1P1 | 48 | 49 | 48.5 | 0.58 | 5.5 | 0 | 11 | 11 | 1.2 | 0 | 0 |
| C1P1 | 49 | 50 | 49.5 | 0.58 | 5 | 2 | 8 | 10 | 1.2 | 0 | 0 |
| C1P1 | 50 | 51 | 50.5 | 0.58 | 5 | 0 | 4 | 4 | 0.5 | 0 | 1 |
| C1P1 | 51 | 52 | 51.5 | 0.58 | 5.5 | 0 | 13 | 13 | 1.4 | 0 | 1 |
| C1P1 | 52 | 53 | 52.5 | 0.58 | 6.5 | 4 | 8 | 12 | 1.1 | 1 | 0 |
| C1P1 | 53 | 54 | 53.5 | 0.58 | 5 | 4 | 12 | 16 | 1.8 | 3 | 0 |
| C1P1 | 54 | 55 | 54.5 | 0.58 | 5 | 2 | 7 | 9 | 1 | 8 | 3 |
| C1P1 | 55 | 56 | 55.5 | 0.58 | 8 | 2 | 22 | 24 | 1.7 | 15 | 3 |
| C1P1 | 56 | 57 | 56.5 | 0.58 | 5 | 3 | 29 | 32 | 3.7 | 6 | 2 |
| C1P1 | 57 | 58 | 57.5 | 0.58 | 7 | 4 | 72 | 76 | 6.2 | 1 | 5 |
| C1P1 | 58 | 59 | 58.5 | 0.58 | 5 | 45 | 251 | 296 | 34.1 | 2 | 0 |
| C1P1 | 59 | 60 | 59.5 | 0.58 | 6.5 | 5 | 275 | 280 | 24.8 | 2 | 1 |
| C1P1 | 60 | 61 | 60.5 | 0.58 | 5 | 25 | 239 | 264 | 30.4 | 1 | 0 |
| C1P1 | 61 | 62 | 61.5 | 0.58 | 5 | 4 | 73 | 77 | 8.9 | 0 | 8 |
| C1P1 | 62 | 63 | 62.5 | 0.58 | 6 | 2 | 27 | 29 | 2.8 | 1 | 10 |
| C1P1 | 63 | 62.5 | 62.8 | 0.58 | 3.5 | 0 | 34 | 34 | 5.6 | 0 | 6 |
| C1P1 | 63.5 | 65 | 64.3 | 0.58 | 5 | 2 | 22 | 24 | 2.8 | 1 | 7 |
| C1P1 | 65 | 66 | 65.5 | 0.58 | 5 | 3 | 7 | 10 | 1.2 | 0 | 0 |
| C1P1 | 66 | 67 | 66.5 | 0.58 | 5 | 0 | 19 | 19 | 2.2 | 0 | 1 |
| C1P1 | 67 | 68 | 67.5 | 0.58 | 5 | 3 | 33 | 36 | 4.1 | 0 | 5 |
| C1P1 | 68 | 69 | 68.5 | 0.58 | 6 | 0 | 24 | 24 | 2.3 | 0 | 2 |
| C1P1 | 69 | 70 | 69.5 | 0.58 | 5 | 0 | 23 | 23 | 2.6 | 0 | 6 |
| C1P1 | 70 | 71 | 70.5 | 0.58 | 5 | 1 | 25 | 26 | 3 | 0 | 13 |
| C1P1 | 71 | 72 | 71.5 | 0.58 | 5 | 4 | 52 | 56 | 6.4 | 0 | 11 |
| C1P1 | 72 | 73 | 72.5 | 0.58 | 5 | 0 | 32 | 32 | 3.7 | 0 | 2 |

| Core Label | Segment depth start (cm) | Segment depth end (cm) | Core Depth (cm) | Sed rate (cm/yr) | Sample Volume ($cm^3$) | Charcoal pieces >250um | Charcoal pieces >125um | Total Charcoal | CHAR | Chara-phytes | Stato-blasts |
|---|---|---|---|---|---|---|---|---|---|---|---|
| C1P1 | 73 | 74 | 73.5 | 0.58 | 5 | 0 | 17 | 17 | 2 | 0 | 6 |
| C1P1 | 74 | 75 | 74.5 | 0.58 | 5 | 1 | 20 | 21 | 2.4 | 0 | 7 |
| C1P1 | 75 | 76 | 75.5 | 0.58 | 5 | 0 | 32 | 32 | 3.7 | 0 | 10 |
| C1P1 | 76 | 77 | 76.5 | 0.58 | 5 | 4 | 27 | 31 | 3.6 | 0 | 7 |
| C1P1 | 77 | 78 | 77.5 | 0.58 | 5 | 3 | 75 | 78 | 9 | 0 | 5 |
| C1P1 | 78 | 79 | 78.5 | 0.58 | 5 | 5 | 217 | 222 | 25.6 | 2 | 18 |
| C1P1 | 79 | 80 | 79.5 | 0.58 | 5 | 6 | 322 | 328 | 37.8 | 3 | 8 |
| C1P1 | 80 | 81 | 80.5 | 0.58 | 5 | 2 | 42 | 44 | 5.1 | 0 | 10 |
| C1P1 | 81 | 82 | 81.5 | 0.58 | 5.5 | 1 | 16 | 17 | 1.8 | 0 | 9 |
| C1P1 | 82 | 83 | 82.5 | 0.58 | 5 | 0 | 71 | 71 | 8.2 | 0 | 4 |
| C1P1 | 83 | 84 | 83.5 | 0.58 | 5.5 | 1 | 198 | 199 | 20.8 | 0 | 16 |
| C1P1 | 84 | 85 | 84.5 | 0.58 | 5 | 0 | 26 | 26 | 3 | 1 | 6 |
| C1P1 | 85 | 86 | 85.5 | 0.58 | 5 | 1 | 37 | 38 | 4.4 | 0 | 19 |
| C1P1 | 86 | 87 | 86.5 | 0.58 | 5 | 2 | 10 | 12 | 1.4 | 3 | 6 |
| C1P1 | 87 | 88 | 87.5 | 0.58 | 5 | 2 | 39 | 41 | 4.7 | 0 | 9 |
| C1P1 | 88 | 89 | 88.5 | 0.58 | 5 | 0 | 6 | 6 | 0.7 | 2 | 3 |
| C1P1 | 89 | 90 | 89.5 | 0.58 | 5 | 2 | 27 | 29 | 3.3 | 24 | 17 |
| C1P1 | 90 | 91 | 90.5 | 0.58 | 5 | 1 | 50 | 51 | 5.9 | 5 | 6 |
| C1P1 | 91 | 92 | 91.5 | 0.58 | 5 | 0 | 3 | 3 | 0.3 | 0 | 1 |
| C1P1 | 92 | 93 | 92.5 | 0.58 | 4.5 | 0 | 7 | 7 | 0.9 | 0 | 2 |
| C1P1 | 93 | 94 | 93.5 | 0.58 | 5 | 0 | 3 | 3 | 0.3 | 2 | 7 |
| C1P1 | 94 | 95 | 94.5 | 0.58 | 5 | 0 | 12 | 12 | 1.4 | 2 | 3 |
| C1P1 | 95 | 96 | 95.5 | 0.58 | 4.5 | 0 | 3 | 3 | 0.4 | 2 | 2 |
| C1P1 | 96 | 97 | 96.5 | 0.58 | 5 | 2 | 11 | 13 | 1.5 | 2 | 3 |
| C1P1 | 97 | 98 | 97.5 | 0.58 | 3.5 | 1 | 12 | 13 | 2.1 | 5 | 2 |
| C1P1 | 98 | 99 | 98.5 | 0.58 | 6 | 0 | 7 | 7 | 0.7 | 7 | 5 |
| C1P1 | 99 | 99.5 | 99.3 | 0.58 | 2.5 | 0 | 7 | 7 | 1.6 | 12 | 2 |
| | | | | | | | | | | | |
| C1P2 | 0 | 1 | 101.5 | 0.58 | 5 | 1 | 6 | 7 | 0.8 | 2 | 4 |
| C1P2 | 1 | 2 | 102.6 | 0.58 | 5 | 0 | 7 | 7 | 0.8 | 2 | 2 |
| C1P2 | 2 | 3 | 103.7 | 0.58 | 5 | 18 | 35 | 53 | 6.1 | 4 | 2 |
| C1P2 | 3 | 4 | 104.8 | 0.58 | 5 | 18 | 35 | 53 | 6.1 | 4 | 2 |
| C1P2 | 4 | 5 | 105.9 | 0.58 | 4 | 3 | 10 | 13 | 1.9 | 13 | 7 |
| C1P2 | 5 | 6 | 107 | 0.58 | 4 | 2 | 29 | 31 | 4.5 | 18 | 10 |
| C1P2 | 6 | 7 | 108 | 0.58 | 5 | 7 | 34 | 41 | 4.7 | 10 | 18 |

| Core Label | Segment depth start (cm) | Segment depth end (cm) | Core Depth (cm) | Sed rate (cm/yr) | Sample Volume ($cm^3$) | Charcoal pieces >250um | Charcoal pieces >125um | Total Charcoal | CHAR | Chara-phytes | Stato-blasts |
|---|---|---|---|---|---|---|---|---|---|---|---|
| C1P2 | 7 | 8 | 109.1 | 0.58 | 5 | 5 | 15 | 20 | 2.3 | 11 | 9 |
| C1P2 | 8 | 9 | 110.2 | 0.58 | 5 | 4 | 25 | 29 | 3.3 | 5 | 8 |
| C1P2 | 9 | 10 | 111.3 | 0.58 | 4.5 | 2 | 65 | 67 | 8.6 | 1 | 10 |
| C1P2 | 10 | 11 | 112.4 | 0.58 | 5 | 1 | 22 | 23 | 2.6 | 6 | 8 |
| C1P2 | 11 | 12 | 113.5 | 0.58 | 5 | 1 | 64 | 65 | 7.5 | 2 | 49 |
| C1P2 | 12 | 13 | 114.5 | 0.58 | 5 | 1 | 64 | 65 | 7.5 | 2 | 49 |
| C1P2 | 13 | 14 | 115.6 | 0.58 | 4.5 | 4 | 102 | 106 | 13.6 | 8 | 28 |
| C1P2 | 14 | 15 | 116.7 | 0.58 | 4.5 | 3 | 99 | 102 | 13 | 2 | 26 |
| C1P2 | 15 | 16 | 117.8 | 0.58 | 5 | 1 | 53 | 54 | 6.2 | 3 | 19 |
| C1P2 | 16 | 17 | 118.9 | 0.58 | 5 | 8 | 52 | 60 | 6.9 | 5 | 24 |
| C1P2 | 17 | 18 | 120 | 0.58 | 5 | 8 | 52 | 60 | 6.9 | 5 | 24 |
| C1P2 | 18 | 19 | 121 | 0.58 | 5 | 1 | 67 | 68 | 7.8 | 6 | 47 |
| C1P2 | 19 | 20 | 122.1 | 0.58 | 5 | 5 | 81 | 86 | 9.9 | 24 | 80 |
| C1P2 | 20 | 21 | 123.2 | 0.58 | 5 | 5 | 49 | 54 | 6.2 | 13 | 62 |
| C1P2 | 21 | 22 | 124.3 | 0.58 | 4.5 | 8 | 73 | 81 | 10.4 | 25 | 62 |
| C1P2 | 22 | 23 | 125.4 | 0.58 | 5 | 4 | 188 | 192 | 22.1 | 12 | 296 |
| C1P2 | 23 | 24 | 126.5 | 0.58 | 5 | 5 | 224 | 229 | 26.4 | 19 | 357 |
| C1P2 | 24 | 25 | 127.5 | 0.58 | 5 | 5 | 135 | 140 | 16.1 | 57 | 137 |
| C1P2 | 25 | 26 | 128.6 | 0.58 | 5 | 3 | 138 | 141 | 16.2 | 46 | 18 |
| C1P2 | 26 | 27 | 129.7 | 0.58 | 5 | 4 | 119 | 123 | 14.2 | 26 | 22 |
| C1P2 | 27 | 28 | 130.8 | 0.58 | 5 | 12 | 163 | 175 | 20.1 | 36 | 56 |
| C1P2 | 28 | 29 | 131.9 | 0.58 | 5 | 4 | 137 | 141 | 16.2 | 20 | 65 |
| C1P2 | 29 | 30 | 133 | 0.58 | 5 | 2 | 130 | 132 | 15.2 | 9 | 41 |
| C1P2 | 30 | 31 | 134 | 0.58 | 6 | 3 | 159 | 162 | 15.5 | 10 | 23 |
| C1P2 | 31 | 32 | 135.1 | 0.58 | 5 | 1 | 170 | 171 | 19.7 | 5 | 30 |
| C1P2 | 32 | 33 | 136.2 | 0.58 | 5 | 3 | 134 | 137 | 15.8 | 4 | 20 |
| C1P2 | 33 | 34 | 137.3 | 0.58 | 5 | 4 | 197 | 201 | 23.1 | 10 | 22 |
| C1P2 | 34 | 35 | 138.4 | 0.22 | 5 | 2 | 316 | 318 | 14 | 7 | 22 |
| C1P2 | 35 | 36 | 139.5 | 0.22 | 6 | 14 | 402 | 416 | 15.2 | 1 | 0 |
| C1P2 | 36 | 37 | 140.5 | 0.22 | 5 | 18 | 381 | 399 | 17.5 | 0 | 1 |
| C1P2 | 37 | 38 | 141.6 | 0.22 | 5 | 19 | 274 | 293 | 12.9 | 7 | 0 |
| C1P2 | 38 | 39 | 142.7 | 0.22 | 5 | 19 | 147 | 166 | 7.3 | 30 | 34 |
| C1P2 | 39 | 40 | 143.8 | 0.22 | 5 | 20 | 284 | 304 | 13.3 | 25 | 7 |
| C1P2 | 40 | 41 | 144.9 | 0.22 | 5 | 44 | 358 | 402 | 17.6 | 0 | 2 |
| C1P2 | 41 | 42 | 146 | 0.22 | 5 | 15 | 240 | 255 | 11.2 | 0 | 0 |

| Core Label | Segment depth start (cm) | Segment depth end (cm) | Core Depth (cm) | Sed rate (cm/yr) | Sample Volume ($cm^3$) | Charcoal pieces >250um | Charcoal pieces >125um | Total Charcoal | CHAR | Chara-phytes | Stato-blasts |
|---|---|---|---|---|---|---|---|---|---|---|---|
| C1P2 | 42 | 43 | 147 | 0.22 | 5 | 5 | 127 | 132 | 5.8 | 0 | 0 |
| C1P2 | 43 | 44 | 148.1 | 0.22 | 5 | 3 | 81 | 84 | 3.7 | 0 | 0 |
| C1P2 | 44 | 45 | 149.2 | 0.22 | 4 | 35 | 434 | 469 | 25.7 | 0 | 0 |
| C1P2 | 45 | 46 | 150.3 | 0.22 | 4 | 6 | 109 | 115 | 6.3 | 0 | 0 |
| C1P2 | 46 | 47 | 151.4 | 0.22 | 5 | 2 | 124 | 126 | 5.5 | 0 | 0 |
| C1P2 | 47 | 48 | 152.5 | 0.22 | 5 | 6 | 74 | 80 | 3.5 | 0 | 0 |
| C1P2 | 48 | 49 | 153.5 | 0.22 | 5 | 2 | 133 | 135 | 5.9 | 0 | 0 |
| C1P2 | 49 | 50 | 154.6 | 0.22 | 5 | 6 | 121 | 127 | 5.6 | 0 | 0 |
| C1P2 | 50 | 51 | 155.7 | 0.22 | 5 | 4 | 149 | 153 | 6.7 | 0 | 0 |
| C1P2 | 51 | 52 | 156.8 | 0.22 | 5 | 17 | 150 | 167 | 7.3 | 0 | 0 |
| C1P2 | 52 | 53 | 157.9 | 0.22 | 5 | 6 | 151 | 157 | 6.9 | 0 | 0 |
| C1P2 | 53 | 54 | 159 | 0.22 | 5 | 10 | 215 | 225 | 9.9 | 0 | 0 |
| C1P2 | 54 | 55 | 160 | 0.22 | 4.5 | 10 | 199 | 209 | 10.2 | 0 | 0 |
| C1P2 | 55 | 56 | 161.1 | 0.22 | 6 | 11 | 112 | 123 | 4.5 | 0 | 0 |
| C1P2 | 56 | 57 | 162.2 | 0.22 | 5 | 12 | 140 | 152 | 6.7 | 0 | 0 |
| C1P2 | 57 | 58 | 163.3 | 0.22 | 5 | 17 | 173 | 190 | 8.3 | 0 | 0 |
| C1P2 | 58 | 59 | 164.4 | 0.22 | 5 | 14 | 207 | 221 | 9.7 | 0 | 0 |
| C1P2 | 59 | 60 | 165.5 | 0.22 | 5 | 8 | 181 | 189 | 8.3 | 0 | 0 |
| C1P2 | 60 | 61 | 166.5 | 0.22 | 5 | 10 | 207 | 217 | 9.5 | 0 | 0 |
| C1P2 | 61 | 62 | 167.6 | 0.22 | 5 | 16 | 237 | 253 | 11.1 | 0 | 0 |
| C1P2 | 62 | 63 | 168.7 | 0.22 | 5 | 9 | 212 | 221 | 9.7 | 0 | 0 |
| C1P2 | 63 | 64 | 169.8 | 0.22 | 5 | 13 | 237 | 250 | 11 | 0 | 0 |
| C1P2 | 64 | 65 | 170.9 | 0.22 | 5 | 9 | 160 | 169 | 7.4 | 0 | 0 |
| C1P2 | 65 | 66 | 172 | 0.22 | 5 | 5 | 146 | 151 | 6.6 | 0 | 0 |
| C1P2 | 66 | 67 | 173 | 0.22 | 4.5 | 7 | 295 | 302 | 14.7 | 0 | 0 |
| C1P2 | 67 | 68 | 174.1 | 0.22 | 4 | 10 | 120 | 130 | 7.1 | 0 | 0 |
| C1P2 | 68 | 69 | 175.2 | 0.22 | 4.5 | 10 | 104 | 114 | 5.6 | 0 | 0 |
| C1P2 | 69 | 70 | 176.3 | 0.22 | 4.5 | 15 | 249 | 264 | 12.9 | 0 | 2 |
| | | | | | | | | | | | |
| C1P3 | 1 | 2 | 179.7 | 0.22 | 4 | 10 | 78 | 88 | 4.8 | 0 | 0 |
| C1P3 | 2 | 3 | 180.8 | 0.22 | 5 | 9 | 149 | 158 | 6.9 | 0 | 0 |
| C1P3 | 3 | 4 | 181.9 | 0.22 | 5 | 5 | 257 | 262 | 11.5 | 0 | 0 |
| C1P3 | 4 | 5 | 183 | 0.22 | 2 | 5 | 30 | 35 | 3.8 | 0 | 0 |
| C1P3 | 5 | 6 | 184.1 | 0.22 | 2 | 10 | 57 | 67 | 7.4 | 0 | 0 |
| C1P3 | 6 | 7 | 185.2 | 0.22 | 2.5 | 2 | 36 | 38 | 3.3 | 0 | 0 |

| Core Label | Segment depth start (cm) | Segment depth end (cm) | Core Depth (cm) | Sed rate (cm/yr) | Sample Volume ($cm^3$) | Charcoal pieces >250um | Charcoal pieces >125um | Total Charcoal | CHAR | Chara-phytes | Stato-blasts |
|---|---|---|---|---|---|---|---|---|---|---|---|
| C1P3 | 7 | 8 | 186.3 | 0.22 | 5 | 3 | 116 | 119 | 5.2 | 0 | 0 |
| C1P3 | 8 | 9 | 187.4 | 0.22 | 4 | 4 | 91 | 95 | 5.2 | 0 | 0 |
| C1P3 | 9 | 10 | 188.5 | 0.22 | 4 | 20 | 138 | 158 | 8.7 | 0 | 0 |
| C1P3 | 10 | 11 | 189.6 | 0.22 | 3.5 | 12 | 180 | 192 | 12 | 0 | 0 |
| C1P3 | 11 | 12 | 190.7 | 0.22 | 4 | 2 | 89 | 91 | 5 | 4 | 0 |
| C1P3 | 12 | 13 | 191.8 | 0.22 | 4 | 6 | 74 | 80 | 4.4 | 0 | 0 |
| C1P3 | 13 | 14 | 192.9 | 0.22 | 4 | 8 | 268 | 276 | 15.1 | 0 | 0 |
| C1P3 | 14 | 15 | 194 | 0.22 | 4 | 8 | 252 | 260 | 14.3 | 3 | 0 |
| C1P3 | 15 | 16 | 195.1 | 0.22 | 4 | 0 | 27 | 27 | 1.5 | 0 | 0 |
| C1P3 | 17 | 18 | 197.3 | 0.22 | 4 | 2 | 57 | 59 | 3.2 | 0 | 0 |
| C1P3 | 18 | 19 | 198.4 | 0.22 | 5 | 1 | 38 | 39 | 1.7 | 0 | 0 |

Appendix 2. LOMC2 Raw Charcoal, Charaphyte, Statoblast data

| Core Label | Segment depth start (cm) | Segment depth end (cm) | Core Depth (cm) | Sed rate (cm/yr) | Sample Volume ($cm^3$) | Charcoal pieces >250um | Charcoal pieces >125um | Total Charcoal | CHAR | Chara-phytes | Stato-blasts |
|---|---|---|---|---|---|---|---|---|---|---|---|
| c2p2 | 1 | 2 | 101.3 | 0.84 | 2.5 | 1 | 2 | 3 | 1 | 0 | 15 |
| c2p2 | 2 | 3 | 102.2 | 0.84 | 2 | 0 | 33 | 33 | 13.9 | 0 | 15 |
| c2p2 | 3 | 4 | 103 | 0.84 | 3 | 3 | 31 | 34 | 9.5 | 1 | 0 |
| c2p2 | 4 | 5 | 103.9 | 0.84 | 2.5 | 0 | 7 | 7 | 2.4 | 5 | 2 |
| c2p2 | 5 | 6 | 104.8 | 0.84 | 5 | 4 | 5 | 9 | 1.5 | 7 | |
| c2p2 | 7 | 8 | 106.5 | 0.84 | 2.5 | 0 | 26 | 26 | 8.7 | 5 | 1 |
| c2p2 | 8 | 9 | 107.3 | 0.84 | 3.5 | 0 | 13 | 13 | 3.1 | 0 | |
| c2p2 | 9 | 10 | 108.2 | 0.84 | 2 | 10 | 278 | 288 | 121 | 0 | 2 |
| c2p2 | 10 | 11 | 109.1 | 0.84 | 3 | 13 | 142 | 155 | 43.4 | 2 | 0 |
| c2p2 | 11 | 12 | 109.9 | 0.84 | 4 | 10 | 295 | 305 | 64.1 | 0 | 0 |
| c2p2 | 12 | 13 | 110.8 | 0.84 | 4 | 2 | 227 | 229 | 48.1 | 3 | |
| c2p2 | 13 | 14 | 111.7 | 0.84 | 4 | 26 | 193 | 219 | 46 | 0 | 0 |
| c2p2 | 14 | 15 | 112.5 | 0.84 | 4 | 19 | 156 | 175 | 36.8 | 0 | 1 |
| c2p2 | 15 | 16 | 113.4 | 0.84 | 4 | 1 | 5 | 6 | 1.3 | 0 | |
| c2p2 | 16 | 17 | 114.3 | 0.84 | 3.5 | 0 | 10 | 10 | 2.4 | 0 | 4 |
| c2p2 | 17 | 18 | 115.1 | 0.84 | 3 | 5 | 41 | 46 | 12.9 | 1 | 3 |
| c2p2 | 18 | 19 | 116 | 0.84 | 3.5 | 0 | 17 | 17 | 4.1 | 0 | 4 |
| c2p2 | 19 | 20 | 116.8 | 0.84 | 4 | 5 | 5 | 10 | 2.1 | 7 | |
| c2p2 | 20 | 21 | 117.7 | 0.84 | 5 | 3 | 24 | 27 | 4.5 | 3 | 0 |
| c2p2 | 21 | 22 | 118.6 | 0.84 | 4 | 0 | 14 | 14 | 2.9 | 0 | 0 |
| c2p2 | 22 | 23 | 119.4 | 0.84 | 3 | 11 | 36 | 47 | 13.2 | 0 | |
| c2p2 | 23 | 24 | 120.3 | 0.84 | 4.5 | 20 | 139 | 159 | 29.7 | 8 | 0 |
| c2p2 | 24 | 25 | 121.2 | 0.84 | 4 | 20 | 139 | 159 | 33.4 | 8 | 0 |
| c2p2 | 25 | 26 | 122 | 0.84 | 4 | 27 | 97 | 124 | 26 | 2 | 0 |
| c2p2 | 26 | 27 | 122.9 | 0.84 | 4 | 2 | 1 | 3 | 0.6 | 17 | |
| c2p2 | 27 | 28 | 123.8 | 0.84 | 3 | 24 | 48 | 72 | 20.2 | 32 | 0 |
| c2p2 | 28 | 29 | 124.6 | 0.84 | 3.5 | 3 | 31 | 34 | 8.2 | 14 | 28 |
| c2p2 | 30 | 31 | 126.3 | 0.84 | 5 | 1 | 4 | 5 | 0.8 | 23 | 0 |
| c2p2 | 31 | 32 | 127.2 | 0.84 | 4.5 | 0 | 12 | 12 | 2.2 | 11 | 20 |
| c2p2 | 32 | 33 | 128.1 | 0.84 | 4 | 0 | 38 | 38 | 8 | 22 | 30 |
| c2p2 | 33 | 34 | 128.9 | 0.84 | 3.5 | 0 | 13 | 13 | 3.1 | 28 | 3 |
| c2p2 | 34 | 35 | 129.8 | 0.84 | 4 | 3 | 22 | 25 | 5.3 | 1 | 3 |
| c2p2 | 35 | 36 | 130.7 | 0.84 | 4 | 9 | 42 | 51 | 10.7 | 11 | |
| c2p2 | 36 | 37 | 131.5 | 0.84 | 4 | 1 | 15 | 16 | 3.4 | 0 | |

| Core Label | Segment depth start (cm) | Segment depth end (cm) | Core Depth (cm) | Sed rate (cm/yr) | Sample Volume ($cm^3$) | Charcoal pieces >250um | Charcoal pieces >125um | Total Charcoal | CHAR | Chara-phytes | Stato-blasts |
|---|---|---|---|---|---|---|---|---|---|---|---|
| c2p2 | 37 | 38 | 132.4 | 0.84 | 5 | 3 | 44 | 47 | 7.9 | 21 | |
| c2p2 | 38 | 39 | 133.3 | 0.84 | 4.5 | 5 | 22 | 27 | 5 | 70 | |
| c2p2 | 39 | 40 | 134.1 | 0.84 | 4.5 | 1 | 7 | 8 | 1.5 | 18 | |
| c2p2 | 40 | 41 | 135 | 0.84 | 3 | 2 | 0 | 2 | 0.6 | 13 | |
| c2p2 | 41 | 42 | 135.8 | 0.84 | 4 | 6 | 28 | 34 | 7.1 | 3 | |
| c2p2 | 42 | 43 | 136.7 | 0.84 | 4 | 4 | 72 | 76 | 16 | 2 | 3 |
| c2p2 | 43 | 44 | 137.6 | 0.84 | 4.5 | 32 | 370 | 402 | 75 | 30 | |
| c2p2 | 44 | 45 | 138.4 | 0.84 | 4 | 8 | 154 | 162 | 34 | 65 | 2 |
| c2p2 | 45 | 46 | 139.3 | 0.84 | 4 | 9 | 181 | 190 | 39.9 | 6 | 0 |
| c2p2 | 46 | 47 | 140.2 | 0.84 | 3.5 | 0 | 54 | 54 | 13 | 2 | 10 |
| c2p2 | 47 | 48 | 141 | 0.84 | 4 | 9 | 101 | 110 | 23.1 | 3 | |
| c2p2 | 48 | 49 | 141.9 | 0.84 | 4.5 | 0 | 22 | 22 | 4.1 | 20 | 22 |
| c2p2 | 49 | 50 | 142.8 | 0.84 | 4.5 | 1 | 49 | 50 | 9.3 | 12 | 35 |
| c2p2 | 51 | 52 | 144.5 | 0.84 | 4.5 | 15 | 54 | 69 | 12.9 | 21 | |
| c2p2 | 52 | 53 | 145.3 | 0.84 | 5 | 0 | 85 | 85 | 14.3 | 28 | |
| c2p2 | 53 | 54 | 146.2 | 0.84 | 5 | 9 | 42 | 51 | 8.6 | 2 | 30 |
| c2p2 | 54 | 55 | 147.1 | 0.84 | 4.5 | 6 | 64 | 70 | 13.1 | 2 | 60 |
| c2p2 | 55 | 56.5 | 148.1 | 0.84 | 3 | 8 | 337 | 345 | 96.6 | 0 | |
| c2p2 | 60 | 62 | 152.7 | 0.84 | 3 | 3 | 105 | 108 | 30.2 | 67 | |
| c2p2 | 62.5 | 65 | 155.1 | 0.84 | 3.5 | 6 | 103 | 109 | 26.2 | 12 | 25 |
| | | | | | | | | | | | |
| c2p3 | 0 | 2 | 158.1 | 0.84 | 3.5 | 2 | 80 | 82 | 19.7 | 8 | |
| c2p3 | 2 | 3 | 159.7 | 0.84 | 3.5 | 0 | 2 | 2 | 0.5 | 6 | |
| c2p3 | 3 | 4 | 160.8 | 0.84 | 4.5 | 19 | 66 | 85 | 15.9 | 1 | |
| c2p3 | 4 | 5 | 161.9 | 0.84 | 3 | 1 | 87 | 88 | 24.6 | 1 | |
| c2p3 | 5 | 6 | 163 | 0.84 | 4 | 18 | 145 | 163 | 34.2 | 1 | |
| c2p3 | 6 | 7 | 164.1 | 0.84 | 5 | 3 | 122 | 125 | 21 | 1 | |
| c2p3 | 7 | 8 | 165.1 | 0.84 | 5 | 1 | 53 | 54 | 9.1 | 0 | |
| c2p3 | 8 | 9 | 166.2 | 0.84 | 5 | 6 | 221 | 227 | 38.1 | 2 | |
| c2p3 | 10 | 11 | 168.4 | 0.84 | 5 | 20 | 509 | 529 | 88.9 | 0 | |
| c2p3 | 11 | 12 | 169.5 | 0.84 | 5 | 35 | 548 | 583 | 97.9 | 0 | |
| c2p3 | 12 | 13 | 170.6 | 0.84 | 4 | 23 | 390 | 413 | 86.7 | 0 | |
| c2p3 | 13 | 14 | 171.7 | 0.84 | 4.5 | 3 | 102 | 105 | 19.6 | 0 | |
| c2p3 | 14 | 16 | 173.3 | 0.84 | 5 | 14 | 272 | 286 | 48 | 0 | |
| c2p3 | 16 | 17 | 174.9 | 0.84 | 3 | 8 | 337 | 345 | 96.6 | 0 | |

| Core Label | Segment depth start (cm) | Segment depth end (cm) | Core Depth (cm) | Sed rate (cm/yr) | Sample Volume ($cm^3$) | Charcoal pieces >250um | Charcoal pieces >125um | Total Charcoal | CHAR | Chara-phytes | Stato-blasts |
|---|---|---|---|---|---|---|---|---|---|---|---|
| c2p3 | 17 | 18 | 176 | 0.84 | 5 | 16 | 206 | 222 | 37.3 | 0 | |
| c2p3 | 18 | 19 | 177.1 | 0.84 | 5 | 33 | 303 | 336 | 56.4 | 0 | |
| c2p3 | 19 | 20 | 178.2 | 0.84 | 5 | 8 | 269 | 277 | 46.5 | 0 | |
| c2p3 | 20 | 21 | 179.3 | 0.84 | 3 | 1 | 239 | 240 | 67.2 | 24 | |
| c2p3 | 21 | 22 | 180.3 | 0.84 | 5 | 2 | 124 | 126 | 21.2 | 46 | |
| c2p3 | 22 | 23 | 181.4 | 0.84 | 5 | 1 | 91 | 92 | 15.5 | 32 | |
| c2p3 | 23 | 24 | 182.5 | 0.84 | 4 | 3 | 241 | 244 | 51.2 | 22 | |
| c2p3 | 24 | 25 | 183.6 | 0.84 | 4 | 6 | 179 | 185 | 38.9 | 20 | |
| c2p3 | 25 | 26 | 184.7 | 0.84 | 4 | 2 | 334 | 336 | 70.6 | 8 | |
| c2p3 | 26 | 27 | 185.8 | 0.84 | 5 | 12 | 240 | 252 | 42.3 | 8 | |
| c2p3 | 27 | 28 | 186.9 | 0.84 | 3.5 | 3 | 163 | 166 | 39.8 | 12 | |
| c2p3 | 28 | 29 | 187.9 | 0.84 | 1.5 | 4 | 60 | 64 | 35.8 | 3 | |
| c2p3 | 29 | 30 | 189 | 0.84 | 4.5 | 3 | 235 | 238 | 44.4 | 13 | |
| c2p3 | 30 | 31 | 190.1 | 0.84 | 3 | 3 | 118 | 121 | 33.9 | 12 | |
| c2p3 | 33 | 34 | 193.4 | 0.84 | 3.5 | 2 | 110 | 112 | 26.9 | 33 | |
| c2p3 | 34 | 35 | 194.5 | 0.84 | 3 | 2 | 79 | 81 | 22.7 | 20 | |
| | | | | | | | | | | | |
| c2p4 | 0 | 1 | 195.5 | 0.84 | 3 | 8 | 42 | 50 | 14 | 22 | |
| c2p4 | 1 | 2 | 196.5 | 0.84 | 2 | 0 | 29 | 29 | 12.2 | 12 | |
| c2p4 | 2 | 3 | 197.5 | 0.84 | 2 | 5 | 36 | 41 | 17.2 | 7 | |
| c2p4 | 3 | 4 | 198.5 | 0.84 | 2 | 4 | 27 | 31 | 13 | 7 | |
| c2p4 | 4 | 5 | 199.4 | 0.84 | 3 | 2 | 65 | 67 | 18.8 | 5 | |
| c2p4 | 5 | 6 | 200.4 | 0.31 | 3 | 9 | 183 | 192 | 19.8 | 2 | |
| c2p4 | 6 | 7 | 201.4 | 0.31 | 3 | 6 | 54 | 60 | 6.2 | 2 | |
| c2p4 | 7 | 8 | 202.4 | 0.31 | 2.5 | 5 | 148 | 153 | 19 | 2 | |
| c2p4 | 8 | 9 | 203.4 | 0.31 | 3.5 | 23 | 127 | 150 | 13.3 | 0 | |
| c2p4 | 9 | 10 | 204.4 | 0.31 | 3.5 | 6 | 292 | 298 | 26.4 | 2 | |
| c2p4 | 10 | 11 | 205.4 | 0.31 | 3.5 | 19 | 75 | 94 | 8.3 | 4 | |
| c2p4 | 11 | 12 | 206.4 | 0.31 | 3 | 7 | 37 | 44 | 4.5 | 0 | |
| c2p4 | 12 | 13 | 207.4 | 0.31 | 3.5 | 5 | 102 | 107 | 9.5 | 2 | |
| c2p4 | 13 | 14 | 208.3 | 0.31 | 3 | 5 | 91 | 96 | 9.9 | 3 | |
| c2p4 | 14 | 15 | 209.3 | 0.31 | 2 | 2 | 27 | 29 | 4.5 | 3 | |
| c2p4 | 15 | 16 | 210.3 | 0.31 | 3.5 | 1 | 26 | 27 | 2.4 | 0 | |
| c2p4 | 16 | 17 | 211.3 | 0.31 | 3 | 2 | 34 | 36 | 3.7 | 0 | |
| c2p4 | 17 | 18 | 212.3 | 0.31 | 3 | 10 | 91 | 101 | 10.4 | 1 | |

| Core Label | Segment depth start (cm) | Segment depth end (cm) | Core Depth (cm) | Sed rate (cm/yr) | Sample Volume (cm$^3$) | Charcoal pieces >250um | Charcoal pieces >125um | Total Charcoal | CHAR | Chara-phytes | Stato-blasts |
|---|---|---|---|---|---|---|---|---|---|---|---|
| c2p4 | 18 | 19 | 213.3 | 0.31 | 3.5 | 5 | 33 | 38 | 3.4 | 0 | |
| c2p4 | 19 | 20 | 214.3 | 0.31 | 4 | 12 | 92 | 104 | 8.1 | 2 | |
| c2p4 | 20 | 21 | 215.3 | 0.31 | 2.5 | 0 | 10 | 10 | 1.2 | 0 | |
| c2p4 | 21 | 22 | 216.3 | 0.31 | 2 | 11 | 119 | 130 | 20.2 | 1 | |
| c2p4 | 22 | 23 | 217.2 | 0.31 | 4 | 9 | 73 | 82 | 6.4 | 0 | |
| c2p4 | 23 | 24 | 218.2 | 0.31 | 4 | 7 | 66 | 73 | 5.7 | 0 | |
| c2p4 | 24 | 25 | 219.2 | 0.31 | 3.5 | 4 | 121 | 125 | 11.1 | 2 | |
| c2p4 | 25 | 26 | 220.2 | 0.31 | 3 | 5 | 70 | 75 | 7.8 | 0 | |
| c2p4 | 26 | 27 | 221.2 | 0.31 | 4 | 19 | 125 | 144 | 11.2 | 0 | |
| c2p4 | 27 | 28 | 222.2 | 0.31 | 3.5 | 0 | 6 | 6 | 0.5 | 0 | |
| c2p4 | 28 | 29 | 223.2 | 0.31 | 5.5 | 2 | 293 | 295 | 16.6 | 1 | |
| c2p4 | 29 | 30 | 224.2 | 0.31 | 3 | 5 | 34 | 39 | 4 | 7 | |
| c2p4 | 30 | 31 | 225.2 | 0.31 | 3 | 1 | 109 | 110 | 11.4 | 0 | |
| c2p4 | 31 | 32 | 226.1 | 0.31 | 5 | 19 | 183 | 202 | 12.5 | 0 | |
| c2p4 | 32 | 33 | 227.1 | 0.31 | 2.5 | 1 | 92 | 93 | 11.5 | 0 | |
| c2p4 | 33 | 34 | 228.1 | 0.31 | 3.5 | 4 | 48 | 52 | 4.6 | 0 | |
| c2p4 | 34 | 35 | 229.1 | 0.31 | 4 | 23 | 218 | 241 | 18.7 | 3 | |
| c2p4 | 35 | 36 | 230.1 | 0.31 | 3.5 | 22 | 114 | 136 | 12 | 0 | |
| c2p4 | 36 | 37 | 231.1 | 0.31 | 5 | 49 | 768 | 817 | 50.7 | 8 | |
| c2p4 | 37 | 38 | 232.1 | 0.31 | 3.5 | 6 | 72 | 78 | 6.9 | 0 | |
| c2p4 | 38 | 39 | 233.1 | 0.31 | 5 | 15 | 248 | 263 | 16.3 | 3 | |
| c2p4 | 39 | 40 | 234.1 | 0.31 | 4 | 12 | 135 | 147 | 11.4 | 0 | |
| c2p4 | 40 | 41 | 235 | 0.31 | 5 | 25 | 209 | 234 | 14.5 | 1 | |
| c2p4 | 41 | 42 | 236 | 0.31 | 3.5 | 12 | 60 | 72 | 6.4 | 12 | |
| c2p4 | 42 | 43.5 | 237.3 | 0.31 | 5 | 3 | 135 | 138 | 8.6 | 33 | |
| | | | | | | | | | | | |
| c2p5 | 0 | 1 | 239.4 | 0.31 | 2.5 | 6 | 211 | 217 | 26.9 | 3 | |
| c2p5 | 1 | 2 | 240.2 | 0.31 | 3 | 0 | 135 | 135 | 14 | 7 | |
| c2p5 | 2 | 3 | 240.9 | 0.31 | 4.5 | 20 | 956 | 976 | 67.2 | 20 | |
| c2p5 | 3 | 4 | 241.7 | 0.31 | 2 | 15 | 184 | 199 | 30.8 | 42 | |
| c2p5 | 4 | 5 | 242.5 | 0.31 | 3.5 | 5 | 362 | 367 | 32.5 | 49 | |
| c2p5 | 5 | 6 | 243.2 | 0.31 | 3.5 | 30 | 347 | 377 | 33.4 | 25 | |
| c2p5 | 6 | 7 | 244 | 0.31 | 5 | 22 | 237 | 259 | 16.1 | 26 | |
| c2p5 | 7 | 8 | 244.8 | 0.31 | 2.5 | 2 | 75 | 77 | 9.5 | 30 | |
| c2p5 | 8 | 9 | 245.6 | 0.31 | 2.5 | 12 | 170 | 182 | 22.6 | 5 | |

| Core Label | Segment depth start (cm) | Segment depth end (cm) | Core Depth (cm) | Sed rate (cm/yr) | Sample Volume ($cm^3$) | Charcoal pieces >250um | Charcoal pieces >125um | Total Charcoal | CHAR | Chara-phytes | Stato-blasts |
|---|---|---|---|---|---|---|---|---|---|---|---|
| c2p5 | 9 | 10 | 246.3 | 0.31 | 4 | 8 | 277 | 285 | 22.1 | 8 | |
| c2p5 | 10 | 11 | 247.1 | 0.31 | 5.5 | 23 | 308 | 331 | 18.7 | 22 | |
| c2p5 | 11 | 12 | 247.9 | 0.31 | 5 | 11 | 163 | 174 | 10.8 | 3 | |
| c2p5 | 12 | 13 | 248.6 | 0.31 | 5 | 4 | 313 | 317 | 19.7 | 7 | |
| c2p5 | 13 | 14 | 249.4 | 0.31 | 3 | 0 | 135 | 135 | 14 | 0 | |
| c2p5 | 14 | 15 | 250.2 | 0.31 | 4.5 | 4 | 101 | 105 | 7.2 | 1 | |
| c2p5 | 15 | 16 | 251 | 0.31 | 5 | 14 | 293 | 307 | 19 | 3 | |
| c2p5 | 16 | 17 | 251.7 | 0.31 | 5 | 20 | 186 | 206 | 12.8 | 3 | |
| c2p5 | 17 | 18 | 252.5 | 0.31 | 2 | 4 | 34 | 38 | 5.9 | 1 | |
| c2p5 | 18 | 19 | 253.3 | 0.31 | 7 | 12 | 189 | 201 | 8.9 | 8 | |
| c2p5 | 19 | 20 | 254 | 0.31 | 5 | 5 | 237 | 242 | 15 | 2 | |
| c2p5 | 20 | 21 | 254.8 | 0.31 | 5 | 21 | 394 | 415 | 25.7 | 14 | |
| c2p5 | 21 | 22 | 255.6 | 0.31 | 3 | 11 | 201 | 212 | 21.9 | 26 | |
| c2p5 | 22 | 23 | 256.4 | 0.31 | 5 | 24 | 136 | 160 | 9.9 | 23 | |
| c2p5 | 23 | 24 | 257.1 | 0.31 | 5 | 2 | 84 | 86 | 5.3 | 3 | |
| c2p5 | 24 | 25 | 257.9 | 0.31 | 4 | 2 | 170 | 172 | 13.3 | 0 | |
| c2p5 | 25 | 26 | 258.7 | 0.31 | 3.5 | 2 | 121 | 123 | 10.9 | 0 | |
| c2p5 | 26 | 27 | 259.4 | 0.31 | 4 | 3 | 69 | 72 | 5.6 | 3 | |
| c2p5 | 27 | 28 | 260.2 | 0.31 | 6 | 4 | 85 | 89 | 4.6 | 12 | |
| c2p5 | 28 | 29 | 261 | 0.31 | 5 | 3 | 91 | 94 | 5.8 | 12 | |
| c2p5 | 29 | 30 | 261.8 | 0.31 | 3.5 | 0 | 80 | 80 | 7.1 | 6 | |
| c2p5 | 30 | 31 | 262.5 | 0.31 | 4 | 1 | 19 | 20 | 1.6 | 0 | |
| c2p5 | 31 | 32 | 263.3 | 0.31 | 3.5 | 0 | 27 | 27 | 2.4 | 0 | |
| c2p5 | 32 | 33 | 264.1 | 0.31 | 3.5 | 3 | 22 | 25 | 2.2 | 0 | |
| c2p5 | 33 | 34 | 264.8 | 0.31 | 3.5 | 9 | 124 | 133 | 11.8 | 0 | |
| c2p5 | 34 | 35 | 265.6 | 0.31 | 4 | 0 | 13 | 13 | 1 | 1 | |
| | | | | | | | | | | | |
| c2p6 | 0 | 1 | 266.6 | 0.31 | 2 | 17 | 167 | 184 | 28.5 | 5 | |
| c2p6 | 1 | 2 | 267.9 | 0.31 | 3 | 14 | 134 | 148 | 15.3 | 6 | |
| c2p6 | 2 | 3 | 269.2 | 0.31 | 2 | 19 | 166 | 185 | 28.7 | 6 | |
| c2p6 | 3 | 4 | 270.4 | 0.31 | 3.5 | 2 | 191 | 193 | 17.1 | 6 | |
| c2p6 | 4 | 5 | 271.7 | 0.31 | 3 | 6 | 55 | 61 | 6.3 | 3 | |
| c2p6 | 5 | 6 | 272.9 | 0.31 | 3.5 | 3 | 501 | 504 | 44.6 | 7 | |
| c2p6 | 6 | 7 | 274.2 | 0.31 | 1 | 0 | 8 | 8 | 2.5 | 0 | |
| c2p6 | 7 | 8 | 275.5 | 0.31 | 3 | 5 | 335 | 340 | 35.1 | 7 | |

| Core Label | Segment depth start (cm) | Segment depth end (cm) | Core Depth (cm) | Sed rate (cm/yr) | Sample Volume ($cm^3$) | Charcoal pieces >250um | Charcoal pieces >125um | Total Charcoal | CHAR | Chara-phytes | Stato-blasts |
|---|---|---|---|---|---|---|---|---|---|---|---|
| c2p6 | 8 | 9 | 276.7 | 0.31 | 3 | 7 | 80 | 87 | 9 | 2 | |
| c2p6 | 9 | 10 | 278 | 0.31 | 4 | 2 | 41 | 43 | 3.3 | 1 | |
| c2p6 | 10 | 11 | 279.3 | 0.31 | 4 | 2 | 80 | 82 | 6.4 | 28 | |
| c2p6 | 11 | 12 | 280.5 | 0.31 | 4.5 | 7 | 61 | 68 | 4.7 | 2 | |
| c2p6 | 12 | 13 | 281.8 | 0.31 | 5 | 1 | 85 | 86 | 5.3 | 1 | |
| c2p6 | 13 | 14 | 283.1 | 0.31 | 4 | 1 | 60 | 61 | 4.7 | 2 | |
| c2p6 | 14 | 15 | 284.3 | 0.31 | 3 | 0 | 28 | 28 | 2.9 | 1 | |
| c2p6 | 15 | 16 | 285.6 | 0.31 | 1.5 | 2 | 8 | 10 | 2.1 | 1 | |
| c2p6 | 16 | 17 | 286.8 | 0.31 | 3 | 2 | 62 | 64 | 6.6 | 0 | |
| c2p6 | 17 | 18 | 288.1 | 0.31 | 4 | 0 | 23 | 23 | 1.8 | 2 | |
| c2p6 | 18 | 19 | 289.4 | 0.31 | 2.5 | 0 | 11 | 11 | 1.4 | 1 | |

Appendix 3. LOMC1 Raw Loss on Ignition Data

| Core Label | Segment depth start (cm) | Segment depth end (cm) | Overall Core Depth (cm) | Crucible (cruc) wt. (g) | Wet wt w/cruc (g) | Dry wt w/cruc (g) | After 550C w/cruc (g) | After 950C w/cruc (g) | Wet wt (g) | Dry wt (g) | % water | weight after 550C (g) | % org of dry wt | % inorg C of dry wt |
|---|---|---|---|---|---|---|---|---|---|---|---|---|---|---|
| C1P1 | 0 | 1 | 0.5 | 4.226 | 6.007 | 5.968 | 5.858 | 5.778 | 1.781 | 1.742 | 2.18978 | 1.632 | 6.31458 | 4.59242 |
| C1P1 | 1 | 2 | 1.5 | 4.826 | 6.84 | 6.791 | 6.67 | 6.584 | 2.014 | 1.965 | 2.43297 | 1.844 | 6.15776 | 4.37659 |
| C1P1 | 3 | 4 | 3.6 | 4.602 | 7.403 | 6.112 | 6.035 | 5.914 | 2.801 | 1.51 | 46.0907 | 1.433 | 5.09934 | 8.01325 |
| C1P1 | 4 | 5 | 4.6 | 4.903 | 7.09 | 7.045 | 6.928 | 6.76 | 2.187 | 2.142 | 2.05761 | 2.025 | 5.46218 | 7.84314 |
| C1P1 | 5 | 6 | 5.6 | 4.899 | 7.102 | 6.13 | 6.074 | 5.987 | 2.203 | 1.231 | 44.1217 | 1.175 | 4.54915 | 7.06742 |
| C1P1 | 6 | 7 | 6.6 | 4.644 | 6.2 | 6.162 | 6.074 | 6.008 | 1.556 | 1.518 | 2.44216 | 1.43 | 5.7971 | 4.34783 |
| C1P1 | 7 | 8 | 7.7 | 4.944 | 6.862 | 6.035 | 5.98 | 5.913 | 1.918 | 1.091 | 43.1178 | 1.036 | 5.04125 | 6.14115 |
| C1P1 | 8 | 9 | 8.7 | 4.909 | 7.154 | 6.079 | 6.011 | 5.889 | 2.245 | 1.17 | 47.8842 | 1.102 | 5.81197 | 10.4274 |
| C1P1 | 9 | 10 | 9.7 | 4.982 | 7.582 | 6.404 | 6.328 | 6.165 | 2.6 | 1.422 | 45.3077 | 1.346 | 5.34459 | 11.4627 |
| C1P1 | 10 | 11 | 10.7 | 4.944 | 6.74 | 5.891 | 5.835 | 5.761 | 1.796 | 0.947 | 47.2717 | 0.891 | 5.91341 | 7.81415 |
| C1P1 | 11 | 12 | 11.7 | 4.781 | 7.197 | 6.066 | 6.005 | 5.905 | 2.416 | 1.285 | 46.8129 | 1.224 | 4.74708 | 7.7821 |
| C1P1 | 12 | 13 | 12.8 | 4.321 | 7.254 | 5.924 | 5.837 | 5.715 | 2.933 | 1.603 | 45.3461 | 1.516 | 5.42732 | 7.61073 |
| C1P1 | 13 | 14 | 13.8 | 4.314 | 6.87 | 5.745 | 5.676 | 5.553 | 2.556 | 1.431 | 44.0141 | 1.362 | 4.8218 | 8.59539 |
| C1P1 | 14 | 15 | 14.8 | 4.848 | 6.661 | 5.841 | 5.787 | 5.709 | 1.813 | 0.993 | 45.2289 | 0.939 | 5.43807 | 7.85498 |
| C1P1 | 15 | 16 | 15.8 | 4.801 | 7.427 | 6.248 | 6.178 | 6.03 | 2.626 | 1.447 | 44.8972 | 1.377 | 4.8376 | 10.2281 |
| C1P1 | 16 | 17 | 16.8 | 5.328 | 7.368 | 6.403 | 6.342 | 6.224 | 2.04 | 1.075 | 47.3039 | 1.014 | 5.67442 | 10.9767 |
| C1P1 | 17 | 18 | 17.9 | 4.287 | 6.763 | 5.668 | 5.601 | 5.448 | 2.476 | 1.381 | 44.2246 | 1.314 | 4.85156 | 11.0789 |
| C1P1 | 18 | 19 | 18.9 | 4.837 | 7.112 | 6.108 | 6.044 | 5.889 | 2.275 | 1.271 | 44.1319 | 1.207 | 5.03541 | 12.1951 |
| C1P1 | 19 | 20 | 19.9 | 4.961 | 6.781 | 5.91 | 5.855 | 5.751 | 1.82 | 0.949 | 47.8571 | 0.894 | 5.79557 | 10.9589 |
| C1P1 | 20 | 21 | 20.9 | 4.908 | 7.149 | 6.081 | 6.017 | 5.857 | 2.241 | 1.173 | 47.6573 | 1.109 | 5.4561 | 13.6402 |
| C1P1 | 21 | 22 | 21.9 | 4.643 | 7.408 | 6.104 | 6.033 | 5.874 | 2.765 | 1.461 | 47.1609 | 1.39 | 4.85969 | 10.883 |
| C1P1 | 22 | 23 | 23 | 5.112 | 7.342 | 6.298 | 6.234 | 6.117 | 2.23 | 1.186 | 46.8161 | 1.122 | 5.39629 | 9.86509 |
| C1P1 | 23 | 24 | 24 | 4.226 | 6.818 | 5.771 | 5.699 | 5.557 | 2.592 | 1.545 | 40.3935 | 1.473 | 4.66019 | 9.19094 |
| C1P1 | 24 | 25 | 25 | 4.764 | 7.851 | 6.532 | 6.452 | 6.259 | 3.087 | 1.768 | 42.7276 | 1.688 | 4.52489 | 10.9163 |
| C1P1 | 25 | 26 | 26 | 4.933 | 6.775 | 6.028 | 5.975 | 5.873 | 1.842 | 1.095 | 40.5537 | 1.042 | 4.84018 | 9.31507 |
| C1P1 | 26 | 27 | 27 | 4.936 | 8.902 | 7.306 | 7.204 | 6.993 | 3.966 | 2.37 | 40.2421 | 2.268 | 4.3038 | 8.90295 |
| C1P1 | 27 | 28 | 28.1 | 4.367 | 7.421 | 6.175 | 6.093 | 5.929 | 3.054 | 1.808 | 40.799 | 1.726 | 4.5354 | 9.0708 |
| C1P1 | 28 | 29 | 29.1 | 4.6 | 6.095 | 5.473 | 5.429 | 5.332 | 1.495 | 0.873 | 41.6054 | 0.829 | 5.04009 | 11.1111 |
| C1P1 | 29 | 30 | 30.1 | 4.76 | 8.261 | 6.66 | 6.576 | 6.363 | 3.501 | 1.9 | 45.7298 | 1.816 | 4.42105 | 11.2105 |
| C1P1 | 30 | 31 | 31.1 | 5.292 | 8.636 | 7.168 | 7.08 | 6.917 | 3.344 | 1.876 | 43.8995 | 1.788 | 4.69083 | 8.6887 |
| C1P1 | 31 | 32 | 32.1 | 4.773 | 6.358 | 5.668 | 5.64 | 5.568 | 1.585 | 0.895 | 43.5331 | 0.867 | 3.12849 | 8.04469 |
| C1P1 | 32 | 33 | 33.2 | 4.878 | 7.454 | 6.451 | 6.366 | 6.226 | 2.576 | 1.573 | 38.9363 | 1.488 | 5.40369 | 8.90019 |

| Core Label | Segment depth start (cm) | Segment depth end (cm) | Overall Core Depth (cm) | Crucible (cruc) wt. (g) | Wet wt w/cruc (g) | Dry wt w/cruc (g) | After 550C w/cruc (g) | After 950C w/cruc (g) | Wet wt (g) | Dry wt (g) | % water | weight after 550C (g) | % org of dry wt | % inorg C of dry wt |
|---|---|---|---|---|---|---|---|---|---|---|---|---|---|---|
| C1P1 | 33 | 34 | 34.2 | 4.227 | 6.676 | 5.705 | 5.625 | 5.495 | 2.449 | 1.478 | 39.6488 | 1.398 | 5.41272 | 8.79567 |
| C1P1 | 34 | 35 | 35.2 | 5.22 | 7.869 | 6.79 | 6.709 | 6.561 | 2.649 | 1.57 | 40.7324 | 1.489 | 5.15924 | 9.42675 |
| C1P1 | 35 | 36 | 36.2 | 5.274 | 7.455 | 6.63 | 6.568 | 6.35 | 2.181 | 1.356 | 37.8267 | 1.294 | 4.57227 | 16.0767 |
| C1P1 | 36 | 37 | 37.2 | 4.766 | 7.243 | 6.256 | 6.176 | 6.052 | 2.477 | 1.49 | 39.8466 | 1.41 | 5.36913 | 8.32215 |
| C1P1 | 37 | 38 | 38.3 | 4.885 | 8.037 | 6.823 | 6.722 | 6.578 | 3.152 | 1.938 | 38.5152 | 1.837 | 5.21156 | 7.43034 |
| C1P1 | 38 | 39 | 39.3 | 4.558 | 7.616 | 6.44 | 6.346 | 6.196 | 3.058 | 1.882 | 38.4565 | 1.788 | 4.99469 | 7.97024 |
| C1P1 | 39 | 40 | 40.3 | 4.885 | 8.054 | 6.776 | 6.681 | 6.545 | 3.169 | 1.891 | 40.3282 | 1.796 | 5.0238 | 7.19196 |
| C1P1 | 40 | 41 | 41.3 | 4.588 | 7.786 | 6.639 | 6.549 | 6.446 | 3.198 | 2.051 | 35.8662 | 1.961 | 4.3881 | 5.02194 |
| C1P1 | 41 | 42 | 42.3 | 4.836 | 8.186 | 6.859 | 6.758 | 6.646 | 3.35 | 2.023 | 39.6119 | 1.922 | 4.99259 | 5.53633 |
| C1P1 | 42 | 43 | 43.4 | 4.9 | 7.554 | 6.242 | 6.138 | 6.032 | 2.654 | 1.342 | 49.4348 | 1.238 | 7.74963 | 7.89866 |
| C1P1 | 43 | 44 | 44.4 | 4.932 | 7.614 | 6.471 | 6.384 | 6.281 | 2.682 | 1.539 | 42.6174 | 1.452 | 5.65302 | 6.69266 |
| C1P1 | 44 | 45 | 45.4 | 4.312 | 7.486 | 6.24 | 6.148 | 6.043 | 3.174 | 1.928 | 39.2565 | 1.836 | 4.77178 | 5.44606 |
| C1P1 | 45 | 46 | 46.4 | 4.773 | 8.316 | 7.096 | 7.012 | 6.904 | 3.543 | 2.323 | 34.4341 | 2.239 | 3.61601 | 4.64916 |
| C1P1 | 46 | 47 | 47.4 | 4.375 | 7.407 | 6.291 | 6.215 | 6.114 | 3.032 | 1.916 | 36.8074 | 1.84 | 3.9666 | 5.2714 |
| C1P1 | 47 | 48 | 48.5 | 5.296 | 7.506 | 6.486 | 6.415 | 6.327 | 2.21 | 1.19 | 46.1538 | 1.119 | 5.96639 | 7.39496 |
| C1P1 | 48 | 49 | 49.5 | 4.645 | 7.885 | 6.701 | 6.616 | 6.519 | 3.24 | 2.056 | 36.5432 | 1.971 | 4.13424 | 4.7179 |
| C1P1 | 49 | 50 | 50.5 | 4.984 | 7.625 | 6.479 | 6.403 | 6.299 | 2.641 | 1.495 | 43.3927 | 1.419 | 5.08361 | 6.95652 |
| C1P1 | 50 | 51 | 51.5 | 4.692 | 7.743 | 6.507 | 6.42 | 6.322 | 3.051 | 1.815 | 40.5113 | 1.728 | 4.79339 | 5.39945 |
| C1P1 | 51 | 52 | 52.5 | 4.961 | 7.78 | 6.617 | 6.526 | 6.431 | 2.819 | 1.656 | 41.2558 | 1.565 | 5.49517 | 5.73671 |
| C1P1 | 52 | 53 | 53.6 | 5.139 | 9.395 | 7.636 | 7.493 | 7.357 | 4.256 | 2.497 | 41.3299 | 2.354 | 5.72687 | 5.44654 |
| C1P1 | 53 | 54 | 54.6 | 5.257 | 8.828 | 7.425 | 7.321 | 7.148 | 3.571 | 2.168 | 39.2887 | 2.064 | 4.79705 | 7.9797 |
| C1P1 | 54 | 55 | 55.6 | 4.764 | 8.286 | 7.398 | 7.339 | 7.038 | 3.522 | 2.634 | 25.2129 | 2.575 | 2.23994 | 11.4275 |
| C1P1 | 55 | 56 | 56.6 | 4.77 | 8.08 | 7.118 | 7.026 | 6.84 | 3.31 | 2.348 | 29.0634 | 2.256 | 3.91823 | 7.92164 |
| C1P1 | 56 | 57 | 57.6 | 4.91 | 8.037 | 7.09 | 6.998 | 6.817 | 3.127 | 2.18 | 30.2846 | 2.088 | 4.22018 | 8.30275 |
| C1P1 | 57 | 58 | 58.7 | 5.122 | 8.256 | 7.317 | 7.218 | 7.105 | 3.134 | 2.195 | 29.9617 | 2.096 | 4.51025 | 5.14806 |
| C1P1 | 58 | 59 | 59.7 | 4.551 | 8.336 | 7.24 | 7.13 | 7.01 | 3.785 | 2.689 | 28.9564 | 2.579 | 4.09074 | 4.46263 |
| C1P1 | 59 | 60 | 60.7 | 5.109 | 8.917 | 7.885 | 7.773 | 7.646 | 3.808 | 2.776 | 27.1008 | 2.664 | 4.03458 | 4.57493 |
| C1P1 | 60 | 61 | 61.7 | 4.809 | 8.066 | 7.125 | 7.028 | 6.918 | 3.257 | 2.316 | 28.8916 | 2.219 | 4.18826 | 4.74957 |
| C1P1 | 61 | 62 | 62.7 | 4.291 | 8.336 | 6.989 | 6.858 | 6.725 | 4.045 | 2.698 | 33.3004 | 2.567 | 4.85545 | 4.92958 |
| C1P1 | 62 | 63 | 63.8 | 4.823 | 8.505 | 7.236 | 7.118 | 6.979 | 3.682 | 2.413 | 34.465 | 2.295 | 4.89018 | 5.76046 |
| C1P1 | 63 | 63.5 | 64.5 | 4.945 | 7.553 | 6.661 | 6.577 | 6.487 | 2.608 | 1.716 | 34.2025 | 1.632 | 4.8951 | 5.24476 |
| C1P1 | 63.5 | 65 | 65.5 | 4.908 | 7.846 | 7.015 | 6.898 | 6.794 | 2.938 | 2.107 | 28.2845 | 1.99 | 5.55292 | 4.93593 |
| C1P1 | 65 | 66 | 66.8 | 4.377 | 7.094 | 6.281 | 6.168 | 6.029 | 2.717 | 1.904 | 29.9227 | 1.791 | 5.93487 | 7.30042 |
| C1P1 | 66 | 67 | 67.8 | 4.765 | 7.467 | 6.663 | 6.549 | 6.432 | 2.702 | 1.898 | 29.7557 | 1.784 | 6.00632 | 6.16438 |

| Core Label | Segment depth start (cm) | Segment depth end (cm) | Overall Core Depth (cm) | Crucible (cruc) wt. (g) | Wet wt w/cruc (g) | Dry wt w/cruc (g) | After 550C w/cruc (g) | After 950C w/cruc (g) | Wet wt (g) | Dry wt (g) | % water | weight after 550C (g) | % org of dry wt | % inorg C of dry wt |
|---|---|---|---|---|---|---|---|---|---|---|---|---|---|---|
| C1P1 | 67 | 68 | 68.9 | 4.964 | 8.084 | 7.126 | 6.999 | 6.883 | 3.12 | 2.162 | 30.7051 | 2.035 | 5.87419 | 5.3654 |
| C1P1 | 68 | 69 | 69.9 | 4.289 | 7.041 | 6.178 | 6.063 | 5.947 | 2.752 | 1.889 | 31.359 | 1.774 | 6.08788 | 6.14082 |
| C1P1 | 69 | 70 | 70.9 | 4.805 | 8.168 | 7.106 | 6.971 | 6.852 | 3.363 | 2.301 | 31.5789 | 2.166 | 5.86701 | 5.17166 |
| C1P1 | 70 | 71 | 71.9 | 5.107 | 8.651 | 7.543 | 7.406 | 7.28 | 3.544 | 2.436 | 31.2641 | 2.299 | 5.62397 | 5.17241 |
| C1P1 | 71 | 72 | 72.9 | 4.645 | 7.422 | 6.6 | 6.487 | 6.371 | 2.777 | 1.955 | 29.6003 | 1.842 | 5.78005 | 5.9335 |
| C1P1 | 72 | 73 | 74 | 4.553 | 8.005 | 6.969 | 6.832 | 6.718 | 3.452 | 2.416 | 30.0116 | 2.279 | 5.67053 | 4.71854 |
| C1P1 | 73 | 74 | 75 | 5.122 | 8.528 | 7.498 | 7.365 | 7.25 | 3.406 | 2.376 | 30.2408 | 2.243 | 5.59764 | 4.84007 |
| C1P1 | 74 | 75 | 76 | 4.985 | 8.019 | 7.066 | 6.95 | 6.853 | 3.034 | 2.081 | 31.4107 | 1.965 | 5.57424 | 4.66122 |
| C1P1 | 75 | 76 | 77 | 4.845 | 7.765 | 6.837 | 6.726 | 6.624 | 2.92 | 1.992 | 31.7808 | 1.881 | 5.57229 | 5.12048 |
| C1P1 | 76 | 77 | 78 | 4.692 | 8.173 | 7.036 | 6.906 | 6.784 | 3.481 | 2.344 | 32.663 | 2.214 | 5.54608 | 5.20478 |
| C1P1 | 77 | 78 | 79.1 | 4.601 | 7.375 | 6.461 | 6.357 | 6.251 | 2.774 | 1.86 | 32.9488 | 1.756 | 5.5914 | 5.69892 |
| C1P1 | 78 | 79 | 80.1 | 5.302 | 8.528 | 7.535 | 7.409 | 7.292 | 3.226 | 2.233 | 30.7812 | 2.107 | 5.64263 | 5.23959 |
| C1P1 | 79 | 80 | 81.1 | 4.764 | 8.421 | 7.303 | 7.163 | 7.021 | 3.657 | 2.539 | 30.5715 | 2.399 | 5.51398 | 5.59275 |
| C1P1 | 80 | 81 | 82.1 | 4.944 | 7.48 | 6.675 | 6.582 | 6.458 | 2.536 | 1.731 | 31.7429 | 1.638 | 5.37262 | 7.16349 |
| C1P1 | 81 | 82 | 83.1 | 5.138 | 8.181 | 7.203 | 7.089 | 6.954 | 3.043 | 2.065 | 32.1393 | 1.951 | 5.52058 | 6.53753 |
| C1P1 | 82 | 83 | 84.2 | 5.065 | 8.308 | 7.305 | 7.183 | 7.016 | 3.243 | 2.24 | 30.9282 | 2.118 | 5.44643 | 7.45536 |
| C1P1 | 83 | 84 | 85.2 | 4.961 | 8.699 | 7.575 | 7.431 | 7.253 | 3.738 | 2.614 | 30.0696 | 2.47 | 5.5088 | 6.80949 |
| C1P1 | 84 | 85 | 86.2 | 4.86 | 8.033 | 7.074 | 6.955 | 6.831 | 3.173 | 2.214 | 30.2238 | 2.095 | 5.37489 | 5.60072 |
| C1P1 | 85 | 86 | 87.2 | 5.256 | 7.983 | 7.145 | 7.041 | 6.942 | 2.727 | 1.889 | 30.7297 | 1.785 | 5.50556 | 5.24087 |
| C1P1 | 86 | 87 | 88.2 | 4.535 | 7.573 | 6.581 | 6.467 | 6.333 | 3.038 | 2.046 | 32.6531 | 1.932 | 5.57185 | 6.54936 |
| C1P1 | 87 | 88 | 89.3 | 4.981 | 8.213 | 7.142 | 7.024 | 6.892 | 3.232 | 2.161 | 33.1374 | 2.043 | 5.46043 | 6.10828 |
| C1P1 | 88 | 89 | 90.3 | 4.677 | 7.671 | 6.621 | 6.515 | 6.369 | 2.994 | 1.944 | 35.0701 | 1.838 | 5.45267 | 7.51029 |
| C1P1 | 89 | 90 | 91.3 | 5.14 | 8.446 | 7.357 | 7.261 | 6.911 | 3.306 | 2.217 | 32.9401 | 2.121 | 4.33018 | 15.7871 |
| C1P1 | 90 | 91 | 92.3 | 4.723 | 7.556 | 6.488 | 6.388 | 6.171 | 2.833 | 1.765 | 37.6986 | 1.665 | 5.66572 | 12.2946 |
| C1P1 | 91 | 92 | 93.3 | 4.824 | 7.692 | 6.765 | 6.652 | 6.581 | 2.868 | 1.941 | 32.3222 | 1.828 | 5.82174 | 3.65791 |
| C1P1 | 92 | 93 | 94.4 | 5.112 | 8.307 | 7.213 | 7.093 | 6.958 | 3.195 | 2.101 | 34.241 | 1.981 | 5.71157 | 6.42551 |
| C1P1 | 93 | 94 | 95.4 | 4.384 | 7.337 | 6.241 | 6.14 | 5.927 | 2.953 | 1.857 | 37.1148 | 1.756 | 5.43888 | 11.4701 |
| C1P1 | 94 | 95 | 96.4 | 4.369 | 7.222 | 6.132 | 6.03 | 5.86 | 2.853 | 1.763 | 38.2054 | 1.661 | 5.78559 | 9.64265 |
| C1P1 | 95 | 96 | 97.4 | 5.33 | 7.972 | 7.034 | 6.946 | 6.73 | 2.642 | 1.704 | 35.5034 | 1.616 | 5.16432 | 12.6761 |
| C1P1 | 96 | 97 | 98.4 | 4.817 | 7.322 | 6.172 | 6.102 | 5.739 | 2.505 | 1.355 | 45.9082 | 1.285 | 5.16605 | 26.7897 |
| C1P1 | 97 | 98 | 99.5 | 5.031 | 6.473 | 5.835 | 5.785 | 5.584 | 1.442 | 0.804 | 44.2441 | 0.754 | 6.21891 | 25 |
| C1P1 | 98 | 99 | 100.5 | 4.345 | 6.846 | 5.739 | 5.657 | 5.398 | 2.501 | 1.394 | 44.2623 | 1.312 | 5.88235 | 18.5796 |
| C1P1 | 99 | 100 | 101.5 | 4.673 | 6.737 | 5.93 | 5.873 | 5.602 | 2.064 | 1.257 | 39.0988 | 1.2 | 4.53461 | 21.5593 |
| C1P2 | 0 | 1 | 101.5 | 4.598 | 8.108 | 7.191 | 7.062 | 6.858 | 3.51 | 2.593 | 26.1254 | 2.464 | 4.97493 | 7.86734 |

| Core Label | Segment depth start (cm) | Segment depth end (cm) | Overall Core Depth (cm) | Crucible (cruc) wt. (g) | Wet wt w/cruc (g) | Dry wt w/cruc (g) | After 550C w/cruc (g) | After 950C w/cruc (g) | Wet wt (g) | Dry wt (g) | % water | weight after 550C (g) | % org of dry wt | % inorg C of dry wt |
|---|---|---|---|---|---|---|---|---|---|---|---|---|---|---|
| C1P2 | 1 | 2 | 102.6 | 5.135 | 8.14 | 7.33 | 7.214 | 7.068 | 3.005 | 2.195 | 26.9551 | 2.079 | 5.28474 | 6.65148 |
| C1P2 | 2 | 3 | 103.7 | 4.982 | 7.848 | 6.967 | 6.858 | 6.699 | 2.866 | 1.985 | 30.7397 | 1.876 | 5.49118 | 8.01008 |
| C1P2 | 3 | 4 | 104.8 | 4.763 | 7.332 | 6.523 | 6.43 | 6.239 | 2.569 | 1.76 | 31.4909 | 1.667 | 5.28409 | 10.8523 |
| C1P2 | 4 | 5 | 105.9 | 5.302 | 7.259 | 6.536 | 6.475 | 6.165 | 1.957 | 1.234 | 36.9443 | 1.173 | 4.94327 | 25.1216 |
| C1P2 | 5 | 6 | 107 | 4.764 | 7.143 | 6.256 | 6.18 | 5.842 | 2.379 | 1.492 | 37.2846 | 1.416 | 5.09383 | 22.6542 |
| C1P2 | 6 | 7 | 108 | 4.764 | 7.744 | 6.639 | 6.542 | 6.144 | 2.98 | 1.875 | 37.0805 | 1.778 | 5.17333 | 21.2267 |
| C1P2 | 7 | 8 | 109.1 | 4.909 | 7.533 | 6.569 | 6.473 | 6.193 | 2.624 | 1.66 | 36.7378 | 1.564 | 5.78313 | 16.8675 |
| C1P2 | 8 | 9 | 110.2 | 4.551 | 7.378 | 6.313 | 6.193 | 6.04 | 2.827 | 1.762 | 37.6724 | 1.642 | 6.81044 | 8.68331 |
| C1P2 | 9 | 10 | 111.3 | 4.289 | 7.153 | 6.077 | 5.951 | 5.75 | 2.864 | 1.788 | 37.5698 | 1.662 | 7.04698 | 11.2416 |
| C1P2 | 10 | 11 | 112.4 | 5.221 | 8.051 | 6.904 | 6.788 | 6.481 | 2.83 | 1.683 | 40.53 | 1.567 | 6.89245 | 18.2412 |
| C1P2 | 11 | 12 | 113.5 | 4.807 | 7.41 | 6.347 | 6.242 | 5.826 | 2.603 | 1.54 | 40.8375 | 1.435 | 6.81818 | 27.013 |
| C1P2 | 12 | 13 | 114.5 | 4.694 | 6.787 | 6.049 | 5.982 | 5.599 | 2.093 | 1.355 | 35.2604 | 1.288 | 4.94465 | 28.2657 |
| C1P2 | 13 | 14 | 115.6 | 4.836 | 7.431 | 6.585 | 6.509 | 6.014 | 2.595 | 1.749 | 32.6012 | 1.673 | 4.34534 | 28.3019 |
| C1P2 | 14 | 15 | 116.7 | 4.74 | 7.238 | 6.447 | 6.379 | 5.881 | 2.498 | 1.707 | 31.6653 | 1.639 | 3.9836 | 29.174 |
| C1P2 | 15 | 16 | 117.8 | 5.107 | 7.386 | 6.791 | 6.732 | 6.212 | 2.279 | 1.684 | 26.1079 | 1.625 | 3.50356 | 30.8789 |
| C1P2 | 16 | 17 | 118.9 | 4.321 | 6.885 | 6.151 | 6.084 | 5.53 | 2.564 | 1.83 | 28.6271 | 1.763 | 3.6612 | 30.2732 |
| C1P2 | 17 | 18 | 120 | 4.849 | 7.44 | 6.555 | 6.48 | 6.017 | 2.591 | 1.706 | 34.1567 | 1.631 | 4.39625 | 27.1395 |
| C1P2 | 18 | 19 | 121 | 4.558 | 7.229 | 6.427 | 6.355 | 5.83 | 2.671 | 1.869 | 30.0262 | 1.797 | 3.85233 | 28.0899 |
| C1P2 | 19 | 20 | 122.1 | 4.967 | 7.101 | 6.502 | 6.454 | 5.985 | 2.134 | 1.535 | 28.0694 | 1.487 | 3.12704 | 30.5537 |
| C1P2 | 20 | 21 | 123.2 | 4.373 | 6.378 | 5.812 | 5.764 | na | 2.005 | 1.439 | 28.2294 | 1.391 | 3.33565 | |
| C1P2 | 21 | 22 | 124.3 | 5.275 | 7.925 | 7.162 | 7.095 | 6.771 | 2.65 | 1.887 | 28.7925 | 1.82 | 3.55061 | 17.1701 |
| C1P2 | 23 | 24 | 126.5 | 4.936 | 7.788 | 6.925 | 6.848 | 6.541 | 2.852 | 1.989 | 30.2595 | 1.912 | 3.87129 | 15.4349 |
| C1P2 | 24 | 25 | 127.5 | 5.123 | 8.864 | 7.725 | 7.598 | 7.457 | 3.741 | 2.602 | 30.4464 | 2.475 | 4.88086 | 5.41891 |
| C1P2 | 25 | 26 | 128.6 | 4.88 | 8.996 | 7.762 | 7.627 | 7.471 | 4.116 | 2.882 | 29.9806 | 2.747 | 4.68425 | 5.41291 |
| C1P2 | 26 | 27 | 129.7 | 4.705 | 8.425 | 7.331 | 7.218 | 7.027 | 3.72 | 2.626 | 29.4086 | 2.513 | 4.30312 | 7.27342 |
| C1P2 | 27 | 28 | 130.8 | 4.831 | 8.059 | 7.237 | 7.144 | 6.89 | 3.228 | 2.406 | 25.4647 | 2.313 | 3.86534 | 10.5569 |
| C1P2 | 28 | 29 | 131.9 | 4.316 | 7.702 | 6.823 | 6.723 | 6.431 | 3.386 | 2.507 | 25.9598 | 2.407 | 3.98883 | 11.6474 |
| C1P2 | 29 | 30 | 133 | 4.901 | 8.999 | 7.874 | 7.755 | 7.485 | 4.098 | 2.973 | 27.4524 | 2.854 | 4.00269 | 9.08174 |
| C1P2 | 30 | 31 | 134 | 4.944 | 8.706 | 7.708 | 7.611 | 7.283 | 3.762 | 2.764 | 26.5284 | 2.667 | 3.50941 | 11.8669 |
| C1P2 | 31 | 32 | 135.1 | 4.645 | 7.667 | 6.885 | 6.808 | 6.467 | 3.022 | 2.24 | 25.8769 | 2.163 | 3.4375 | 15.2232 |
| C1P2 | 32 | 33 | 136.2 | 4.228 | 7.779 | 6.821 | 6.717 | 6.421 | 3.551 | 2.593 | 26.9783 | 2.489 | 4.0108 | 11.4153 |
| C1P2 | 33 | 34 | 137.3 | 4.886 | 7.932 | 7.132 | 7.038 | 6.876 | 3.046 | 2.246 | 26.264 | 2.152 | 4.18522 | 7.21282 |
| C1P2 | 34 | 35 | 138.4 | 4.698 | 8.336 | 7.469 | 7.346 | 7.224 | 3.638 | 2.771 | 23.8318 | 2.648 | 4.43883 | 4.40274 |
| C1P2 | 35 | 36 | 139.5 | 4.226 | 7.642 | 6.897 | 6.775 | 6.659 | 3.416 | 2.671 | 21.8091 | 2.549 | 4.56758 | 4.34294 |

| Core Label | Segment depth start (cm) | Segment depth end (cm) | Overall Core Depth (cm) | Crucible (cruc) wt. (g) | Wet wt w/cruc (g) | Dry wt w/cruc (g) | After 550C w/cruc (g) | After 950C w/cruc (g) | Wet wt (g) | Dry wt (g) | % water | weight after 550C (g) | % org of dry wt | % inorg C of dry wt |
|---|---|---|---|---|---|---|---|---|---|---|---|---|---|---|
| C1P2 | 36 | 37 | 140.5 | 4.832 | 7.879 | 7.22 | 7.092 | 6.991 | 3.047 | 2.388 | 21.6278 | 2.26 | 5.36013 | 4.22948 |
| C1P2 | 37 | 38 | 141.6 | 4.701 | 7.713 | 7.055 | 6.941 | 6.841 | 3.012 | 2.354 | 21.8459 | 2.24 | 4.84282 | 4.24809 |
| C1P2 | 38 | 39 | 142.7 | 4.966 | 7.642 | 7.087 | 6.993 | 6.83 | 2.676 | 2.121 | 20.7399 | 2.027 | 4.43187 | 7.68505 |
| C1P2 | 39 | 40 | 143.8 | 4.902 | 8.342 | 7.574 | 7.438 | 7.329 | 3.44 | 2.672 | 22.3256 | 2.536 | 5.08982 | 4.07934 |
| C1P2 | 40 | 41 | 144.9 | 4.807 | 8.217 | 7.461 | 7.322 | 7.239 | 3.41 | 2.654 | 22.1701 | 2.515 | 5.23738 | 3.12735 |
| C1P2 | 41 | 42 | 146 | 4.838 | 8.333 | 7.583 | 7.445 | 7.349 | 3.495 | 2.745 | 21.4592 | 2.607 | 5.02732 | 3.49727 |
| C1P2 | 42 | 43 | 147 | 4.317 | 7.116 | 6.532 | 6.427 | 6.317 | 2.799 | 2.215 | 20.8646 | 2.11 | 4.74041 | 4.96614 |
| C1P2 | 43 | 44 | 148.1 | 4.645 | 7.603 | 6.976 | 6.869 | 6.733 | 2.958 | 2.331 | 21.1968 | 2.224 | 4.5903 | 5.83441 |
| C1P2 | 44 | 45 | 149.2 | 4.885 | 7.776 | 7.226 | 7.128 | 7.039 | 2.891 | 2.341 | 19.0246 | 2.243 | 4.18625 | 3.80179 |
| C1P2 | 45 | 46 | 150.3 | 4.552 | 8.312 | 7.683 | 7.564 | 7.458 | 3.76 | 3.131 | 16.7287 | 3.012 | 3.8007 | 3.3855 |
| C1P2 | 46 | 47 | 151.4 | 4.878 | 8.574 | 7.979 | 7.867 | 7.768 | 3.696 | 3.101 | 16.0985 | 2.989 | 3.61174 | 3.19252 |
| C1P2 | 47 | 48 | 152.5 | 4.765 | 7.672 | 7.227 | 7.138 | 7.053 | 2.907 | 2.462 | 15.3079 | 2.373 | 3.61495 | 3.45248 |
| C1P2 | 48 | 49 | 153.5 | 4.768 | 7.879 | 7.477 | 7.394 | 7.299 | 3.111 | 2.709 | 12.9219 | 2.626 | 3.06386 | 3.50683 |
| C1P2 | 49 | 50 | 154.6 | 4.678 | 7.292 | 7.018 | 6.955 | 6.833 | 2.614 | 2.34 | 10.482 | 2.277 | 2.69231 | 5.21368 |
| C1P2 | 50 | 51 | 155.7 | 4.559 | 8.286 | 7.905 | 7.817 | 7.652 | 3.727 | 3.346 | 10.2227 | 3.258 | 2.63001 | 4.93126 |
| C1P2 | 51 | 52 | 156.8 | 4.533 | 8.338 | 7.891 | 7.802 | 7.658 | 3.805 | 3.358 | 11.7477 | 3.269 | 2.65039 | 4.28827 |
| C1P2 | 52 | 53 | 157.9 | 4.977 | 7.973 | 7.601 | 7.526 | 7.427 | 2.996 | 2.624 | 12.4166 | 2.549 | 2.85823 | 3.77287 |
| C1P2 | 53 | 54 | 159 | 4.767 | 8.524 | 8.098 | 8.007 | 7.893 | 3.757 | 3.331 | 11.3388 | 3.24 | 2.73191 | 3.4224 |
| C1P2 | 54 | 55 | 160 | 4.931 | 7.283 | 6.99 | 6.931 | 6.891 | 2.352 | 2.059 | 12.4575 | 2 | 2.86547 | 1.94269 |
| C1P2 | 55 | 56 | 161.1 | 5.125 | 9.196 | 8.684 | 8.58 | 8.518 | 4.071 | 3.559 | 12.5768 | 3.455 | 2.92217 | 1.74206 |
| C1P2 | 56 | 57 | 162.2 | 4.705 | 8.432 | 7.993 | 7.897 | 7.832 | 3.727 | 3.288 | 11.7789 | 3.192 | 2.91971 | 1.97689 |
| C1P2 | 57 | 58 | 163.3 | 4.723 | 8.168 | 7.634 | 7.534 | 7.42 | 3.445 | 2.911 | 15.5007 | 2.811 | 3.43525 | 3.91618 |
| C1P2 | 58 | 59 | 164.4 | 5.142 | 8.945 | 8.268 | 8.143 | 8.049 | 3.803 | 3.126 | 17.8017 | 3.001 | 3.99872 | 3.00704 |
| C1P2 | 59 | 60 | 165.5 | 4.817 | 8.776 | 8.09 | 7.958 | 7.844 | 3.959 | 3.273 | 17.3276 | 3.141 | 4.033 | 3.48304 |
| C1P2 | 60 | 61 | 166.5 | 4.986 | 8.116 | 7.632 | 7.544 | 7.425 | 3.13 | 2.646 | 15.4633 | 2.558 | 3.32577 | 4.49735 |
| C1P2 | 61 | 62 | 167.6 | 5.301 | 8.674 | 8.108 | 8.007 | 7.878 | 3.373 | 2.807 | 16.7803 | 2.706 | 3.59815 | 4.59565 |
| C1P2 | 62 | 63 | 168.7 | 4.347 | 7.623 | 7.039 | 6.932 | 6.825 | 3.276 | 2.692 | 17.8266 | 2.585 | 3.97474 | 3.97474 |
| C1P2 | 63 | 64 | 169.8 | 5.258 | 8.608 | 7.965 | 7.842 | 7.78 | 3.35 | 2.707 | 19.194 | 2.584 | 4.54378 | 2.29036 |
| C1P2 | 64 | 65 | 170.9 | 5.065 | 8.14 | 7.56 | 7.457 | 7.408 | 3.075 | 2.495 | 18.8618 | 2.392 | 4.12826 | 1.96393 |
| C1P2 | 65 | 66 | 172 | 4.674 | 8.055 | 7.362 | 7.242 | 7.155 | 3.381 | 2.688 | 20.4969 | 2.568 | 4.46429 | 3.23661 |
| C1P2 | 66 | 67 | 173 | 4.386 | 7.464 | 6.807 | 6.697 | 6.6 | 3.078 | 2.421 | 21.345 | 2.311 | 4.54358 | 4.00661 |
| C1P2 | 67 | 68 | 174.1 | 4.693 | 7.189 | 6.645 | 6.548 | 6.47 | 2.496 | 1.952 | 21.7949 | 1.855 | 4.96926 | 3.9959 |
| C1P3 | 0 | 1 | 175 | 4.844 | 8.079 | 7.735 | 7.648 | 7.538 | 3.235 | 2.891 | 10.6337 | 2.804 | 3.00934 | 3.80491 |
| C1P2 | 68 | 69 | 175.2 | 4.739 | 8.101 | 7.425 | 7.286 | 7.187 | 3.362 | 2.686 | 20.1071 | 2.547 | 5.17498 | 3.68578 |

| Core Label | Segment depth start (cm) | Segment depth end (cm) | Overall Core Depth (cm) | Crucible (cruc) wt. (g) | Wet wt w/cruc (g) | Dry wt w/cruc (g) | After 550C w/cruc (g) | After 950C w/cruc (g) | Wet wt (g) | Dry wt (g) | % water | weight after 550C (g) | % org of dry wt | % inorg C of dry wt |
|---|---|---|---|---|---|---|---|---|---|---|---|---|---|---|
| C1P2 | 69 | 70 | 176.3 | 4.291 | 7.703 | 6.931 | 6.797 | 6.638 | 3.412 | 2.64 | 22.626 | 2.506 | 5.07576 | 6.02273 |
| C1P3 | 1 | 2 | 175.7 | 4.824 | 8.856 | 8.384 | 8.27 | 8.164 | 4.032 | 3.56 | 11.7063 | 3.446 | 3.20225 | 2.97753 |
| C1P3 | 2 | 3 | 176.8 | 4.677 | 8.643 | 8.121 | 8.005 | 7.879 | 3.966 | 3.444 | 13.1619 | 3.328 | 3.36818 | 3.65854 |
| C1P3 | 3 | 4 | 177.9 | 5.254 | 9.275 | 8.687 | 8.564 | 8.39 | 4.021 | 3.433 | 14.6232 | 3.31 | 3.58287 | 5.06845 |
| C1P3 | 4 | 5 | 179 | 5.065 | 9.707 | 9.012 | 8.873 | 8.765 | 4.642 | 3.947 | 14.972 | 3.808 | 3.52166 | 2.73626 |
| C1P3 | 5 | 6 | 180.1 | 4.691 | 6.86 | 6.57 | 6.513 | 6.442 | 2.169 | 1.879 | 13.3702 | 1.822 | 3.03353 | 3.77861 |
| C1P3 | 6 | 7 | 181.2 | 4.552 | 7.963 | 7.52 | 7.417 | 7.336 | 3.411 | 2.968 | 12.9874 | 2.865 | 3.47035 | 2.72911 |
| C1P3 | 7 | 8 | 182.3 | 5.121 | 8.434 | 7.982 | 7.887 | 7.776 | 3.313 | 2.861 | 13.6432 | 2.766 | 3.32052 | 3.87976 |
| C1P3 | 8 | 9 | 183.4 | 4.763 | 8.707 | 8.103 | 7.993 | 7.923 | 3.944 | 3.34 | 15.3144 | 3.23 | 3.29341 | 2.09581 |
| C1P3 | 9 | 10 | 184.5 | 4.863 | 9.045 | 8.496 | 8.38 | 8.279 | 4.182 | 3.633 | 13.1277 | 3.517 | 3.19295 | 2.78007 |
| C1P3 | 10 | 11 | 185.6 | 5.137 | 8.876 | 8.393 | 8.293 | 8.171 | 3.739 | 3.256 | 12.9179 | 3.156 | 3.07125 | 3.74693 |
| C1P3 | 11 | 12 | 186.7 | 4.375 | 8.564 | 7.851 | 7.7 | 7.569 | 4.189 | 3.476 | 17.0208 | 3.325 | 4.34407 | 3.7687 |
| C1P3 | 12 | 13 | 187.8 | 4.96 | 8.631 | 7.955 | 7.817 | 7.711 | 3.671 | 2.995 | 18.4146 | 2.857 | 4.60768 | 3.53923 |
| C1P3 | 13 | 14 | 188.9 | 4.705 | 8.931 | 8.169 | 8.02 | 7.859 | 4.226 | 3.464 | 18.0312 | 3.315 | 4.30139 | 4.64781 |
| C1P3 | 14 | 15 | 190 | 4.963 | 9.737 | 8.835 | 8.638 | 8.528 | 4.774 | 3.872 | 18.894 | 3.675 | 5.08781 | 2.84091 |
| C1P3 | 15 | 16 | 191.1 | 4.807 | 8.802 | 8.038 | 7.891 | 7.741 | 3.995 | 3.231 | 19.1239 | 3.084 | 4.54968 | 4.64253 |
| C1P3 | 16 | 17 | 192.2 | 4.386 | 8.203 | 7.486 | 7.366 | 7.195 | 3.817 | 3.1 | 18.7844 | 2.98 | 3.87097 | 5.51613 |
| C1P3 | 17 | 18 | 193.3 | 4.725 | 8.697 | 7.954 | 7.808 | 7.67 | 3.972 | 3.229 | 18.7059 | 3.083 | 4.52152 | 4.27377 |
| C1P3 | 18 | 19 | 194.4 | 5.11 | 9.067 | 8.215 | 8.094 | 7.968 | 3.957 | 3.105 | 21.5315 | 2.984 | 3.89694 | 4.05797 |
| C1P3 | 19 | 20 | 195.6 | 5.143 | 9.277 | 8.535 | 8.403 | 8.258 | 4.134 | 3.392 | 17.9487 | 3.26 | 3.89151 | 4.27476 |

Appendix 4. LOMC2 Raw Loss on Ignition Data

| Core Label | Segment depth start (cm) | Segment depth end (cm) | Overall Core Depth | Crucible (cruc) wt. (g) | Wet wt w/cruc (g) | Dry wt w/cruc (g) | After 550C w/cruc | After 950C w/cruc | Wet wt (g) | Dry wt (g) | % water | weight after 550C (g) | % org of dry wt | % inorg C of dry wt |
|---|---|---|---|---|---|---|---|---|---|---|---|---|---|---|
| c2 p2 | 1 | 2 | 101.3 | 4.377 | 5.104 | 5.062 | 4.988 | 4.953 | 0.727 | 0.685 | 5.77717 | 0.611 | 10.8029 | 5.10949 |
| c2 p2 | 2 | 3 | 102.2 | 4.723 | 6.065 | 5.961 | 5.896 | 5.832 | 1.342 | 1.238 | 7.74963 | 1.173 | 5.2504 | 5.16963 |
| c2 p2 | 3 | 4 | 103 | 4.694 | 6.541 | 6.38 | 6.293 | 6.212 | 1.847 | 1.686 | 8.71684 | 1.599 | 5.16014 | 4.80427 |
| c2 p2 | 4 | 5 | 103.9 | 4.864 | 6.588 | 6.443 | 6.36 | 6.296 | 1.724 | 1.579 | 8.41067 | 1.496 | 5.25649 | 4.0532 |
| c2 p2 | 5 | 6 | 104.8 | 4.899 | 6.466 | 6.311 | 6.237 | 6.153 | 1.567 | 1.412 | 9.89151 | 1.338 | 5.24079 | 5.94901 |
| c2 p2 | 6 | 7 | 105.6 | 4.773 | 6.983 | 6.772 | 6.678 | 6.529 | 2.21 | 1.999 | 9.54751 | 1.905 | 4.70235 | 7.45373 |
| c2 p2 | 7 | 8 | 106.5 | 4.76 | 6.816 | 6.553 | 6.461 | 6.388 | 2.056 | 1.793 | 12.7918 | 1.701 | 5.13107 | 4.07139 |
| c2 p2 | 8 | 9 | 107.3 | 4.788 | 8.071 | 7.162 | 7.04 | 6.947 | 3.283 | 2.374 | 27.6881 | 2.252 | 5.13901 | 3.91744 |
| c2 p2 | 9 | 10 | 108.2 | 5.292 | 7.332 | 6.883 | 6.792 | 6.68 | 2.04 | 1.591 | 22.0098 | 1.5 | 5.71967 | 7.0396 |
| c2 p2 | 10 | 11 | 109.1 | 4.229 | 6.38 | 5.75 | 5.662 | 5.598 | 2.151 | 1.521 | 29.2887 | 1.433 | 5.78567 | 4.20776 |
| c2 p2 | 11 | 12 | 109.9 | 4.55 | 7.075 | 6.288 | 6.204 | 6.126 | 2.525 | 1.738 | 31.1683 | 1.654 | 4.83314 | 4.48792 |
| c2 p2 | 12 | 13 | 110.8 | 4.842 | 7.023 | 6.38 | 6.293 | 6.168 | 2.181 | 1.538 | 29.4819 | 1.451 | 5.6567 | 8.12744 |
| c2 p2 | 13 | 14 | 111.7 | 5.277 | 8.018 | 7.169 | 7.065 | 6.91 | 2.741 | 1.892 | 30.9741 | 1.788 | 5.49683 | 8.19239 |
| c2 p2 | 14 | 15 | 112.5 | 5.254 | 7.76 | 6.955 | 6.861 | 6.703 | 2.506 | 1.701 | 32.1229 | 1.607 | 5.52616 | 9.28865 |
| c2 p2 | 15 | 16 | 113.4 | 5.153 | 7.942 | 7.048 | 6.95 | 6.812 | 2.789 | 1.895 | 32.0545 | 1.797 | 5.1715 | 7.28232 |
| c2 p2 | 16 | 17 | 114.3 | 5.078 | 6.951 | 6.35 | 6.278 | 6.174 | 1.873 | 1.272 | 32.0876 | 1.2 | 5.66038 | 8.1761 |
| c2 p2 | 17 | 18 | 115.1 | 4.552 | 7.727 | 6.598 | 6.492 | 6.327 | 3.175 | 2.046 | 35.5591 | 1.94 | 5.18084 | 8.06452 |
| c2 p2 | 18 | 19 | 116 | 4.941 | 7.464 | 6.623 | 6.53 | 6.396 | 2.523 | 1.682 | 33.3333 | 1.589 | 5.52913 | 7.96671 |
| c2 p2 | 19 | 20 | 116.8 | 5.113 | 6.987 | 6.369 | 6.295 | 6.215 | 1.874 | 1.256 | 32.9776 | 1.182 | 5.89172 | 6.36943 |
| c2 p2 | 20 | 21 | 117.7 | 4.963 | 7.524 | 6.688 | 6.596 | 6.48 | 2.561 | 1.725 | 32.6435 | 1.633 | 5.33333 | 6.72464 |
| c2 p2 | 21 | 22 | 118.6 | 5.142 | 7.137 | 6.497 | 6.427 | 6.364 | 1.995 | 1.355 | 32.0802 | 1.285 | 5.16605 | 4.64945 |
| c2 p2 | 22 | 23 | 119.4 | 4.547 | 6.76 | 6.053 | 5.974 | 5.92 | 2.213 | 1.506 | 31.9476 | 1.427 | 5.24568 | 3.58566 |
| c2 p2 | 23 | 24 | 120.3 | 5.219 | 8.406 | 7.441 | 7.313 | 7.238 | 3.187 | 2.222 | 30.2793 | 2.094 | 5.76058 | 3.37534 |
| c2 p2 | 24 | 25 | 121.2 | 4.855 | 7.101 | 6.414 | 6.326 | 6.274 | 2.246 | 1.559 | 30.5877 | 1.471 | 5.64464 | 3.33547 |
| c2 p2 | 25 | 26 | 122 | 4.836 | 7.568 | 6.71 | 6.602 | 6.532 | 2.732 | 1.874 | 31.4056 | 1.766 | 5.76307 | 3.73533 |
| c2 p2 | 26 | 27 | 122.9 | 4.893 | 8.043 | 7.064 | 6.939 | 6.853 | 3.15 | 2.171 | 31.0794 | 2.046 | 5.75772 | 3.96131 |
| c2 p2 | 27 | 28 | 123.8 | 5.334 | 8.441 | 7.341 | 7.232 | 7.139 | 3.107 | 2.007 | 35.4039 | 1.898 | 5.43099 | 4.63378 |
| c2 p2 | 28 | 29 | 124.6 | 4.642 | 7.083 | 6.342 | 6.245 | 6.158 | 2.441 | 1.7 | 30.3564 | 1.603 | 5.70588 | 5.11765 |
| c2 p2 | 29 | 30 | 125.5 | 4.355 | 7.312 | 6.495 | 6.383 | 6.304 | 2.957 | 2.14 | 27.6294 | 2.028 | 5.23364 | 3.69159 |
| c2 p2 | 30 | 31 | 126.3 | 4.701 | 7.052 | 6.341 | 6.249 | 6.178 | 2.351 | 1.64 | 30.2425 | 1.548 | 5.60976 | 4.32927 |
| c2 p2 | 31 | 32 | 127.2 | 4.906 | 7.493 | 6.714 | 6.614 | 6.538 | 2.587 | 1.808 | 30.1121 | 1.708 | 5.53097 | 4.20354 |
| c2 p2 | 32 | 33 | 128.1 | 4.719 | 7.353 | 6.52 | 6.424 | 6.291 | 2.634 | 1.801 | 31.6249 | 1.705 | 5.33037 | 7.38479 |
| c2 p2 | 33 | 34 | 128.9 | 4.695 | 7.676 | 6.453 | 6.369 | 6.107 | 2.981 | 1.758 | 41.0265 | 1.674 | 4.77816 | 14.9033 |

| Core Label | Segment depth start (cm) | Segment depth end (cm) | Overall Core Depth (cm) | Crucible (cruc) wt. (g) | Wet wt w/cruc (g) | Dry wt w/cruc (g) | After 550C w/cruc (g) | After 950C w/cruc (g) | Wet wt (g) | Dry wt (g) | % water | weight after 550C (g) | % org of dry wt | % inorg C of dry wt |
|---|---|---|---|---|---|---|---|---|---|---|---|---|---|---|
| c2 p2 | 35 | 36 | 130.7 | 4.884 | 6.972 | 6.322 | 6.238 | 6.186 | 2.088 | 1.438 | 31.1303 | 1.354 | 5.84145 | 3.61613 |
| c2 p2 | 36 | 37 | 131.5 | 4.836 | | 6.767 | 6.658 | 6.572 | | 1.931 | | 1.822 | 5.64474 | 4.45365 |
| c2 p2 | 37 | 38 | 132.4 | 4.883 | 8.055 | 6.891 | 6.788 | 6.586 | 3.172 | 2.008 | 36.6961 | 1.905 | 5.12948 | 10.0598 |
| c2 p2 | 38 | 39 | 133.3 | 4.843 | | 6.392 | 6.315 | 6.102 | | 1.549 | | 1.472 | 4.97095 | 13.7508 |
| c2 p2 | 39 | 40 | 134.1 | 4.718 | | 6.186 | 6.105 | 5.781 | | 1.468 | | 1.387 | 5.51771 | 22.0708 |
| c2 p2 | 41 | 42 | 135.8 | 4.84 | 7.492 | 6.341 | 6.299 | 5.763 | 2.652 | 1.501 | 43.4012 | 1.459 | 2.79813 | 35.7095 |
| c2 p2 | 42 | 43 | 136.7 | 4.7 | | 6.238 | 6.12 | 5.79 | | 1.538 | | 1.42 | 7.6723 | 21.4564 |
| c2 p2 | 43 | 44 | 137.6 | 4.854 | | 6.569 | 6.451 | 6.13 | | 1.715 | | 1.597 | 6.88047 | 18.7172 |
| c2 p2 | 44 | 45 | 138.4 | 5.077 | | 6.754 | 6.649 | 6.373 | | 1.677 | | 1.572 | 6.26118 | 16.458 |
| c2 p2 | 45 | 46 | 139.3 | 4.76 | | 6.188 | 6.106 | 5.868 | | 1.428 | | 1.346 | 5.7423 | 16.6667 |
| c2 p2 | 47 | 48 | 141 | 4.838 | 7.817 | 6.641 | 6.55 | 6.284 | 2.979 | 1.803 | 39.4763 | 1.712 | 5.04714 | 14.7532 |
| c2 p2 | 48 | 49 | 141.9 | 5.113 | | 6.826 | 6.738 | 6.5 | | 1.713 | | 1.625 | 5.13719 | 13.8938 |
| c2 p2 | 49 | 50 | 142.8 | 4.228 | | 5.802 | 5.717 | 5.5 | | 1.574 | | 1.489 | 5.40025 | 13.7865 |
| c2 p2 | 50 | 51 | 143.6 | 5.142 | | 6.296 | 6.23 | 6.019 | | 1.154 | | 1.088 | 5.71924 | 18.2842 |
| c2 p2 | 51 | 52 | 144.5 | 5.292 | | 6.828 | 6.755 | 6.452 | | 1.536 | | 1.463 | 4.7526 | 19.7266 |
| c2 p2 | 52 | 53 | 145.3 | 4.455 | | 6.295 | 6.213 | 5.885 | | 1.84 | | 1.758 | 4.45652 | 17.8261 |
| c2 p2 | 53 | 54 | 146.2 | 4.885 | | 6.569 | 6.483 | 6.218 | | 1.684 | | 1.598 | 5.10689 | 15.7363 |
| c2 p2 | 54 | 55 | 147.1 | 5.218 | 8.28 | 7.053 | 6.962 | 6.696 | 3.062 | 1.835 | 40.0718 | 1.744 | 4.95913 | 14.4959 |
| c2 p2 | 55 | 56.5 | 148.1 | 4.773 | | 6.247 | 6.183 | 5.788 | | 1.474 | | 1.41 | 4.34193 | 26.7978 |
| c2 p2 | 58 | 59 | 150.5 | 4.44 | 6.243 | 5.585 | 5.542 | 5.205 | 1.803 | 1.145 | 36.4947 | 1.102 | 3.75546 | 29.4323 |
| c2 p2 | 60 | 62.5 | 152.9 | 4.694 | | 5.938 | 5.881 | 5.544 | | 1.244 | | 1.187 | 4.58199 | 27.09 |
| c2 p2 | 62 | 65 | 154.8 | 4.899 | | 7.287 | 7.137 | 6.966 | | 2.388 | | 2.238 | 6.28141 | 7.1608 |
| c2p3 | 0 | 2 | 158.1 | 4.943 | 6.977 | 6.665 | 6.562 | 6.233 | 2.034 | 1.722 | 15.3392 | 1.619 | 5.98142 | 19.1057 |
| c2p3 | 2 | 3 | 159.7 | 4.678 | 7.546 | 6.921 | 6.745 | 6.592 | 2.868 | 2.243 | 21.7922 | 2.067 | 7.84663 | 6.82122 |
| c2p3 | 3 | 4 | 160.8 | 4.551 | 7.356 | 6.993 | 6.518 | 6.416 | 2.805 | 2.442 | 12.9412 | 1.967 | 19.4513 | 4.1769 |
| c2p3 | 4 | 5 | 161.9 | 4.315 | 6.341 | 5.806 | 5.678 | 5.618 | 2.026 | 1.491 | 26.4067 | 1.363 | 8.58484 | 4.02414 |
| c2p3 | 5 | 6 | 163 | 4.32 | 7.296 | 6.01 | 5.888 | 5.827 | 2.976 | 1.69 | 43.2124 | 1.568 | 7.21893 | 3.60947 |
| c2p3 | 6 | 7 | 164.1 | 4.8 | 7.018 | 6.278 | 6.159 | 6.111 | 2.218 | 1.478 | 33.3634 | 1.359 | 8.05142 | 3.24763 |
| c2p3 | 7 | 8 | 165.1 | 5.218 | 7.204 | 6.529 | 6.422 | 6.379 | 1.986 | 1.311 | 33.9879 | 1.204 | 8.16171 | 3.27994 |
| c2p3 | 8 | 9 | 166.2 | 4.717 | 6.555 | 5.948 | 5.862 | 5.817 | 1.838 | 1.231 | 33.025 | 1.145 | 6.98619 | 3.65556 |
| c2p3 | 9 | 10 | 167.3 | 5.273 | 7.777 | 6.978 | 6.858 | 6.785 | 2.504 | 1.705 | 31.9089 | 1.585 | 7.03812 | 4.28152 |
| c2p3 | 10 | 11 | 168.4 | 4.807 | 7.063 | 6.329 | 6.22 | 6.159 | 2.256 | 1.522 | 32.5355 | 1.413 | 7.16163 | 4.00788 |
| c2p3 | 11 | 12 | 169.5 | 4.899 | 7.503 | 6.676 | 6.539 | 6.467 | 2.604 | 1.777 | 31.7588 | 1.64 | 7.70962 | 4.05177 |
| c2p3 | 12 | 13 | 170.6 | 4.837 | 7.537 | 6.661 | 6.533 | 6.476 | 2.7 | 1.824 | 32.4444 | 1.696 | 7.01754 | 3.125 |

| Core Label | Segment depth start (cm) | Segment depth end (cm) | Overall Core Depth (cm) | Crucible (cruc) wt. (g) | Wet wt w/cruc (g) | Dry wt w/cruc (g) | After 550C w/cruc (g) | After 950C w/cruc (g) | Wet wt (g) | Dry wt (g) | % water | weight after 550C (g) | % org of dry wt | % inorg C of dry wt |
|---|---|---|---|---|---|---|---|---|---|---|---|---|---|---|
| c2p3 | 13 | 14 | 171.7 | 4.843 | 7.307 | 6.583 | 6.459 | 6.4 | 2.464 | 1.74 | 29.3831 | 1.616 | 7.12644 | 3.3908 |
| c2p3 | 15 | 16 | 173.8 | 4.863 | 7.789 | 6.546 | 6.444 | 6.377 | 2.926 | 1.683 | 42.4812 | 1.581 | 6.06061 | 3.98099 |
| c2p3 | 16 | 17 | 174.9 | 4.377 | 6.681 | 5.935 | 5.822 | 5.772 | 2.304 | 1.558 | 32.3785 | 1.445 | 7.25289 | 3.20924 |
| c2p3 | 17 | 18 | 176 | 4.289 | 6.704 | 5.933 | 5.81 | 5.755 | 2.415 | 1.644 | 31.9255 | 1.521 | 7.48175 | 3.3455 |
| c2p3 | 18 | 19 | 177.1 | 4.959 | 7.945 | 7 | 6.851 | 6.774 | 2.986 | 2.041 | 31.6477 | 1.892 | 7.30034 | 3.77266 |
| c2p3 | 19 | 20 | 178.2 | 4.534 | 7.079 | 6.27 | 6.151 | 6.082 | 2.545 | 1.736 | 31.7878 | 1.617 | 6.85484 | 3.97465 |
| c2p3 | 20 | 21 | 179.3 | 5.294 | 6.646 | 6.301 | 6.25 | 6.083 | 1.352 | 1.007 | 25.5178 | 0.956 | 5.06455 | 16.5839 |
| c2p3 | 21 | 22 | 180.3 | 4.605 | 6.659 | 6.038 | 5.964 | 5.75 | 2.054 | 1.433 | 30.2337 | 1.359 | 5.16399 | 14.9337 |
| c2p3 | 22 | 23 | 181.4 | 4.907 | 7.123 | 6.474 | 6.395 | 6.201 | 2.216 | 1.567 | 29.287 | 1.488 | 5.04148 | 12.3803 |
| c2p3 | 23 | 24 | 182.5 | 5.255 | 7.332 | 6.751 | 6.683 | 6.466 | 2.077 | 1.496 | 27.973 | 1.428 | 4.54545 | 14.5053 |
| c2p3 | 24 | 25 | 183.6 | 4.965 | 7.008 | 6.442 | 6.365 | 6.205 | 2.043 | 1.477 | 27.7044 | 1.4 | 5.21327 | 10.8328 |
| c2p3 | 25 | 26 | 184.7 | 4.83 | 7.603 | 6.4 |  |  | 2.773 | 1.57 | 43.3826 |  |  |  |
| c2p3 | 26 | 27 | 185.8 | 4.825 | 6.92 | 6.285 | 6.196 | 6.072 | 2.095 | 1.46 | 30.3103 | 1.371 | 6.09589 | 8.49315 |
| c2p3 | 27 | 28 | 186.9 | 4.878 | 6.793 | 6.141 | 6.03 | 5.876 | 1.915 | 1.263 | 34.047 | 1.152 | 8.7886 | 12.1932 |
| c2p3 | 28 | 29 | 187.9 | 4.367 | 6.351 | 5.783 | 5.699 | 5.483 | 1.984 | 1.416 | 28.629 | 1.332 | 5.9322 | 15.2542 |
| c2p3 | 29 | 30 | 189 | 5.066 | 6.883 | 6.372 | 6.309 | 6.123 | 1.817 | 1.306 | 28.1233 | 1.243 | 4.82389 | 14.242 |
| c2p3 | 30 | 31 | 190.1 | 5.112 | 6.012 | 5.881 | 5.853 | 5.601 | 0.9 | 0.769 | 14.5556 | 0.741 | 3.64109 | 32.7698 |
| c2p3 | 31 | 32 | 191.2 | 4.983 | 6.687 | 6.27 | 6.233 | 5.771 | 1.704 | 1.287 | 24.4718 | 1.25 | 2.8749 | 35.8974 |
| c2p3 | 32 | 33 | 192.3 | 5.112 | 6.492 | 6.301 | 6.248 | 5.9 | 1.38 | 1.189 | 13.8406 | 1.136 | 4.45753 | 29.2683 |
| c2p3 | 33 | 34 | 193.4 | 5.328 | 6.75 | 6.557 | 6.51 | 6.197 | 1.422 | 1.229 | 13.5724 | 1.182 | 3.82425 | 25.4679 |
| c2p4 | 0 | 1 | 195.5 | 4.706 | 6.496 | 6.389 | 6.29 | 6.182 | 1.79 | 1.683 | 5.97765 | 1.584 | 5.88235 | 6.41711 |
| c2p4 | 2 | 3 | 197.5 | 4.76 | 7.948 | 7.077 | 6.958 | 6.82 | 3.188 | 2.317 | 27.3212 | 2.198 | 5.13595 | 5.95598 |
| c2p4 | 3 | 4 | 198.5 | 4.773 | 7.347 | 7.162 | 7.023 | 6.897 | 2.574 | 2.389 | 7.18726 | 2.25 | 5.81833 | 5.27417 |
| c2p4 | 4 | 5 | 199.4 | 4.227 | 5.717 | 5.646 | 5.584 | 5.504 | 1.49 | 1.419 | 4.7651 | 1.357 | 4.36927 | 5.63777 |
| c2p4 | 5 | 6 | 200.4 | 4.937 | 6.629 | 6.526 | 6.452 | 6.373 | 1.692 | 1.589 | 6.08747 | 1.515 | 4.65702 | 4.97168 |
| c2p4 | 6 | 7 | 201.4 | 4.963 | 8.186 | 7.938 | 7.795 | 7.647 | 3.223 | 2.975 | 7.69469 | 2.832 | 4.80672 | 4.97479 |
| c2p4 | 7 | 8 | 202.4 | 5.142 | 8.589 | 7.793 | 7.671 | 7.567 | 3.447 | 2.651 | 23.0925 | 2.529 | 4.60204 | 3.92305 |
| c2p4 | 8 | 9 | 203.4 | 5.274 | 7.148 | 6.987 | 6.905 | 6.833 | 1.874 | 1.713 | 8.59125 | 1.631 | 4.78692 | 4.20315 |
| c2p4 | 9 | 10 | 204.4 | 5.228 | 7.09 | 6.948 | 6.867 | 6.786 | 1.862 | 1.72 | 7.62621 | 1.639 | 4.7093 | 4.7093 |
| c2p4 | 10 | 11 | 205.4 | 4.878 | 8.196 | 7.887 | 7.739 | 7.605 | 3.318 | 3.009 | 9.31284 | 2.861 | 4.91858 | 4.45331 |
| c2p4 | 11 | 12 | 206.4 | 4.708 | 7.213 | 6.99 | 6.876 | 6.782 | 2.505 | 2.282 | 8.9022 | 2.168 | 4.99562 | 4.11919 |
| c2p4 | 12 | 13 | 207.4 | 5.113 | 7.868 | 7.607 | 7.492 | 7.387 | 2.755 | 2.494 | 9.47368 | 2.379 | 4.61107 | 4.2101 |
| c2p4 | 13 | 14 | 208.3 | 4.287 | 7.101 | 6.836 | 6.717 | 6.616 | 2.814 | 2.549 | 9.4172 | 2.43 | 4.6685 | 3.96234 |
| c2p4 | 14 | 15 | 209.3 | 4.366 | 7.8 | 7.083 | 6.914 | 6.754 | 3.434 | 2.717 | 20.8794 | 2.548 | 6.2201 | 5.88885 |

| Core Label | Segment depth start (cm) | Segment depth end (cm) | Overall Core Depth (cm) | Crucible (cruc) wt. (g) | Wet wt w/cruc (g) | Dry wt w/cruc (g) | After 550C w/cruc (g) | After 950C w/cruc (g) | Wet wt (g) | Dry wt (g) | % water | weight after 550C (g) | % org of dry wt | % inorg C of dry wt |
|---|---|---|---|---|---|---|---|---|---|---|---|---|---|---|
| c2p4 | 15 | 16 | 210.3 | 5.292 | 7.975 | 7.698 | 7.581 | 7.47 | 2.683 | 2.406 | 10.3243 | 2.289 | 4.86284 | 4.61347 |
| c2p4 | 16 | 17 | 211.3 | 4.724 | 7.338 | 7.044 | 6.933 | 6.825 | 2.614 | 2.32 | 11.2471 | 2.209 | 4.78448 | 4.65517 |
| c2p4 | 17 | 18 | 212.3 | 4.7 | 7.526 | 7.189 | 7.067 | 6.97 | 2.826 | 2.489 | 11.925 | 2.367 | 4.90157 | 3.89715 |
| c2p4 | 18 | 19 | 213.3 | 4.983 | 8.559 | 8.121 | 7.961 | 7.844 | 3.576 | 3.138 | 12.2483 | 2.978 | 5.09879 | 3.72849 |
| c2p4 | 19 | 20 | 214.3 | 5.328 | 8.107 | 7.767 | 7.647 | 7.557 | 2.779 | 2.439 | 12.2346 | 2.319 | 4.92005 | 3.69004 |
| c2p4 | 20 | 21 | 215.3 | 4.864 | 6.744 | 6.541 | 6.477 | 6.384 | 1.88 | 1.677 | 10.7979 | 1.613 | 3.81634 | 5.54562 |
| c2p4 | 21 | 22 | 216.3 | 4.909 | 6.515 | 6.355 | 6.279 | 6.231 | 1.606 | 1.446 | 9.96264 | 1.37 | 5.25588 | 3.3195 |
| c2p4 | 22 | 23 | 217.2 | 4.844 | 7.523 | 7.183 | 7.067 | 6.981 | 2.679 | 2.339 | 12.6913 | 2.223 | 4.95938 | 3.67678 |
| c2p4 | 23 | 24 | 218.2 | 5.067 | 8.17 | 7.735 | 7.604 | 7.507 | 3.103 | 2.668 | 14.0187 | 2.537 | 4.91004 | 3.63568 |
| c2p4 | 24 | 25 | 219.2 | 4.761 | 7.596 |  | 7.056 | 6.969 |  |  |  |  |  |  |
| c2p4 | 25 | 26 | 220.2 | 4.995 | 8.435 | 7.629 | 7.509 | 7.402 | 3.44 | 2.634 | 23.4302 | 2.514 | 4.55581 | 4.06226 |
| c2p4 | 26 | 27 | 221.2 | 4.807 | 7.322 | 6.93 | 6.828 | 6.747 | 2.515 | 2.123 | 15.5865 | 2.021 | 4.80452 | 3.81536 |
| c2p4 | 27 | 28 | 222.2 | 4.762 | 8.506 | 7.839 | 7.689 | 7.577 | 3.744 | 3.077 | 17.8152 | 2.927 | 4.87488 | 3.63991 |
| c2p4 | 28 | 29 | 223.2 | 4.961 | 7.843 | 7.33 | 7.207 | 7.128 | 2.882 | 2.369 | 17.8001 | 2.246 | 5.19206 | 3.33474 |
| c2p4 | 29 | 30 | 224.2 | 4.749 | 8.028 | 7.453 | 7.316 | 7.223 | 3.279 | 2.704 | 17.5358 | 2.567 | 5.06657 | 3.43935 |
| c2p4 | 30 | 31 | 225.2 | 5.138 | 7.491 | 7.064 | 6.974 | 6.907 | 2.353 | 1.926 | 18.147 | 1.836 | 4.6729 | 3.47871 |
| c2p4 | 31 | 32 | 226.1 | 5.143 | 8.614 | 7.963 | 7.83 | 7.727 | 3.471 | 2.82 | 18.7554 | 2.687 | 4.71631 | 3.65248 |
| c2p4 | 32 | 33 | 227.1 | 4.901 | 8.738 | 7.964 | 7.809 | 7.709 | 3.837 | 3.063 | 20.172 | 2.908 | 5.0604 | 3.26477 |
| c2p4 | 33 | 34 | 228.1 | 4.644 | 8.111 | 7.436 | 7.297 | 7.194 | 3.467 | 2.792 | 19.4693 | 2.653 | 4.97851 | 3.68911 |
| c2p4 | 34 | 35 | 229.1 | 5.09 | 8.454 | 7.711 | 7.583 | 7.471 | 3.364 | 2.621 | 22.0868 | 2.493 | 4.88363 | 4.27318 |
| c2p4 | 35 | 36 | 230.1 | 4.386 | 7.577 | 6.926 | 6.802 | 6.694 | 3.191 | 2.54 | 20.4011 | 2.416 | 4.88189 | 4.25197 |
| c2p4 | 36 | 37 | 231.1 | 4.822 | 7.577 | 7.009 | 6.9 | 6.819 | 2.755 | 2.187 | 20.6171 | 2.078 | 4.984 | 3.7037 |
| c2p4 | 37 | 38 | 232.1 | 4.838 | 9.159 | 8.252 | 8.085 | 7.959 | 4.321 | 3.414 | 20.9905 | 3.247 | 4.89162 | 3.69069 |
| c2p4 | 38 | 39 | 233.1 | 4.484 | 8.03 | 7.445 | 7.317 | 7.24 | 3.546 | 2.961 | 16.4975 | 2.833 | 4.32286 | 2.60047 |
| c2p4 | 39 | 40 | 234.1 | 4.938 | 8.181 | 7.537 | 7.413 | 7.325 | 3.243 | 2.599 | 19.8582 | 2.475 | 4.77107 | 3.38592 |
| c2p4 | 40 | 41 | 235 | 4.09 | 8.405 | 7.673 | 7.528 | 7.425 | 4.315 | 3.583 | 16.9641 | 3.438 | 4.04689 | 2.87469 |
| c2p4 | 41 | 42 | 236 | 4.555 | 7.503 | 6.867 | 6.748 | 6.639 | 2.948 | 2.312 | 21.5739 | 2.193 | 5.14706 | 4.71453 |
| c2p4 | 42 | 44.5 | 237.8 | 5.122 | 8.43 | 7.703 | 7.577 | 7.463 | 3.308 | 2.581 | 21.977 | 2.455 | 4.88183 | 4.41689 |
| c2p5 | 0 | 1 | 239.4 | 4.934 | 7.364 | 7.093 | 6.971 | 6.892 | 2.43 | 2.159 | 11.1523 | 2.037 | 5.65076 | 3.6591 |
| c2p5 | 1 | 2 | 240.2 | 4.959 | 7.327 | 7.067 | 6.944 | 6.867 | 2.368 | 2.108 | 10.9797 | 1.985 | 5.83491 | 3.65275 |
| c2p5 | 2 | 3 | 240.9 | 4.384 | 7.236 | 6.941 | 6.798 | 6.625 | 2.852 | 2.557 | 10.3436 | 2.414 | 5.59249 | 6.76574 |
| c2p5 | 3 | 4 | 241.7 | 4.901 | 8.053 | 7.701 | 7.546 | 7.383 | 3.152 | 2.8 | 11.1675 | 2.645 | 5.53571 | 5.82143 |
| c2p5 | 4 | 5 | 242.5 | 4.761 | 7.352 | 7.073 | 6.929 | 6.835 | 2.591 | 2.312 | 10.768 | 2.168 | 6.22837 | 4.06574 |
| c2p5 | 5 | 6 | 243.2 | 5.254 | 8.672 | 7.757 | 7.635 | 7.54 | 3.418 | 2.503 | 26.77 | 2.381 | 4.87415 | 3.79545 |

| Core Label | Segment depth start (cm) | Segment depth end (cm) | Overall Core Depth (cm) | Crucible (cruc) wt. (g) | Wet wt w/cruc (g) | Dry wt w/cruc (g) | After 550C w/cruc (g) | After 950C w/cruc (g) | Wet wt (g) | Dry wt (g) | % water | weight after 550C (g) | % org of dry wt | % inorg C of dry wt |
|---|---|---|---|---|---|---|---|---|---|---|---|---|---|---|
| c2p5 | 6 | 7 | 244 | 4.743 | 8.283 | 7.835 | 7.659 | spilled | 3.54 | 3.092 | 12.6554 | 2.916 | 5.69211 | |
| c2p5 | 7 | 8 | 244.8 | 4.557 | 7.04 | 6.776 | 6.648 | 6.547 | 2.483 | 2.219 | 10.6323 | 2.091 | 5.76836 | 4.5516 |
| c2p5 | 8 | 9 | 245.6 | 4.806 | 7.241 | 6.901 | 6.777 | 6.698 | 2.435 | 2.095 | 13.963 | 1.971 | 5.91885 | 3.77088 |
| c2p5 | 9 | 10 | 246.3 | 4.841 | 8.625 | 7.989 | 7.82 | 7.708 | 3.784 | 3.148 | 16.8076 | 2.979 | 5.36849 | 3.55781 |
| c2p5 | 10 | 11 | 247.1 | 5.12 | 8.453 | 7.903 | 7.748 | 7.648 | 3.333 | 2.783 | 16.5017 | 2.628 | 5.56953 | 3.59324 |
| c2p5 | 11 | 12 | 247.9 | 5.135 | 8.486 | 7.953 | 7.799 | 7.699 | 3.351 | 2.818 | 15.9057 | 2.664 | 5.46487 | 3.54862 |
| c2p5 | 12 | 13 | 248.6 | 4.822 | 8.67 | 8.045 | 7.865 | 7.744 | 3.848 | 3.223 | 16.2422 | 3.043 | 5.58486 | 3.75427 |
| c2p5 | 13 | 14 | 249.4 | 4.983 | 8.763 | 8.146 | 7.94 | 7.818 | 3.78 | 3.163 | 16.3228 | 2.957 | 6.5128 | 3.8571 |
| c2p5 | 14 | 15 | 250.2 | 4.691 | 8.678 | 7.925 | 7.746 | 7.632 | 3.987 | 3.234 | 18.8864 | 3.055 | 5.53494 | 3.52505 |
| c2p5 | 15 | 16 | 251 | 5.231 | 8.759 | 7.828 | 7.694 | 7.593 | 3.528 | 2.597 | 26.3889 | 2.463 | 5.1598 | 3.8891 |
| c2p5 | 16 | 17 | 251.7 | 4.643 | 8.211 | 7.567 | 7.402 | 7.298 | 3.568 | 2.924 | 18.0493 | 2.759 | 5.64295 | 3.55677 |
| c2p5 | 17 | 18 | 252.5 | 4.349 | 8.342 | 7.514 | 7.354 | 7.228 | 3.993 | 3.165 | 20.7363 | 3.005 | 5.05529 | 3.98104 |
| c2p5 | 18 | 19 | 253.3 | 5.064 | 9.126 | 8.25 | 8.089 | 7.972 | 4.062 | 3.186 | 21.5657 | 3.025 | 5.05336 | 3.67232 |
| c2p5 | 19 | 20 | 254 | 4.377 | 8.81 | 7.823 | 7.656 | 7.534 | 4.433 | 3.446 | 22.2648 | 3.279 | 4.8462 | 3.54034 |
| c2p5 | 20 | 21 | 254.8 | 5.115 | 8.951 | 8.044 | 7.894 | 7.781 | 3.836 | 2.929 | 23.6444 | 2.779 | 5.1212 | 3.85797 |
| c2p5 | 21 | 22 | 255.6 | 4.603 | 8.331 | 7.481 | 7.334 | 7.236 | 3.728 | 2.878 | 22.8004 | 2.731 | 5.10771 | 3.40514 |
| c2p5 | 22 | 23 | 256.4 | 5.22 | 9.382 | 8.415 | 8.255 | 8.143 | 4.162 | 3.195 | 23.234 | 3.035 | 5.00782 | 3.50548 |
| c2p5 | 23 | 24 | 257.1 | 4.552 | 8.082 | 7.212 | 7.072 | 6.971 | 3.53 | 2.66 | 24.6459 | 2.52 | 5.26316 | 3.79699 |
| c2p5 | 24 | 25 | 257.9 | 4.899 | 8.358 | 7.427 | 7.294 | 7.196 | 3.459 | 2.528 | 26.9153 | 2.395 | 5.26108 | 3.87658 |
| c2p5 | 25 | 26 | 258.7 | 4.718 | 9.176 | 8.057 | 7.889 | 7.777 | 4.458 | 3.339 | 25.1009 | 3.171 | 5.03145 | 3.3543 |
| c2p5 | 26 | 27 | 259.4 | 4.837 | 9.374 | 8.22 | 8.045 | 7.926 | 4.537 | 3.383 | 25.4353 | 3.208 | 5.17292 | 3.51759 |
| c2p5 | 27 | 28 | 260.2 | 5.254 | 9.502 | 8.391 | 8.225 | 8.106 | 4.248 | 3.137 | 26.1535 | 2.971 | 5.29168 | 3.79343 |
| c2p5 | 28 | 29 | 261 | 4.844 | 8.101 | 7.247 | 7.11 | 6.97 | 3.257 | 2.403 | 26.2204 | 2.266 | 5.70121 | 5.82605 |
| c2p5 | 29 | 30 | 261.8 | 4.799 | 8.693 | 7.654 | 7.51 | 7.351 | 3.894 | 2.855 | 26.6821 | 2.711 | 5.04378 | 5.56918 |
| c2p5 | 30 | 31 | 262.5 | 4.678 | 7.916 | 7.052 | 6.931 | 6.781 | 3.238 | 2.374 | 26.6831 | 2.253 | 5.09688 | 6.31845 |
| c2p5 | 31 | 32 | 263.3 | 4.535 | 8.256 | 7.275 | 7.135 | 6.968 | 3.721 | 2.74 | 26.3639 | 2.6 | 5.10949 | 6.09489 |
| c2p5 | 32 | 33 | 264.1 | 4.377 | 7.402 | 6.523 | 6.417 | 6.18 | 3.025 | 2.146 | 29.0579 | 2.04 | 4.93942 | 11.0438 |
| c2p5 | 33 | 34 | 264.8 | 4.546 | 8.457 | 7.658 | 7.507 | 7.282 | 3.911 | 3.112 | 20.4296 | 2.961 | 4.85219 | 7.23008 |
| c2p5 | 34 | 35 | 265.6 | 4.761 | 8.766 | 7.904 | 7.747 | 7.575 | 4.005 | 3.143 | 21.5231 | 2.986 | 4.99523 | 5.47248 |
| c2p6 | 0 | 1 | 266.6 | 4.901 | 7.944 | 7.165 | 7.037 | 6.936 | 3.043 | 2.264 | 25.5997 | 2.136 | 5.65371 | 4.46113 |
| c2p6 | 1 | 2 | 267.9 | 4.987 | 7.589 | 6.966 | 6.849 | 6.763 | 2.602 | 1.979 | 23.9431 | 1.862 | 5.91208 | 4.34563 |
| c2p6 | 2 | 3 | 269.2 | 5.006 | 8.127 | 7.38 | 7.251 | 7.134 | 3.121 | 2.374 | 23.9346 | 2.245 | 5.43387 | 4.92839 |
| c2p6 | 3 | 4 | 270.4 | 4.552 | 8.023 | 7.128 | 6.983 | 6.846 | 3.471 | 2.576 | 25.7851 | 2.431 | 5.62888 | 5.31832 |
| c2p6 | 4 | 5 | 271.7 | 4.603 | 7.59 | 6.84 | 6.715 | 6.62 | 2.987 | 2.237 | 25.1088 | 2.112 | 5.58784 | 4.24676 |

| Core Label | Segment depth start (cm) | Segment depth end (cm) | Overall Core Depth (cm) | Crucible (cruc) wt. (g) | Wet wt w/cruc (g) | Dry wt w/cruc (g) | After 550C w/cruc (g) | After 950C w/cruc (g) | Wet wt (g) | Dry wt (g) | % water | weight after 550C (g) | % org of dry wt | % inorg C of dry wt |
|---|---|---|---|---|---|---|---|---|---|---|---|---|---|---|
| c2p6 | 5 | 6 | 272.9 | 4.677 | 7.812 | 7.012 | 6.881 | 6.79 | 3.135 | 2.335 | 25.5183 | 2.204 | 5.61028 | 3.89722 |
| c2p6 | 6 | 7 | 274.2 | 4.842 | 7.768 | 7.058 | 6.924 | 6.842 | 2.926 | 2.216 | 24.2652 | 2.082 | 6.04693 | 3.70036 |
| c2p6 | 7 | 8 | 275.5 | 4.841 | 7.886 | 7.14 | 7.005 | 6.913 | 3.045 | 2.299 | 24.4992 | 2.164 | 5.87212 | 4.00174 |
| c2p6 | 8 | 9 | 276.7 | 4.378 | 7.629 | 6.809 | 6.66 | 6.562 | 3.251 | 2.431 | 25.223 | 2.282 | 6.12916 | 4.03126 |
| c2p6 | 9 | 10 | 278 | 5.218 | 8.574 | 7.728 | 7.598 | 7.507 | 3.356 | 2.51 | 25.2086 | 2.38 | 5.17928 | 3.6255 |
| c2p6 | 10 | 11 | 279.3 | 4.802 | 8.406 | 7.498 | 7.342 | 7.228 | 3.604 | 2.696 | 25.1942 | 2.54 | 5.78635 | 4.22849 |
| c2p6 | 11 | 12 | 280.5 | 5.295 | 9.115 | 8.155 | 8.005 | 7.907 | 3.82 | 2.86 | 25.1309 | 2.71 | 5.24476 | 3.42657 |
| c2p6 | 12 | 13 | 281.8 | 4.824 | 8.111 | 7.266 | 7.133 | 6.993 | 3.287 | 2.442 | 25.7073 | 2.309 | 5.44636 | 5.73301 |
| c2p6 | 13 | 14 | 283.1 | 4.936 | 8.757 | 7.741 | 7.578 | 7.428 | 3.821 | 2.805 | 26.5899 | 2.642 | 5.81105 | 5.34759 |
| c2p6 | 14 | 15 | 284.3 | 4.864 | 8.478 | 7.567 | 7.42 | 7.257 | 3.614 | 2.703 | 25.2075 | 2.556 | 5.4384 | 6.03034 |
| c2p6 | 15 | 16 | 285.6 | 4.554 | 7.436 | 6.847 | 6.719 | 6.542 | 2.882 | 2.293 | 20.4372 | 2.165 | 5.58221 | 7.71915 |
| c2p6 | 16 | 17 | 286.8 | 5.113 | 7.902 | 7.334 | 7.221 | 7.061 | 2.789 | 2.221 | 20.3657 | 2.108 | 5.0878 | 7.20396 |
| c2p6 | 17 | 18 | 288.1 | 4.984 | 9.538 | 8.57 | 8.383 | 8.193 | 4.554 | 3.586 | 21.256 | 3.399 | 5.21472 | 5.29838 |
| c2p6 | 18 | 19 | 289.4 | 5.275 | 8.341 | 7.651 | 7.525 | 7.401 | 3.066 | 2.376 | 22.5049 | 2.25 | 5.30303 | 5.21886 |

Appendix 5. LOMC1 High-Resolution Magnetic Susceptibility data

| Core Label | Segment Depth (cm) | Core Depth (cm) | HRMS (SI) | | Core Label | Segment Depth (cm) | Core Depth (cm) | HRMS (SI) |
|---|---|---|---|---|---|---|---|---|
| C1P1 | 0 | 0 | 6 | | C1P1 | 24 | 24.5 | 1.6 |
| C1P1 | 0.5 | 0.5 | 1.8 | | C1P1 | 24.5 | 25 | 2.7 |
| C1P1 | 1 | 1 | 0.8 | | C1P1 | 25 | 25.5 | 1.5 |
| C1P1 | 1.5 | 1.5 | 0.5 | | C1P1 | 25.5 | 26 | 1.7 |
| C1P1 | 2 | 2 | 2.1 | | C1P1 | 26 | 26.5 | 2.8 |
| C1P1 | 2.5 | 2.6 | 2.8 | | C1P1 | 26.5 | 27 | 3.1 |
| C1P1 | 3 | 3.1 | 2.4 | | C1P1 | 27 | 27.5 | 2.7 |
| C1P1 | 3.5 | 3.6 | 3.6 | | C1P1 | 27.5 | 28.1 | 3.7 |
| C1P1 | 4 | 4.1 | 4.8 | | C1P1 | 28 | 28.6 | 4.4 |
| C1P1 | 4.5 | 4.6 | 5.5 | | C1P1 | 28.5 | 29.1 | 4 |
| C1P1 | 5 | 5.1 | 6 | | C1P1 | 29 | 29.6 | 2.9 |
| C1P1 | 5.5 | 5.6 | 7.3 | | C1P1 | 29.5 | 30.1 | 2.2 |
| C1P1 | 6 | 6.1 | 9.5 | | C1P1 | 30 | 30.6 | 2.7 |
| C1P1 | 6.5 | 6.6 | 11.3 | | C1P1 | 30.5 | 31.1 | 3.2 |
| C1P1 | 7 | 7.1 | 13.8 | | C1P1 | 31 | 31.6 | 4.1 |
| C1P1 | 7.5 | 7.7 | 16.3 | | C1P1 | 31.5 | 32.1 | 4.7 |
| C1P1 | 8 | 8.2 | 13.9 | | C1P1 | 32 | 32.6 | 5.6 |
| C1P1 | 8.5 | 8.7 | 10.8 | | C1P1 | 32.5 | 33.2 | 6.4 |
| C1P1 | 9 | 9.2 | 10.2 | | C1P1 | 33 | 33.7 | 7.4 |
| C1P1 | 9.5 | 9.7 | 9.2 | | C1P1 | 33.5 | 34.2 | 8.3 |
| C1P1 | 10 | 10.2 | 8.7 | | C1P1 | 34 | 34.7 | 9.1 |
| C1P1 | 10.5 | 10.7 | 8.8 | | C1P1 | 34.5 | 35.2 | 9.1 |
| C1P1 | 11 | 11.2 | 8.4 | | C1P1 | 35 | 35.7 | 5.3 |
| C1P1 | 11.5 | 11.7 | 7.7 | | C1P1 | 35.5 | 36.2 | 8 |
| C1P1 | 12 | 12.2 | 7.2 | | C1P1 | 36 | 36.7 | 6.8 |
| C1P1 | 12.5 | 12.8 | 6.4 | | C1P1 | 36.5 | 37.2 | 5.8 |
| C1P1 | 13 | 13.3 | 5.8 | | C1P1 | 37 | 37.7 | 5.2 |
| C1P1 | 13.5 | 13.8 | 5.7 | | C1P1 | 37.5 | 38.3 | 7.4 |
| C1P1 | 14 | 14.3 | 5.9 | | C1P1 | 38 | 38.8 | 11.2 |
| C1P1 | 14.5 | 14.8 | 5.5 | | C1P1 | 38.5 | 39.3 | 14.3 |
| C1P1 | 15 | 15.3 | 5.5 | | C1P1 | 39 | 39.8 | 15.2 |
| C1P1 | 15.5 | 15.8 | 4.9 | | C1P1 | 39.5 | 40.3 | 15.5 |
| C1P1 | 16 | 16.3 | 4.7 | | C1P1 | 40 | 40.8 | 16.2 |
| C1P1 | 16.5 | 16.8 | 3.6 | | C1P1 | 40.5 | 41.3 | 19.1 |
| C1P1 | 17 | 17.3 | 2.6 | | C1P1 | 41 | 41.8 | 20.3 |
| C1P1 | 17.5 | 17.9 | 2.3 | | C1P1 | 41.5 | 42.3 | 24 |
| C1P1 | 18 | 18.4 | 2.4 | | C1P1 | 42 | 42.8 | 25.4 |
| C1P1 | 18.5 | 18.9 | 2 | | C1P1 | 42.5 | 43.4 | 25.6 |
| C1P1 | 19 | 19.4 | 1.8 | | C1P1 | 43 | 43.9 | 27.2 |
| C1P1 | 19.5 | 19.9 | 1.9 | | C1P1 | 43.5 | 44.4 | 29.6 |
| C1P1 | 20 | 20.4 | 1.8 | | C1P1 | 44 | 44.9 | 28.9 |
| C1P1 | 20.5 | 20.9 | 1.6 | | C1P1 | 44.5 | 45.4 | 26.2 |
| C1P1 | 21 | 21.4 | 1.7 | | C1P1 | 45 | 45.9 | 27.5 |
| C1P1 | 21.5 | 21.9 | 1.5 | | C1P1 | 45.5 | 46.4 | 28.3 |
| C1P1 | 22 | 22.4 | 1.7 | | C1P1 | 46 | 46.9 | 28 |
| C1P1 | 22.5 | 23 | 1.5 | | C1P1 | 46.5 | 47.4 | 27.8 |
| C1P1 | 23 | 23.5 | 1.5 | | C1P1 | 47 | 47.9 | 26.9 |
| C1P1 | 23.5 | 24 | 2.6 | | C1P1 | 47.5 | 48.5 | 26.3 |

| Core Label | Segment Depth (cm) | Core Depth (cm) | HRMS (SI) | | Core Label | Segment Depth (cm) | Core Depth (cm) | HRMS (SI) |
|---|---|---|---|---|---|---|---|---|
| C1P1 | 48 | 49 | 25.6 | | C1P1 | 73 | 74.5 | 9.3 |
| C1P1 | 48.5 | 49.5 | 26.4 | | C1P1 | 73.5 | 75 | 10 |
| C1P1 | 49 | 50 | 27.1 | | C1P1 | 74 | 75.5 | 9.8 |
| C1P1 | 49.5 | 50.5 | 27 | | C1P1 | 74.5 | 76 | 9.7 |
| C1P1 | 50 | 51 | 23.9 | | C1P1 | 75 | 76.5 | 9.4 |
| C1P1 | 50.5 | 51.5 | 23.6 | | C1P1 | 75.5 | 77 | 9.4 |
| C1P1 | 51 | 52 | 24.1 | | C1P1 | 76 | 77.5 | 9 |
| C1P1 | 51.5 | 52.5 | 24.6 | | C1P1 | 76.5 | 78 | 2.7 |
| C1P1 | 52 | 53 | 13.8 | | C1P1 | 77 | 78.5 | 7.2 |
| C1P1 | 52.5 | 53.6 | 19.4 | | C1P1 | 77.5 | 79.1 | 2.5 |
| C1P1 | 53 | 54.1 | 17 | | C1P1 | 78 | 79.6 | 2.8 |
| C1P1 | 53.5 | 54.6 | 17.8 | | C1P1 | 78.5 | 80.1 | 3.6 |
| C1P1 | 54 | 55.1 | 19 | | C1P1 | 79 | 80.6 | 4.1 |
| C1P1 | 54.5 | 55.6 | 9.9 | | C1P1 | 79.5 | 81.1 | 8.6 |
| C1P1 | 55 | 56.1 | 7 | | C1P1 | 80 | 81.6 | 9.1 |
| C1P1 | 55.5 | 56.6 | 1.7 | | C1P1 | 80.5 | 82.1 | 8.5 |
| C1P1 | 56 | 57.1 | 0.7 | | C1P1 | 81 | 82.6 | 6.2 |
| C1P1 | 56.5 | 57.6 | 1.9 | | C1P1 | 81.5 | 83.1 | 1.8 |
| C1P1 | 57 | 58.1 | 3.5 | | C1P1 | 82 | 83.6 | 6 |
| C1P1 | 57.5 | 58.7 | 6.1 | | C1P1 | 82.5 | 84.2 | 8 |
| C1P1 | 58 | 59.2 | 9.1 | | C1P1 | 83 | 84.7 | 8.6 |
| C1P1 | 58.5 | 59.7 | 11.3 | | C1P1 | 83.5 | 85.2 | 9.2 |
| C1P1 | 59 | 60.2 | 11.2 | | C1P1 | 84 | 85.7 | 8.5 |
| C1P1 | 59.5 | 60.7 | 16.5 | | C1P1 | 84.5 | 86.2 | 12.5 |
| C1P1 | 60 | 61.2 | 10.6 | | C1P1 | 85 | 86.7 | 10.5 |
| C1P1 | 60.5 | 61.7 | 12.3 | | C1P1 | 85.5 | 87.2 | 9.4 |
| C1P1 | 61 | 62.2 | 21.3 | | C1P1 | 86 | 87.7 | 7.8 |
| C1P1 | 61.5 | 62.7 | 19.9 | | C1P1 | 86.5 | 88.2 | 7.5 |
| C1P1 | 62 | 63.2 | 13.4 | | C1P1 | 87 | 88.7 | 6.9 |
| C1P1 | 62.5 | 63.8 | 7.3 | | C1P1 | 87.5 | 89.3 | 4.8 |
| C1P1 | 63 | 64.3 | 8.9 | | C1P1 | 88 | 89.8 | 4 |
| C1P1 | 63.5 | 64.8 | 9 | | C1P1 | 88.5 | 90.3 | 3.4 |
| C1P1 | 64 | 65.3 | 8.7 | | C1P1 | 89 | 90.8 | 3 |
| C1P1 | 64.5 | 65.8 | 8.1 | | C1P1 | 89.5 | 91.3 | 2.6 |
| C1P1 | 65 | 66.3 | 7.2 | | C1P1 | 90 | 91.8 | 1.7 |
| C1P1 | 65.5 | 66.8 | 7.1 | | C1P1 | 90.5 | 92.3 | 0.3 |
| C1P1 | 66 | 67.3 | 5 | | C1P1 | 91 | 92.8 | 1.2 |
| C1P1 | 66.5 | 67.8 | 5.7 | | C1P1 | 91.5 | 93.3 | 2.1 |
| C1P1 | 67 | 68.3 | 6.4 | | C1P1 | 92 | 93.8 | 2.8 |
| C1P1 | 67.5 | 68.9 | 6.7 | | C1P1 | 92.5 | 94.4 | 3.3 |
| C1P1 | 68 | 69.4 | 6.6 | | C1P1 | 93 | 94.9 | 2.7 |
| C1P1 | 68.5 | 69.9 | 6.6 | | C1P1 | 93.5 | 95.4 | 2 |
| C1P1 | 69 | 70.4 | 6.3 | | C1P1 | 94 | 95.9 | 1.5 |
| C1P1 | 69.5 | 70.9 | 6.3 | | C1P1 | 94.5 | 96.4 | 1.6 |
| C1P1 | 70 | 71.4 | 6.6 | | C1P1 | 95 | 96.9 | 1.5 |
| C1P1 | 70.5 | 71.9 | 6.4 | | C1P1 | 95.5 | 97.4 | 1.4 |
| C1P1 | 71 | 72.4 | 7.6 | | C1P1 | 96 | 97.9 | 1.5 |
| C1P1 | 71.5 | 72.9 | 8.1 | | C1P1 | 96.5 | 98.4 | 0.8 |
| C1P1 | 72 | 73.4 | 7.7 | | C1P1 | 97 | 98.9 | 0.2 |
| C1P1 | 72.5 | 74 | 8.5 | | C1P1 | 97.5 | 99.5 | 0.3 |

| Core Label | Segment Depth (cm) | Core Depth (cm) | HRMS (SI) | | Core Label | Segment Depth (cm) | Core Depth (cm) | HRMS (SI) |
|---|---|---|---|---|---|---|---|---|
| C1P1 | 98 | 100 | 0.2 | | C1P2 | 23.5 | 127.2 | 5.7 |
| C1P1 | 98.5 | 100.5 | 0.3 | | C1P2 | 24 | 127.7 | 7 |
| C1P1 | 99 | 101 | 0.7 | | C1P2 | 24.5 | 128.2 | 7.2 |
| C1P2 | 0 | 102 | | | C1P2 | 25 | 128.8 | 6.2 |
| C1P2 | 0.5 | 102.5 | 1.3 | | C1P2 | 25.5 | 129.3 | 6 |
| C1P2 | 1 | 103.1 | 0.7 | | C1P2 | 26 | 129.8 | 6.3 |
| C1P2 | 1.5 | 103.6 | 1.1 | | C1P2 | 26.5 | 130.4 | 7 |
| C1P2 | 2 | 104.1 | 6.1 | | C1P2 | 27 | 130.9 | 7.3 |
| C1P2 | 2.5 | 104.7 | 7.1 | | C1P2 | 27.5 | 131.4 | 8.1 |
| C1P2 | 3 | 105.2 | 5.6 | | C1P2 | 28 | 132 | 8.9 |
| C1P2 | 3.5 | 105.7 | 3.6 | | C1P2 | 28.5 | 132.5 | 6.6 |
| C1P2 | 4 | 106.3 | 4.7 | | C1P2 | 29 | 133 | 7.1 |
| C1P2 | 4.5 | 106.8 | | | C1P2 | 29.5 | 133.6 | 4.8 |
| C1P2 | 5 | 107.4 | 1.1 | | C1P2 | 30 | 134.1 | 3.6 |
| C1P2 | 5.5 | 107.9 | 0.5 | | C1P2 | 30.5 | 134.6 | 4.3 |
| C1P2 | 6 | 108.4 | 0.5 | | C1P2 | 31 | 135.2 | 4.4 |
| C1P2 | 6.5 | 109 | 0.6 | | C1P2 | 31.5 | 135.7 | 5.5 |
| C1P2 | 7 | 109.5 | 0.6 | | C1P2 | 32 | 136.3 | 12.1 |
| C1P2 | 7.5 | 110 | 0.7 | | C1P2 | 32.5 | 136.8 | 21.7 |
| C1P2 | 8 | 110.6 | 0.9 | | C1P2 | 33 | 137.3 | 38.3 |
| C1P2 | 8.5 | 111.1 | 1.7 | | C1P2 | 33.5 | 137.9 | 47 |
| C1P2 | 9 | 111.6 | 2.3 | | C1P2 | 34 | 138.4 | 50.5 |
| C1P2 | 9.5 | 112.2 | 2.3 | | C1P2 | 34.5 | 138.9 | 60.3 |
| C1P2 | 10 | 112.7 | 1.9 | | C1P2 | 35 | 139.5 | 87.5 |
| C1P2 | 10.5 | 113.2 | 1.3 | | C1P2 | 35.5 | 140 | 97.2 |
| C1P2 | 11 | 113.8 | 0.9 | | C1P2 | 36 | 140.5 | 68.1 |
| C1P2 | 11.5 | 114.3 | 0 | | C1P2 | 36.5 | 141.1 | 61.6 |
| C1P2 | 12 | 114.8 | -0.1 | | C1P2 | 37 | 141.6 | 66.4 |
| C1P2 | 12.5 | 115.4 | -0.2 | | C1P2 | 37.5 | 142.1 | 83.1 |
| C1P2 | 13 | 115.9 | -0.5 | | C1P2 | 38 | 142.7 | 77.7 |
| C1P2 | 13.5 | 116.5 | 0 | | C1P2 | 38.5 | 143.2 | 49.1 |
| C1P2 | 14 | 117 | 0 | | C1P2 | 39 | 143.7 | 16.4 |
| C1P2 | 14.5 | 117.5 | 0.1 | | C1P2 | 39.5 | 144.3 | 13.5 |
| C1P2 | 15 | 118.1 | 0.2 | | C1P2 | 40 | 144.8 | 35.4 |
| C1P2 | 15.5 | 118.6 | 0.2 | | C1P2 | 40.5 | 145.4 | 49.6 |
| C1P2 | 16 | 119.1 | 0 | | C1P2 | 41 | 145.9 | 47 |
| C1P2 | 16.5 | 119.7 | 0.1 | | C1P2 | 41.5 | 146.4 | 38.2 |
| C1P2 | 17 | 120.2 | 0 | | C1P2 | 42 | 147 | 43.4 |
| C1P2 | 17.5 | 120.7 | 0.2 | | C1P2 | 42.5 | 147.5 | 55.3 |
| C1P2 | 18 | 121.3 | 0.2 | | C1P2 | 43 | 148 | 49.3 |
| C1P2 | 18.5 | 121.8 | 0.6 | | C1P2 | 43.5 | 148.6 | 34.9 |
| C1P2 | 19 | 122.3 | 1 | | C1P2 | 44 | 149.1 | 23.3 |
| C1P2 | 19.5 | 122.9 | 1.1 | | C1P2 | 44.5 | 149.6 | 22.1 |
| C1P2 | 20 | 123.4 | 1 | | C1P2 | 45 | 150.2 | 21.5 |
| C1P2 | 20.5 | 123.9 | 0.7 | | C1P2 | 45.5 | 150.7 | 21.1 |
| C1P2 | 21 | 124.5 | 0.3 | | C1P2 | 46 | 151.2 | 25.3 |
| C1P2 | 21.5 | 125 | 0.9 | | C1P2 | 46.5 | 151.8 | 27.6 |
| C1P2 | 22 | 125.5 | 1.3 | | C1P2 | 47 | 152.3 | 28.1 |
| C1P2 | 22.5 | 126.1 | 1.1 | | C1P2 | 47.5 | 152.8 | 29.2 |
| C1P2 | 23 | 126.6 | 2.2 | | C1P2 | 48 | 153.4 | 37.5 |

| Core Label | Segment Depth (cm) | Core Depth (cm) | HRMS (SI) |
|---|---|---|---|
| C1P2 | 48.5 | 153.9 | 51.6 |
| C1P2 | 49 | 154.5 | 45.4 |
| C1P2 | 49.5 | 155 | 34.2 |
| C1P2 | 50 | 155.5 | 52.3 |
| C1P2 | 50.5 | 156.1 | 75.5 |
| C1P2 | 51 | 156.6 | 52.8 |
| C1P2 | 51.5 | 157.1 | 31 |
| C1P2 | 52 | 157.7 | 35.1 |
| C1P2 | 52.5 | 158.2 | 37.4 |
| C1P2 | 53 | 158.7 | 37.6 |
| C1P2 | 53.5 | 159.3 | 38.3 |
| C1P2 | 54 | 159.8 | 46.1 |
| C1P2 | 54.5 | 160.3 | 32.8 |
| C1P2 | 55 | 160.9 | 25.6 |
| C1P2 | 55.5 | 161.4 | 43.2 |
| C1P2 | 56 | 161.9 | 66 |
| C1P2 | 56.5 | 162.5 | 66.1 |
| C1P2 | 57 | 163 | 68.7 |
| C1P2 | 57.5 | 163.5 | 56.9 |
| C1P2 | 58 | 164.1 | 53.7 |
| C1P2 | 58.5 | 164.6 | 45.9 |
| C1P2 | 59 | 165.2 | 59.4 |
| C1P2 | 59.5 | 165.7 | 63.6 |
| C1P2 | 60 | 166.2 | 56.2 |
| C1P2 | 60.5 | 166.8 | 43.8 |
| C1P2 | 61 | 167.3 | 49.6 |
| C1P2 | 61.5 | 167.8 | 33.1 |
| C1P2 | 62 | 168.4 | 32.1 |
| C1P2 | 62.5 | 168.9 | 47.8 |
| C1P2 | 63 | 169.4 | 52.5 |
| C1P2 | 63.5 | 170 | 51.3 |
| C1P2 | 64 | 170.5 | 67 |
| C1P2 | 64.5 | 171 | 70.6 |
| C1P2 | 65 | 171.6 | 46 |
| C1P2 | 65.5 | 172.1 | 26.7 |
| C1P2 | 66 | 172.6 | 8.8 |
| C1P2 | 66.5 | 173.2 | 4.9 |
| C1P2 | 67 | 173.7 | 4.6 |
| C1P2 | 67.5 | 174.3 | 6.4 |
| C1P2 | 68 | 174.8 | |
| C1P2 | 68.5 | 175.3 | 6.6 |
| C1P2 | 69 | 175.9 | 24.7 |
| C1P2 | 69.5 | 176.4 | 34.7 |
| C1P2 | 70 | 176.9 | 5.9 |
| C1P2 | 70.5 | 177.5 | 4.4 |
| C1P2 | 71 | 178 | 3.3 |
| | | | |
| C1P3 | 0 | 178 | 4 |
| C1P3 | 0.5 | 178.5 | 9.1 |
| C1P3 | 1 | 179.1 | 35.4 |

| Core Label | Segment Depth (cm) | Core Depth (cm) | HRMS (SI) |
|---|---|---|---|
| C1P3 | 1.5 | 179.6 | 43.5 |
| C1P3 | 2 | 180.1 | 28.8 |
| C1P3 | 2.5 | 180.6 | 17.5 |
| C1P3 | 3 | 181.2 | 11.6 |
| C1P3 | 3.5 | 181.7 | 11.3 |
| C1P3 | 4 | 182.2 | 14.8 |
| C1P3 | 4.5 | 182.7 | 16.3 |
| C1P3 | 5 | 183.3 | 26.9 |
| C1P3 | 5.5 | 183.8 | 20.4 |
| C1P3 | 6 | 184.3 | 12.9 |
| C1P3 | 6.5 | 184.8 | 7.8 |
| C1P3 | 7 | 185.4 | 7.1 |
| C1P3 | 7.5 | 185.9 | 9 |
| C1P3 | 8 | 186.4 | 10.8 |
| C1P3 | 8.5 | 186.9 | 12.5 |
| C1P3 | 9 | 187.5 | 6.7 |
| C1P3 | 9.5 | 188 | 7.7 |
| C1P3 | 10 | 188.5 | 13.7 |
| C1P3 | 10.5 | 189 | 20.8 |
| C1P3 | 11 | 189.6 | 25.4 |
| C1P3 | 11.5 | 190.1 | 36.2 |
| C1P3 | 12 | 190.6 | 36.3 |
| C1P3 | 12.5 | 191.1 | 35.6 |
| C1P3 | 13 | 191.7 | 40.1 |
| C1P3 | 13.5 | 192.2 | 47.7 |
| C1P3 | 14 | 192.7 | 51.1 |
| C1P3 | 14.5 | 193.2 | 51.7 |
| C1P3 | 15 | 193.8 | 56.1 |
| C1P3 | 15.5 | 194.3 | 49.5 |
| C1P3 | 16 | 194.8 | 39.2 |
| C1P3 | 16.5 | 195.3 | 44.2 |
| C1P3 | 17 | 195.9 | 39.5 |
| C1P3 | 17.5 | 196.4 | 38.6 |
| C1P3 | 18 | 196.9 | 45.9 |
| C1P3 | 18.5 | 197.4 | 39 |
| C1P3 | 19 | 198 | 23.4 |
| C1P3 | 19.5 | 198.5 | 10.6 |
| C1P3 | 20 | 199 | 2.4 |

Appendix 6. LOMC2 High-Resolution Magnetic Susceptibility Data

| Core Label | Segment Depth (cm) | Core Depth (cm) | HRMS (SI) | | Core Label | Segment Depth (cm) | Core Depth (cm) | HRMS (SI) |
|---|---|---|---|---|---|---|---|---|
| C2P2 | 0 | 100 | 3.9 | | C2P2 | 24 | 120.7 | 54.5 |
| C2P2 | 0.5 | 100.4 | 1.2 | | C2P2 | 24.5 | 121.2 | 58.7 |
| C2P2 | 1 | 100.9 | 0.4 | | C2P2 | 25 | 121.6 | 63.1 |
| C2P2 | 1.5 | 101.3 | 0 | | C2P2 | 25.5 | 122 | 77.8 |
| C2P2 | 2 | 101.7 | 0.1 | | C2P2 | 26 | 122.5 | 62.2 |
| C2P2 | 2.5 | 102.2 | 0.7 | | C2P2 | 26.5 | 122.9 | 70.6 |
| C2P2 | 3 | 102.6 | 1.2 | | C2P2 | 27 | 123.3 | 76.2 |
| C2P2 | 3.5 | 103 | 1.4 | | C2P2 | 27.5 | 123.8 | 70.9 |
| C2P2 | 4 | 103.5 | 1.4 | | C2P2 | 28 | 124.2 | 88.4 |
| C2P2 | 4.5 | 103.9 | 1.7 | | C2P2 | 28.5 | 124.6 | 62.1 |
| C2P2 | 5 | 104.3 | 2.7 | | C2P2 | 29 | 125 | 56.4 |
| C2P2 | 5.5 | 104.8 | 3.2 | | C2P2 | 29.5 | 125.5 | 56.5 |
| C2P2 | 6 | 105.2 | 3.4 | | C2P2 | 30 | 125.9 | 55.3 |
| C2P2 | 6.5 | 105.6 | 3 | | C2P2 | 30.5 | 126.3 | 55.9 |
| C2P2 | 7 | 106 | 2.5 | | C2P2 | 31 | 126.8 | 53 |
| C2P2 | 7.5 | 106.5 | 2.6 | | C2P2 | 31.5 | 127.2 | 55.6 |
| C2P2 | 8 | 106.9 | 2.8 | | C2P2 | 32 | 127.6 | 54.1 |
| C2P2 | 8.5 | 107.3 | 2.8 | | C2P2 | 32.5 | 128.1 | 48.4 |
| C2P2 | 9 | 107.8 | 2.9 | | C2P2 | 33 | 128.5 | 35.2 |
| C2P2 | 9.5 | 108.2 | 2.8 | | C2P2 | 33.5 | 128.9 | 21.2 |
| C2P2 | 10 | 108.6 | 1.1 | | C2P2 | 34 | 129.4 | 14.3 |
| C2P2 | 10.5 | 109.1 | 1 | | C2P2 | 34.5 | 129.8 | 12 |
| C2P2 | 11 | 109.5 | 1.8 | | C2P2 | 35 | 130.2 | 3.9 |
| C2P2 | 11.5 | 109.9 | 6.2 | | C2P2 | 35.5 | 130.7 | 4.2 |
| C2P2 | 12 | 110.4 | 9.8 | | C2P2 | 36 | 131.1 | 7 |
| C2P2 | 12.5 | 110.8 | 11.5 | | C2P2 | 36.5 | 131.5 | 7.4 |
| C2P2 | 13 | 111.2 | 10.1 | | C2P2 | 37 | 132 | 6.5 |
| C2P2 | 13.5 | 111.7 | 13.6 | | C2P2 | 37.5 | 132.4 | 6.1 |
| C2P2 | 14 | 112.1 | 6.5 | | C2P2 | 38 | 132.8 | 6.1 |
| C2P2 | 14.5 | 112.5 | 5.4 | | C2P2 | 38.5 | 133.3 | 4.8 |
| C2P2 | 15 | 113 | 4.6 | | C2P2 | 39 | 133.7 | 3.8 |
| C2P2 | 15.5 | 113.4 | 4.1 | | C2P2 | 39.5 | 134.1 | 4.1 |
| C2P2 | 16 | 113.8 | 4.4 | | C2P2 | 40 | 134.5 | 3.4 |
| C2P2 | 16.5 | 114.3 | 3.9 | | C2P2 | 40.5 | 135 | 0.9 |
| C2P2 | 17 | 114.7 | 4.6 | | C2P2 | 41 | 135.4 | 1.3 |
| C2P2 | 17.5 | 115.1 | 5.5 | | C2P2 | 41.5 | 135.8 | 1.6 |
| C2P2 | 18 | 115.5 | 5.9 | | C2P2 | 42 | 136.3 | 0.1 |
| C2P2 | 18.5 | 116 | 5.8 | | C2P2 | 42.5 | 136.7 | -0.8 |
| C2P2 | 19 | 116.4 | 6.6 | | C2P2 | 43 | 137.1 | -0.3 |
| C2P2 | 19.5 | 116.8 | 7.9 | | C2P2 | 43.5 | 137.6 | 1.2 |
| C2P2 | 20 | 117.3 | 9.1 | | C2P2 | 44 | 138 | 1.8 |
| C2P2 | 20.5 | 117.7 | 11.1 | | C2P2 | 44.5 | 138.4 | 1.7 |
| C2P2 | 21 | 118.1 | 18.1 | | C2P2 | 45 | 138.9 | 1.5 |
| C2P2 | 21.5 | 118.6 | 21.9 | | C2P2 | 45.5 | 139.3 | 4.6 |
| C2P2 | 22 | 119 | 23.2 | | C2P2 | 46 | 139.7 | 2.6 |
| C2P2 | 22.5 | 119.4 | 22 | | C2P2 | 46.5 | 140.2 | 1.5 |
| C2P2 | 23 | 119.9 | 35.7 | | C2P2 | 47 | 140.6 | 1.4 |
| C2P2 | 23.5 | 120.3 | 48.1 | | C2P2 | 47.5 | 141 | 1.6 |

| Core Label | Sample Depth | Overall Core Depth | HRMS (SI) | | Core Label | Sample Depth | Overall Core Depth | HRMS (SI) |
|---|---|---|---|---|---|---|---|---|
| C2P2 | 48 | 141.5 | 2.6 | | C2P3 | 6 | 163.5 | 5.4 |
| C2P2 | 48.5 | 141.9 | 3.5 | | C2P3 | 6.5 | 164.1 | 5.4 |
| C2P2 | 49 | 142.3 | 3.5 | | C2P3 | 7 | 164.6 | 5.8 |
| C2P2 | 49.5 | 142.8 | 3.7 | | C2P3 | 7.5 | 165.1 | 6.2 |
| C2P2 | 50 | 143.2 | 3.3 | | C2P3 | 8 | 165.7 | 6 |
| C2P2 | 50.5 | 143.6 | 2.9 | | C2P3 | 8.5 | 166.2 | 5.7 |
| C2P2 | 51 | 144 | 3.1 | | C2P3 | 9 | 166.8 | 7.3 |
| C2P2 | 51.5 | 144.5 | 3.1 | | C2P3 | 9.5 | 167.3 | 8.8 |
| C2P2 | 52 | 144.9 | 2.1 | | C2P3 | 10 | 167.9 | 9.4 |
| C2P2 | 52.5 | 145.3 | 1.4 | | C2P3 | 10.5 | 168.4 | 9.9 |
| C2P2 | 53 | 145.8 | 2.6 | | C2P3 | 11 | 168.9 | 9.9 |
| C2P2 | 53.5 | 146.2 | 1.5 | | C2P3 | 11.5 | 169.5 | 9.2 |
| C2P2 | 54 | 146.6 | 1.7 | | C2P3 | 12 | 170 | 10.6 |
| C2P2 | 54.5 | 147.1 | 1.6 | | C2P3 | 12.5 | 170.6 | 11.3 |
| C2P2 | 55 | 147.5 | 1.9 | | C2P3 | 13 | 171.1 | 11.6 |
| C2P2 | 55.5 | 147.9 | 2.3 | | C2P3 | 13.5 | 171.7 | 10.5 |
| C2P2 | 56 | 148.4 | 2.6 | | C2P3 | 14 | 172.2 | 10.2 |
| C2P2 | 56.5 | 148.8 | 3 | | C2P3 | 14.5 | 172.7 | 10.9 |
| C2P2 | 57 | 149.2 | 2.3 | | C2P3 | 15 | 173.3 | 12.4 |
| C2P2 | 57.5 | 149.7 | 0.9 | | C2P3 | 15.5 | 173.8 | 12.3 |
| C2P2 | 58 | 150.1 | 0.5 | | C2P3 | 16 | 174.4 | 15.1 |
| C2P2 | 58.5 | 150.5 | 0.4 | | C2P3 | 16.5 | 174.9 | 17.2 |
| C2P2 | 59 | 151 | 0.2 | | C2P3 | 17 | 175.5 | 16.5 |
| C2P2 | 59.5 | 151.4 | 0.1 | | C2P3 | 17.5 | 176 | 18.4 |
| C2P2 | 60 | 151.8 | 0.1 | | C2P3 | 18 | 176.5 | 18.3 |
| C2P2 | 60.5 | 152.3 | 0 | | C2P3 | 18.5 | 177.1 | 16.7 |
| C2P2 | 61 | 152.7 | 0.5 | | C2P3 | 19 | 177.6 | 9.1 |
| C2P2 | 61.5 | 153.1 | 1.8 | | C2P3 | 19.5 | 178.2 | 7.9 |
| C2P2 | 62 | 153.5 | 3.5 | | C2P3 | 20 | 178.7 | 7.2 |
| C2P2 | 62.5 | 154 | 4.3 | | C2P3 | 20.5 | 179.3 | 6.8 |
| C2P2 | 63 | 154.4 | 4.5 | | C2P3 | 21 | 179.8 | 4.8 |
| C2P2 | 63.5 | 154.8 | 4.9 | | C2P3 | 21.5 | 180.3 | 0.8 |
| C2P2 | 64 | 155.3 | 4.8 | | C2P3 | 22 | 180.9 | 2.3 |
| C2P2 | 64.5 | 155.7 | 4.3 | | C2P3 | 22.5 | 181.4 | 3.4 |
| C2P2 | 65 | 156.1 | 2.6 | | C2P3 | 23 | 182 | 4.8 |
| C2P2 | 65.5 | 156.6 | 0.4 | | C2P3 | 23.5 | 182.5 | 4.5 |
| C2P2 | 66 | 157 | 0.3 | | C2P3 | 24 | 183.1 | 3.7 |
| | | | | | C2P3 | 24.5 | 183.6 | 4.3 |
| C2P3 | 0 | 157 | | | C2P3 | 25 | 184.1 | 3.9 |
| C2P3 | 0.5 | 157.5 | 1.4 | | C2P3 | 25.5 | 184.7 | 3.1 |
| C2P3 | 1 | 158.1 | 0.7 | | C2P3 | 26 | 185.2 | 3 |
| C2P3 | 1.5 | 158.6 | 0.9 | | C2P3 | 26.5 | 185.8 | 6.4 |
| C2P3 | 2 | 159.2 | 3.6 | | C2P3 | 27 | 186.3 | 9.7 |
| C2P3 | 2.5 | 159.7 | 6.7 | | C2P3 | 27.5 | 186.9 | 7.9 |
| C2P3 | 3 | 160.3 | 9.4 | | C2P3 | 28 | 187.4 | 15.7 |
| C2P3 | 3.5 | 160.8 | 7.7 | | C2P3 | 28.5 | 187.9 | 29.7 |
| C2P3 | 4 | 161.3 | 6.1 | | C2P3 | 29 | 188.5 | 38.6 |
| C2P3 | 4.5 | 161.9 | 5.3 | | C2P3 | 29.5 | 189 | 58.3 |
| C2P3 | 5 | 162.4 | 4.9 | | C2P3 | 30 | 189.6 | 32.3 |
| C2P3 | 5.5 | 163 | 5.4 | | C2P3 | 30.5 | 190.1 | 15.6 |

| Core Label | Sample Depth | Overall Core Depth | HRMS (SI) | | Core Label | Sample Depth | Overall Core Depth | HRMS (SI) |
|---|---|---|---|---|---|---|---|---|
| C2P3 | 31 | 190.7 | 6.2 | | C2P4 | 20.5 | 215.3 | 59.3 |
| C2P3 | 31.5 | 191.2 | 2.2 | | C2P4 | 21 | 215.8 | 47.6 |
| C2P3 | 32 | 191.7 | 0.3 | | C2P4 | 21.5 | 216.3 | 40 |
| C2P3 | 32.5 | 192.3 | 0.2 | | C2P4 | 22 | 216.8 | 35.3 |
| C2P3 | 33 | 192.8 | 0.3 | | C2P4 | 22.5 | 217.2 | 42 |
| C2P3 | 33.5 | 193.4 | 0.3 | | C2P4 | 23 | 217.7 | 54 |
| C2P3 | 34 | 193.9 | 1.1 | | C2P4 | 23.5 | 218.2 | 67.4 |
| C2P3 | 34.5 | 194.5 | 3 | | C2P4 | 24 | 218.7 | 67.4 |
| C2P3 | 35 | 195 | 0.5 | | C2P4 | 24.5 | 219.2 | 68.9 |
| | | | | | C2P4 | 25 | 219.7 | 66.6 |
| C2P4 | 0.5 | 195.5 | 2.2 | | C2P4 | 25.5 | 220.2 | 66.5 |
| C2P4 | 1 | 196 | 1.8 | | C2P4 | 26 | 220.7 | 62.2 |
| C2P4 | 1.5 | 196.5 | 8 | | C2P4 | 26.5 | 221.2 | 16.4 |
| C2P4 | 2 | 197 | 14.3 | | C2P4 | 27 | 221.7 | 118.4 |
| C2P4 | 2.5 | 197.5 | 52.1 | | C2P4 | 27.5 | 222.2 | 77.1 |
| C2P4 | 3 | 198 | 59.5 | | C2P4 | 28 | 222.7 | 57.5 |
| C2P4 | 3.5 | 198.5 | 49.7 | | C2P4 | 28.5 | 223.2 | 57.3 |
| C2P4 | 4 | 199 | 21.1 | | C2P4 | 29 | 223.7 | 60.1 |
| C2P4 | 4.5 | 199.4 | 7.3 | | C2P4 | 29.5 | 224.2 | 54 |
| C2P4 | 5 | 199.9 | 5.1 | | C2P4 | 30 | 224.7 | 50.3 |
| C2P4 | 5.5 | 200.4 | 8.7 | | C2P4 | 30.5 | 225.2 | 45.5 |
| C2P4 | 6 | 200.9 | 24.7 | | C2P4 | 31 | 225.7 | 39.2 |
| C2P4 | 6.5 | 201.4 | 53.6 | | C2P4 | 31.5 | 226.1 | 37.5 |
| C2P4 | 7 | 201.9 | 80.6 | | C2P4 | 32 | 226.6 | 26.7 |
| C2P4 | 7.5 | 202.4 | 87.6 | | C2P4 | 32.5 | 227.1 | 28.9 |
| C2P4 | 8 | 202.9 | 92.7 | | C2P4 | 33 | 227.6 | 39.8 |
| C2P4 | 8.5 | 203.4 | 84.9 | | C2P4 | 33.5 | 228.1 | 33.5 |
| C2P4 | 9 | 203.9 | 80 | | C2P4 | 34 | 228.6 | 27.4 |
| C2P4 | 9.5 | 204.4 | 74.1 | | C2P4 | 34.5 | 229.1 | 43.3 |
| C2P4 | 10 | 204.9 | 79.9 | | C2P4 | 35 | 229.6 | 57.4 |
| C2P4 | 10.5 | 205.4 | 79.9 | | C2P4 | 35.5 | 230.1 | 61.9 |
| C2P4 | 11 | 205.9 | 77.3 | | C2P4 | 36 | 230.6 | 56.7 |
| C2P4 | 11.5 | 206.4 | 74.1 | | C2P4 | 36.5 | 231.1 | 45.5 |
| C2P4 | 12 | 206.9 | 72.3 | | C2P4 | 37 | 231.6 | 33.7 |
| C2P4 | 12.5 | 207.4 | 73.4 | | C2P4 | 37.5 | 232.1 | 33.2 |
| C2P4 | 13 | 207.9 | 79.1 | | C2P4 | 38 | 232.6 | 36.4 |
| C2P4 | 13.5 | 208.3 | 75.6 | | C2P4 | 38.5 | 233.1 | 40.9 |
| C2P4 | 14 | 208.8 | 62.4 | | C2P4 | 39 | 233.6 | 50.1 |
| C2P4 | 14.5 | 209.3 | 54 | | C2P4 | 39.5 | 234.1 | 54.5 |
| C2P4 | 15 | 209.8 | 46.3 | | C2P4 | 40 | 234.6 | 58.2 |
| C2P4 | 15.5 | 210.3 | 43.5 | | C2P4 | 40.5 | 235 | 67.8 |
| C2P4 | 16 | 210.8 | 63.6 | | C2P4 | 41 | 235.5 | 70.6 |
| C2P4 | 16.5 | 211.3 | 67.2 | | C2P4 | 41.5 | 236 | 60.2 |
| C2P4 | 17 | 211.8 | 45.9 | | C2P4 | 42 | 236.5 | 47.4 |
| C2P4 | 17.5 | 212.3 | 31.1 | | C2P4 | 42.5 | 237 | 49.3 |
| C2P4 | 18 | 212.8 | 46 | | C2P4 | 43 | 237.5 | 61.1 |
| C2P4 | 18.5 | 213.3 | 57.7 | | C2P4 | 43.5 | 238 | 68.6 |
| C2P4 | 19 | 213.8 | 91.2 | | C2P4 | 44 | 238.5 | 51.4 |
| C2P4 | 19.5 | 214.3 | 82 | | | | | |
| C2P4 | 20 | 214.8 | 71.3 | | C2P5 | 0 | 239 | 6 |

| Core Label | Sample Depth | Overall Core Depth | HRMS (SI) | | Core Label | Sample Depth | Overall Core Depth | HRMS (SI) |
|---|---|---|---|---|---|---|---|---|
| C2P5 | 0.5 | 239.4 | 2.3 | | C2P5 | 25.5 | 258.7 | 43.7 |
| C2P5 | 1 | 239.8 | 2 | | C2P5 | 26 | 259.1 | 49 |
| C2P5 | 1.5 | 240.2 | 8 | | C2P5 | 26.5 | 259.4 | 52.1 |
| C2P5 | 2 | 240.5 | 26.1 | | C2P5 | 27 | 259.8 | 47.2 |
| C2P5 | 2.5 | 240.9 | 44.8 | | C2P5 | 27.5 | 260.2 | 30.8 |
| C2P5 | 3 | 241.3 | 60.3 | | C2P5 | 28 | 260.6 | 40.3 |
| C2P5 | 3.5 | 241.7 | 69.4 | | C2P5 | 28.5 | 261 | 67.2 |
| C2P5 | 4 | 242.1 | 60.7 | | C2P5 | 29 | 261.4 | 75.5 |
| C2P5 | 4.5 | 242.5 | 58 | | C2P5 | 29.5 | 261.8 | 74 |
| C2P5 | 5 | 242.9 | 56.6 | | C2P5 | 30 | 262.1 | 62.6 |
| C2P5 | 5.5 | 243.2 | 58.1 | | C2P5 | 30.5 | 262.5 | 53.2 |
| C2P5 | 6 | 243.6 | 61.6 | | C2P5 | 31 | 262.9 | 41.9 |
| C2P5 | 6.5 | 244 | 64.6 | | C2P5 | 31.5 | 263.3 | 59.6 |
| C2P5 | 7 | 244.4 | 64.5 | | C2P5 | 32 | 263.7 | 52.2 |
| C2P5 | 7.5 | 244.8 | 63.7 | | C2P5 | 32.5 | 264.1 | 47.1 |
| C2P5 | 8 | 245.2 | 59.2 | | C2P5 | 33 | 264.5 | 46.5 |
| C2P5 | 8.5 | 245.6 | 46.1 | | C2P5 | 33.5 | 264.8 | 30.1 |
| C2P5 | 9 | 245.9 | 51.6 | | C2P5 | 34 | 265.2 | 22 |
| C2P5 | 9.5 | 246.3 | 71.6 | | C2P5 | 34.5 | 265.6 | 2.5 |
| C2P5 | 10 | 246.7 | 75.7 | | C2P5 | 35 | 266 | 2.9 |
| C2P5 | 10.5 | 247.1 | 78.1 | | | | | |
| C2P5 | 11 | 247.5 | 78.2 | | C2P6 | 0.5 | 266.6 | 6.6 |
| C2P5 | 11.5 | 247.9 | 70.9 | | C2P6 | 1 | 267.3 | 8.5 |
| C2P5 | 12 | 248.3 | 72.4 | | C2P6 | 1.5 | 267.9 | 16.7 |
| C2P5 | 12.5 | 248.6 | 79.7 | | C2P6 | 2 | 268.5 | 28.1 |
| C2P5 | 13 | 249 | 65.4 | | C2P6 | 2.5 | 269.2 | 27.3 |
| C2P5 | 13.5 | 249.4 | 65.4 | | C2P6 | 3 | 269.8 | 30.4 |
| C2P5 | 14 | 249.8 | 74.2 | | C2P6 | 3.5 | 270.4 | 36.5 |
| C2P5 | 14.5 | 250.2 | 76.7 | | C2P6 | 4 | 271.1 | 42.6 |
| C2P5 | 15 | 250.6 | 82.3 | | C2P6 | 4.5 | 271.7 | 42.9 |
| C2P5 | 15.5 | 251 | 85.8 | | C2P6 | 5 | 272.3 | 42.4 |
| C2P5 | 16 | 251.3 | 76.5 | | C2P6 | 5.5 | 272.9 | 44 |
| C2P5 | 16.5 | 251.7 | 63.1 | | C2P6 | 6 | 273.6 | 41 |
| C2P5 | 17 | 252.1 | 58.5 | | C2P6 | 6.5 | 274.2 | 45.4 |
| C2P5 | 17.5 | 252.5 | 62.2 | | C2P6 | 7 | 274.8 | 46.8 |
| C2P5 | 18 | 252.9 | 65.7 | | C2P6 | 7.5 | 275.5 | 46.2 |
| C2P5 | 18.5 | 253.3 | 73.1 | | C2P6 | 8 | 276.1 | 47.1 |
| C2P5 | 19 | 253.7 | 69.8 | | C2P6 | 8.5 | 276.7 | 46.1 |
| C2P5 | 19.5 | 254 | 68.1 | | C2P6 | 9 | 277.4 | 44.2 |
| C2P5 | 20 | 254.4 | 67.5 | | C2P6 | 9.5 | 278 | 41.6 |
| C2P5 | 20.5 | 254.8 | 61.8 | | C2P6 | 10 | 278.6 | 40.1 |
| C2P5 | 21 | 255.2 | 61.8 | | C2P6 | 10.5 | 279.3 | 43.8 |
| C2P5 | 21.5 | 255.6 | 60.5 | | C2P6 | 11 | 279.9 | 47.1 |
| C2P5 | 22 | 256 | 55.3 | | C2P6 | 11.5 | 280.5 | 53 |
| C2P5 | 22.5 | 256.4 | 50.9 | | C2P6 | 12 | 281.2 | 46.6 |
| C2P5 | 23 | 256.7 | 38.9 | | C2P6 | 12.5 | 281.8 | 33.2 |
| C2P5 | 23.5 | 257.1 | 36.7 | | C2P6 | 13 | 282.4 | 20.9 |
| C2P5 | 24 | 257.5 | 43.7 | | C2P6 | 13.5 | 283.1 | 24.9 |
| C2P5 | 24.5 | 257.9 | 49.6 | | C2P6 | 14 | 283.7 | 49 |
| C2P5 | 25 | 258.3 | 46.5 | | C2P6 | 14.5 | 284.3 | 17.2 |

| Core Label | Sample Depth | Overall Core Depth | HRMS (SI) | |
|---|---|---|---|---|
| C2P6 | 15 | 284.9 | 1.4 | |
| C2P6 | 15.5 | 285.6 | 3.9 | |
| C2P6 | 16 | 286.2 | 23.2 | |
| C2P6 | 16.5 | 286.8 | 37 | |
| C2P6 | 17 | 287.5 | 15.3 | |
| C2P6 | 17.5 | 288.1 | 4.3 | |
| C2P6 | 18 | 288.7 | 3.5 | |
| C2P6 | 18.5 | 289.4 | 10.8 | |
| C2P6 | 19 | 290 | 8.9 | |

Appendix 7. LOMC1 Elemental and Isotopic data

| Core Label | Segment depth start (cm) | Segment depth end (cm) | Overall Core Depth (cm) | Weight. (mg) | N2 Amp | %N | δ15N vs. At. Air | CO2 Amp | %C | δ13C vs. VPDB | C/N ratio |
|---|---|---|---|---|---|---|---|---|---|---|---|
| C1P1 | 2 | 4 | 3.1 | 30.418 | 1226 | 0.1445287 | 4.0410675 | 7727 | 3.0656104 | -14.620177 | 21.2 |
| C1P1 | 6 | 8 | 7.1 | 29.685 | 456 | 0.067779 | 2.0573993 | 1291 | 0.7380945 | -24.294997 | 10.9 |
| C1P1 | 10 | 12 | 11.2 | 31.235 | 1068 | 0.1374072 | 3.4671132 | 6074 | 3.0002687 | -15.709601 | 21.8 |
| C1P1 | 14 | 16 | 15.3 | 28.281 | 942 | 0.1160331 | 3.7100316 | 4813 | 1.9308204 | -17.007163 | 16.6 |
| C1P1 | 18 | 20 | 19.4 | 28.562 | 324 | 0.0516318 | 1.6149198 | 1380 | 0.7794418 | -19.287172 | 15.1 |
| C1P1 | 26 | 28 | 27.5 | 29.811 | 1200 | 0.1412377 | 3.1307186 | 8078 | 3.218787 | -12.55659 | 22.8 |
| C1P1 | 30 | 32 | 31.6 | 32.694 | 749 | 0.0937113 | 2.9132612 | 4681 | 2.1862988 | -15.258044 | 23.3 |
| C1P1 | 34 | 36 | 35.7 | 29.951 | 400 | 0.0669909 | 1.8958592 | 1806 | 1.0674712 | -22.440319 | 15.9 |
| C1P1 | 38 | 40 | 39.8 | 31.846 | 872 | 0.0953196 | 3.9752592 | 3904 | 1.3822631 | -17.134212 | 14.5 |
| C1P1 | 42 | 44 | 43.9 | 31.256 | 890 | 0.0990206 | 3.642229 | 3180 | 1.1406244 | -20.823452 | 11.5 |
| C1P1 | 50 | 52 | 52 | 29.763 | 712 | 0.0842245 | 4.4159757 | 2473 | 0.9379391 | -22.887039 | 11.1 |
| C1P1 | 54 | 56 | 56.1 | 29.614 | 834 | 0.097333 | 4.4249496 | 4367 | 1.6594243 | -16.294917 | 17 |
| C1P1 | 58 | 60 | 60.2 | 31.428 | 807 | 0.09144 | 5.1967021 | 3897 | 1.4346405 | -14.774176 | 15.7 |
| C1P1 | 62 | 64 | 64.3 | 29.934 | 998 | 0.1174454 | 4.3960338 | 4792 | 1.834732 | -16.741514 | 15.6 |
| C1P1 | 66 | 68 | 68.3 | 31.58 | 709 | 0.0790049 | 5.226615 | 3547 | 1.2818881 | -15.378623 | 16.2 |
| C1P1 | 70 | 72 | 72.4 | 28.302 | 745 | 0.0929071 | 4.7460146 | 3301 | 1.3313391 | -17.528834 | 14.3 |
| C1P1 | 74 | 76 | 76.5 | 28.417 | 602 | 0.0839507 | 4.4132771 | 2104 | 1.0926404 | -19.709659 | 13 |
| C1P1 | 78 | 80 | 80.6 | 30.908 | 664 | 0.0957052 | 3.700895 | 3611 | 1.9210486 | -16.522597 | 20.1 |
| C1P1 | 82 | 84 | 84.7 | 30.553 | 905 | 0.10508 | 4.2594316 | 4854 | 1.8440827 | -14.65194 | 17.5 |
| C1P1 | 86 | 88 | 88.7 | 28.9 | 790 | 0.0948634 | 4.9534106 | 3867 | 1.516732 | -15.612509 | 16 |
| C1P1 | 90 | 92 | 92.8 | 29.605 | 555 | 0.0647299 | 3.217466 | 8103 | 3.247173 | -7.1367856 | 50.2 |
| C1P1 | 94 | 96 | 96.9 | 30.612 | 740 | 0.084033 | 4.4229554 | 4492 | 1.675257 | -11.609496 | 19.9 |
| | | | | | | | | | | | |
| C1P2 | 2 | 4 | 104.2 | 31.656 | 770 | 0.0846385 | 3.2144747 | 5911 | 2.1467683 | -9.7249323 | 25.4 |
| C1P2 | 6 | 8 | 107.5 | 28.19 | 741 | 0.0886985 | 2.3041259 | 7628 | 3.1337075 | -7.7085071 | 35.3 |
| C1P2 | 10 | 12 | 111.8 | 30.379 | 691 | 0.080441 | 1.7577171 | 8404 | 3.3588948 | -7.071336 | 41.8 |
| C1P2 | 14 | 16 | 116.1 | 30.748 | 585 | 0.0650088 | 2.8345811 | 10416 | 4.2627371 | -5.3475091 | 65.6 |
| C1P2 | 18 | 20 | 120.3 | 27.747 | 457 | 0.0692638 | 3.1209557 | 4988 | 3.5610687 | -7.4730462 | 51.4 |
| C1P2 | 22 | 24 | 124.6 | 30.46 | 654 | 0.0849348 | 3.0166068 | 7940 | 4.1690131 | -6.2986104 | 49.1 |
| C1P2 | 26 | 28 | 128.9 | 31.246 | 584 | 0.0657143 | 5.3173507 | 3697 | 1.339357 | -11.488221 | 20.4 |
| C1P2 | 30 | 32 | 133.2 | 29.039 | 482 | 0.0565706 | 4.2604287 | 8137 | 3.4567933 | -4.3927149 | 61.1 |
| C1P2 | 38 | 40 | 141.7 | 30.237 | 280 | 0.0436631 | 3.3808247 | 2654 | 1.5987803 | -7.9943716 | 36.6 |
| C1P2 | 42 | 44 | 146 | 29.218 | 317 | 0.0390425 | 6.4560347 | 1169 | 0.4453584 | -20.455779 | 11.4 |

| Core Label | Segment depth start (cm) | Segment depth end (cm) | Overall Core Depth (cm) | Weight. (mg) | N2 Amp | %N | δ15N vs. At. Air | CO2 Amp | %C | δ13C vs. VPDB | C/N ratio |
|---|---|---|---|---|---|---|---|---|---|---|---|
| C1P2 | 46 | 48 | 150.3 | 29.773 | 85 | 0.0151522 | -3.3025235 | 660 | 0.4432987 | -10.425609 | 29.3 |
| C1P2 | 54 | 56 | 158.9 | 32.032 | 108 | 0.0180815 | 2.7958687 | 269 | 0.1555754 | -19.304614 | 8.6 |
| C1P2 | 58 | 60 | 163.2 | 30.409 | 168 | 0.0201031 | 6.3593163 | 467 | 0.1875051 | -21.583822 | 9.3 |
| C1P2 | 62 | 64 | 167.4 | 28.858 | 299 | 0.0415458 | 3.6888547 | 428 | 0.2152781 | -20.691262 | 5.2 |
| C1P2 | 66 | 68 | 171.7 | 31.645 | 279 | 0.0306354 | 6.7441955 | 869 | 0.3017917 | -22.209443 | 9.9 |
| | | | | | | | | | | | |
| C1P3 | 0 | 2 | 175.1 | 31.951 | 132 | 0.0184886 | 3.5513951 | 245 | 0.1374046 | -22.33179 | 7.4 |
| C1P3 | 8 | 10 | 183.5 | 29.953 | 397 | 0.0525239 | 5.3072664 | 940 | 0.4544275 | -18.633093 | 8.7 |
| C1P3 | 12 | 14 | 187.7 | 29.408 | 471 | 0.0639872 | 5.0785015 | 1437 | 0.7161619 | -18.605961 | 11.2 |
| C1P3 | 16 | 18 | 191.9 | 28.563 | 315 | 0.0442643 | 3.7821667 | 559 | 0.2842307 | -20.456763 | 6.4 |

Appendix 8. LOMC2 Elemental and Isotopic data

| Core Label | Segment depth start (cm) | Segment depth end (cm) | Overall Core Depth (cm) | Weight. (mg) | N2 Amp | %N | δ15N vs. At. Air | CO2 Amp | %C | δ13C vs. VPDB | C/N ratio |
|---|---|---|---|---|---|---|---|---|---|---|---|
| C2P2 | 14 | 16 | 113 | 29.48 | 1874 | 0.1809416 | 3.0928422 | 4484 | 2.2635552 | -21.70286 | 12.5 |
| C2P2 | 22 | 24 | 119.9 | 30.47 | 1086 | 0.1175648 | 4.046185 | 2741 | 1.3702199 | -20.96665 | 11.7 |
| C2P2 | 30 | 32 | 126.8 | 29.96 | 952 | 0.1052538 | 4.4905564 | 2727 | 1.3707138 | -19.78561 | 13 |
| C2P2 | 37 | 39 | 132.8 | 28.17 | 1667 | 0.1781273 | 2.5496129 | 4326 | 2.3280403 | -21.91514 | 13.1 |
| C2P2 | 46 | 48 | 140.6 | 27.14 | 2233 | 0.2502205 | 1.4504301 | 5247 | 3.046391 | -26.29577 | 12.2 |
| C2P2 | 54 | 56 | 147.5 | 29.48 | 1890 | 0.1934749 | 1.9838715 | 5039 | 2.6491831 | -25.7506 | 13.7 |
| C2P2 | 60 | 62 | 152.7 | 28.78 | 2027 | 0.2034455 | 2.4390095 | 5862 | 3.1530262 | -22.97556 | 15.5 |
| | | | | | | | | | | | |
| C2P3 | 2 | 4 | 160.3 | 30.76 | 1067 | 0.114202 | 4.8233455 | 2643 | 1.3690178 | -22.00005 | 12 |
| C2P3 | 10 | 12 | 168.9 | 32.35 | 1095 | 0.1070494 | 3.5137225 | 3193 | 1.5665511 | -22.93021 | 14.6 |
| C2P3 | 18 | 20 | 177.6 | 30.97 | 1005 | 0.0955157 | 4.7499361 | 3426 | 1.6336028 | -12.7766 | 17.1 |
| C2P3 | 26 | 28 | 186.3 | 28.83 | 1125 | 0.1201986 | 5.018125 | 2942 | 1.5350397 | -20.67525 | 12.8 |
| | | | | | | | | | | | |
| C2P4 | 2 | 4 | 198 | 15.491 | 612 | 0.1200227 | 4.1704916 | 1605 | 1.6084323 | -23.3538 | 13.4 |
| C2P4 | 26 | 28 | 221.7 | 29.84 | 473 | 0.0495327 | 5.8089885 | 1053 | 0.5313802 | -18.85545 | 10.7 |
| C2P4 | 10 | 12 | 205.9 | 31.93 | 525 | 0.049722 | 5.6885971 | 1182 | 0.5374653 | -17.69661 | 10.8 |
| C2P4 | 18 | 20 | 213.8 | 32.24 | 502 | 0.0488077 | 5.8471613 | 1292 | 0.5913503 | -16.73171 | 12.1 |
| C2P4 | 34 | 36 | 229.6 | 32.64 | 666 | 0.0609849 | 5.9949588 | 2055 | 0.9273896 | -16.10357 | 15.2 |
| C2P4 | 40 | 42 | 235.5 | 31.35 | 461 | 0.0477582 | 6.7251373 | 1585 | 0.7590429 | -15.45516 | 15.9 |
| C2P4 | 18 | 20 | 213.8 | 32.04 | 549 | 0.0603329 | 3.8572783 | 2945 | 1.4563762 | -11.49425 | 24.1 |
| | | | | | | | | | | | |
| C2P5 | 4 | 6 | 242.9 | 32.59 | 602 | 0.0559477 | 5.7306851 | 2061 | 0.9323005 | -14.73438 | 16.7 |
| C2P5 | 12 | 14 | 249 | 32.28 | 452 | 0.0481339 | 4.48762 | 1751 | 0.8349203 | -15.27183 | 17.3 |
| C2P5 | 20 | 22 | 255.2 | 31.61 | 481 | 0.0490976 | 6.13982 | 1896 | 0.8995586 | -14.78069 | 18.3 |
| C2P5 | 28 | 30 | 261.4 | 32.96 | 600 | 0.0559285 | 5.6964274 | 2398 | 1.074345 | -14.07342 | 19.2 |
| | | | | | | | | | | | |
| C2P6 | 2 | 4 | 269.8 | 32.41 | 643 | 0.0623447 | 5.7375367 | 3401 | 1.6088732 | -12.15424 | 25.8 |
| C2P6 | 10 | 12 | 279.9 | 29.37 | 541 | 0.0580176 | 6.9688563 | 1631 | 0.8229142 | -19.09861 | 14.2 |

Appendix 9.  LOMC1 Seed data

| Core Label | Segment depth start (cm) | Segment depth end (cm) | Overall Core Depth (cm) | Carex | Potamogeton | Scirpus | Juncaceae | Cyperaceae | Typha | Glyceria | Renunculus | Scleria |
|---|---|---|---|---|---|---|---|---|---|---|---|---|
| C1P1 | 3 | 4 | 3.6 | 1 | | | | | | | | |
| C1P1 | 6 | 8 | 7.1 | 0 | | | | | | | | |
| C1P1 | 11 | 12 | 11.7 | 2 | | | | | | | | |
| C1P1 | 14 | 15 | 14.8 | 9 | | | | | | | | |
| C1P1 | 18 | 19 | 18.9 | 7 | | | | | | | | |
| C1P1 | 26 | 27 | 27 | 1 | | | | | | | | |
| C1P1 | 30 | 31 | 31.8 | 11 | | 1 | | | | | | |
| C1P1 | 35 | 36 | 36.2 | 4 | | | | | | | | |
| C1P1 | 37 | 38 | 38.3 | 4 | | | | | | | | |
| C1P1 | 42 | 43 | 43.4 | 3 | | | | | | | | |
| C1P1 | 51 | 52 | 52.5 | 3 | | | | | | | | |
| C1P1 | 54 | 55 | 55.6 | 4 | | | | | | | | |
| C1P1 | 58 | 59 | 59.7 | 18 | | 1 | | 1 | | | | |
| C1P1 | 63 | 64 | 64.8 | 1 | | | | 1 | | | | |
| C1P1 | 67 | 68 | 68.9 | 2 | | | | | | | | |
| C1P1 | 71 | 72 | 72.9 | 4 | | | | | | | | |
| C1P1 | 75 | 76 | 77 | 3 | | | | | | | | |
| C1P1 | 79 | 80 | 81.1 | 28 | | 1 | 2 | | | | | |
| C1P1 | 82 | 84 | 84.7 | 18 | | | | | | | | |
| C1P1 | 87 | 88 | 89.3 | 7 | | | | | | | | |
| C1P1 | 90 | 91 | 92.3 | 3 | | | | | | | | |
| C1P1 | 95 | 97 | 97.9 | 1 | | | | | | | | |
| | | | | | | | | | | | | |
| C1P2 | 3 | 4 | 104.7 | 6 | | | | | | | | |
| C1P2 | 7 | 8 | 109 | 2 | | | 1 | | 1 | | | |
| C1P2 | 10 | 11 | 112.2 | 2 | | | 2 | | 2 | | | |
| C1P2 | 15 | 16 | 117.6 | 6 | 2 | 1 | | 1 | | | | |
| C1P2 | 18 | 19 | 120.8 | 2 | 1 | | 2 | 1 | | 1 | | |
| C1P2 | 22 | 23 | 125.1 | 1 | | | | 2 | | 10 | | |
| C1P2 | 27 | 28 | 130.4 | 1 | | | | 1 | 1 | 1 | | |
| C1P2 | 30 | 31 | 133.6 | | 1 | | | | | | | |
| C1P2 | 39 | 40 | 143.3 | | 1 | | | | | | | |

| Core Label | Segment depth start (cm) | Segment depth end (cm) | Overall Core Depth (cm) | Carex | Potamogeton | Scirpus | Juncaceae | Cyperaceae | Typha | Glyceria | Renunculus | Scleria |
|---|---|---|---|---|---|---|---|---|---|---|---|---|
| C1P2 | 42 | 44 | 147 | | | | | | | | | |
| C1P2 | 46 | 48 | 151.3 | | | | | | | | | |
| C1P2 | 54 | 56 | 159.9 | | | | | | | | | |
| C1P2 | 58 | 60 | 164.2 | | | | | | | | | |
| C1P2 | 62 | 64 | 168.4 | | | | | | | | | |
| C1P2 | 66 | 68 | 172.7 | | | | | | | | | |
| | | | | | | | | | | | | |
| C1P3 | 0 | 2 | 175.1 | | | | | | | | | |
| C1P3 | 8 | 10 | 183.5 | | | | | | | | | |
| C1P3 | 12 | 14 | 187.7 | | | | | | | | | |
| C1P3 | 16 | 18 | 191.9 | | | | | | | | | |

Appendix 10.  LOMC2 Seed data

| Core Label | Segment depth start (cm) | Segment depth end (cm) | Overall Core Depth (cm) | Carex | Potamogeton | Scirpus | Juncaceae | Cyperaceae | Typha | Glyceria | Renunculus | Scleria |
|---|---|---|---|---|---|---|---|---|---|---|---|---|
| C2P2 | 14 | 15 | 112.5 | 26 | | | | | | | | |
| C2P2 | 18 | 19 | 116 | 4 | | | | 1 | | | | |
| C2P2 | 22 | 24 | 119.9 | | | | | | | | | |
| C2P2 | 26 | 28 | 123.3 | | | | | | | | | |
| C2P2 | 30 | 31 | 126.3 | 1 | | | | | | | | |
| C2P2 | 35 | 36 | 130.7 | | | | | | | 1 | | |
| C2P2 | 38 | 39 | 133.3 | 1 | | | | | | | | |
| C2P2 | 43 | 44 | 137.6 | 1 | | | | 1 | 5 | 1 | | |
| C2P2 | 46 | 47 | 140.2 | 4 | | | | 4 | 2 | | | |
| C2P2 | 50 | 51 | 143.6 | 4 | | | | | | | | |
| C2P2 | 54 | 55 | 147.1 | | | | | 1 | 1 | | | |
| C2P2 | 60 | 62 | 152.7 | 1 | | | | | | | | |
| | | | | | | | | | | | | |
| C2P3 | 2 | 3 | 159.3 | 7 | | | | | | | | |
| C2P3 | 6 | 8 | 163.4 | | | | | | | | | |
| C2P3 | 11 | 12 | 167.6 | 8 | | | | 5 | | | | |
| C2P3 | 14 | 16 | 170.8 | 2 | | | | | 3 | | | |
| C2P3 | 18 | 19 | 174 | 3 | | 1 | | 4 | | | | |
| C2P3 | 23 | 24 | 178.6 | 11 | | 1 | | | | | | |
| C2P3 | 26 | 28 | 181.9 | 22 | | | | | | | | |
| C2P3 | 30 | 31 | 185.1 | 12 | | 1 | | 2 | 1 | | | |
| | | | | | | | | | | | | |
| C2P4 | 2 | 4 | 198 | | | | | | | | | |
| C2P4 | 6 | 8 | 201.9 | | | | | | | | | |
| C2P4 | 10 | 12 | 205.9 | | | | | | | | | |
| C2P4 | 15 | 16 | 210.3 | 1 | | | | | | | | |
| C2P4 | 19 | 20 | 214.3 | 1 | | | | | | | | |
| C2P4 | 23 | 24 | 218.2 | 1 | | | | | | | | |
| C2P4 | 28 | 29 | 223.2 | 28 | | 2 | | | | | | |
| C2P4 | 30 | 31 | 225.2 | 26 | | 3 | | 1 | | | | 1 |
| C2P4 | 34 | 35 | 229.1 | 1 | | | | | 1 | | | |
| C2P4 | 40 | 41 | 235 | 1 | | | | | | | | |

| Core Label | Segment depth start (cm) | Segment depth end (cm) | Overall Core Depth (cm) | Carex | Potamogeton | Scirpus | Juncaceae | Cyperaceae | Typha | Glyceria | Renunculus | Scleria |
|---|---|---|---|---|---|---|---|---|---|---|---|---|
| C2P5 | 0 | 1 | 235.4 | 23 | | 4 | | 2 | | | | |
| C2P5 | 4 | 5 | 238.5 | 3 | | | | | | 1 | | |
| C2P5 | 8 | 9 | 241.6 | 1 | | | | 1 | | | | |
| C2P5 | 12 | 13 | 244.6 | | | | | | | 2 | | |
| C2P5 | 16 | 18 | 248.1 | | | | | | | | | |
| C2P5 | 20 | 21 | 250.8 | 1 | 1 | | | | | | | |
| C2P5 | 24 | 25 | 253.9 | 1 | | | | | | | | |
| C2P5 | 28 | 29 | 257 | | 6 | | | | | | | |
| C2P5 | 29 | 30 | 257.8 | | 8 | | | | | | | |
| C2P5 | 32 | 33 | 260.1 | | 3 | | | | | | | |
| | | | | | | | | | | | | |
| C2P6 | 3 | 4 | 270.4 | 2 | | | | | | | | |
| C2P6 | 7 | 8 | 275.5 | 1 | | | | | | | | |
| C2P6 | 10 | 11 | 279.3 | 1 | | | | | | | | |
| C2P6 | 14 | 15 | 284.3 | 19 | 2 | | | | | | | |
| C2P6 | 22 | 23 | 294.4 | 6 | | | | | | | | |

Appendix 11. LOMC1 Coring field notes.

Laguna Ojo de mar    W. Pepe, M.

Water depth = 4.50m

$H_2O$ to | $H_2O$ depth

Height to PV = 67cm | Clarity 88cm

44
23

1st mark = ~~48~~ 47cm

1.35
3.82

LOM Core1

P1 = 0-1.2m (+ few cm)    Red tape.

R=100cm

@ least 3 bands of gypsum

1 ~ @ ~ 50cm (not measured)

2 near base of core

all about 1-2cm thick.

C1 P2 1-2M.    Green Tape.

P=78cm.

R=72cm    1-172cm

~23cm light color

Δ to dark grey til 32cm

32-end is a brownish/tan color.

mottled ~~Th~~ w/ blackish then tan

Scale: 1 square = ______

yellow

C1 P3 $178 - 278$cm type

Added shoe onto cores.

$278 - 17 = 261$

17cm From PVC to yellow

~~P = 178 - 261~~

$261 - 178 = 83$

Pos start of push 17cm below yellow
end of push 79cm below yellow

So push start = $178 - 17 = 161$cm
pushed to 38cm lower

= 199cm end sandy
bottom 17cm should be ok, ie new stuff
above that slop?

R = 19cm tan colored
Felt some resistance and couldn't
push to end of P2 so
after p3 cleaned out hole to
point ended last time
again some resistance.

PVC may have shifted after on
2 or 3 remeasure

Scale: 1 square = ________

PVC height is now 44cm
above $H_2O$

Sd $H_2O$ + PV = 450 + 44 = 494
Total drivelength = = 199

693

Distance PVC moved = + 23

6716

−135

581

275

6

C1P4 Blue Tape
E of core too much resistance

Scale: 1 square = _______

Appendix 12. LOMC2 Coring field notes

LOM CORE 2 5/31/08

Water depth 5.07m | ~20m from shore

$H_2O$ to PVC top 30cm

$H_2O$ + PVC = 5.37

Livingston 1.38

4.02m

1.83

rods ↓

2.19

92

27

C2P1

w/ shoe yellow tape.

Push 0–1m

R = 80cm

Platform to $H_2O$

N 17 47.541' elev 2800'

W 092° 33.615'

Nav Datum C2P2

→ Platform above $H_2O$ = 20cm

P = 1–1.57cm

R = ~60cm green tape.

Slight stretching.

Scale: 1 square =

C2P3 Tbar handle

P = 38 cm

P 1.57 ⇒ 1.95

ΣR = 35 cm

bottom 5cm missing possibly b/c
of Δ in up/down motion w/have
been ~40 cm
~silty at base.

C2P4 blue tape

P = 195 - 239 44cm in tape

R = 46 some stretching

Brownish near top
then into black seds.
then mottled brown nr base

C2P5 Orange tape

239

P = 239 - 266 cm 27 in tape

R = 34 266

top stretched out

Strange 30 hard material on outside
bread put in bag
Brownish w/ black mottling

Scale: 1 square = ________

C2P6 Red tape

P = 266cm — 290cm 76 to tape

R = 19cm push 24cm

Core extended 5cm beyond tube.

Cut off so recovery = 266

15cm 19

85

C2P7

280- 285cm indigo tape

No recovery 5cm push

fell out of tube.

E of core

Scale: 1 square =